Petrology, Mineralogy, and Geochemistry of the Lower Coon Mountain Pluton, Northern California, with Respect to the Distribution of Platinum-Group Elements

U.S. GEOLOGICAL SURVEY BULLETIN 2014

Petrology, Mineralogy, and Geochemistry of the Lower Coon Mountain Pluton, Northern California, with Respect to the Distribution of Platinum-Group Elements

By NORMAN J PAGE, FLOYD GRAY, and ANDREW GRISCOM

U.S. GEOLOGICAL SURVEY BULLETIN 2014

U.S. DEPARTMENT OF THE INTERIOR
BRUCE BABBITT, Secretary

U.S. GEOLOGICAL SURVEY
Dallas L. Peck, Director

Text edited by George Havach
Illustrations edited by Carol L. Ostergren

UNITED STATES GOVERNMENT PRINTING OFFICE, WASHINGTON : 1993

For sale by
Book and Open-File Report Sales
U.S. Geological Survey
Federal Center, Box 25286
Denver, CO 80225

Library of Congress Cataloging in Publication Data

Page, Norman J
Petrology, mineralogy, and geochemistry of the Lower Coon Mountain pluton, northern California, with respect to the distribution of platinum-group elements / by Norman J Page, Floyd Gray, and Andrew Griscom.
p. cm. — (U.S. Geological Survey bulletin ; 2014)
Includes bibliographical references.
1. Rocks, Igneous—California—Del Norte County. 2. Geochemistry—California—Del Norte County. I. Gray, Floyd. II. Griscom, Andrew. III. Title. IV. Series.
QE75.89 no. 2014
[QE461]
557.3 s—dc20 92-27975
[552'.3'0979411] CIP

CONTENTS

FIGURES

PLATE

TABLES

Petrology, Mineralogy, and Geochemistry of the Lower Coon Mountain Pluton, Northern California, with Respect to the Distribution of Platinum-Group Elements

By Norman J Page, Floyd Gray, *and* Andrew Griscom

Abstract

The Lower Coon Mountain pluton, south of Gasquet in Del Norte County, northern California, forms a sill-like mass of mafic and ultramafic rocks that crop out over an area of about 8 km^2. It intrudes the central part of a syncline formed by metasedimentary and metavolcanic rocks that overlie the Josephine ophiolite of Jurassic age. The pluton has a minimum age of 142 Ma. Aeromagnetic modeling suggests a maximum thickness of 400 to 500 m, but most of the pluton is much thinner. Two sequences of rocks compose the pluton, a layered and an intrusive sequence. The older, layered sequence consists of repetitive units, ranging in thickness from 10 to 625 m, of clinopyroxene-olivine cumulate and plagioclase-rich clinopyroxene-olivine cumulate. Varying proportions of cumulus diopside, olivine, magnetite, and plagioclase form finer layers, 1 to 50 cm thick; hornblende is present as an accessory mineral. Primary structural features include modal layering, crystal-size layering, and rare basinlike structures. The intrusive sequence, which crosscuts and contains xenoliths and pendants of the layered sequence, consists, in ascending stratigraphic order, of layered olivine-clinopyroxene cumulate, olivine-clinopyroxene cumulate, intrusive feldspathic pyroxenite, olivine cumulate and dunite, and gabbro. The rocks are composed of varying proportions of diopside, olivine, magnetite, plagioclase, and hornblende; pyrrhotite, chalcopyrite, and pyrite occur in trace amounts, and the rocks are altered to combinations of serpentine, magnetite, epidote, carbonate and zeolite minerals, and hydrogarnet. Neither sequence contains orthopyroxene. The general crystallization order is either olivine, magnetite, or both first, followed by diopside or plagioclase with continued crystallization of olivine and magnetite, and, lastly, followed by hornblende. Diopside compositions, which range from $En_{42.3}$ to $En_{49.4}$, from $Fs_{3.6}$ to $Fs_{11.3}$, and from $Wo_{44.9}$ to $Wo_{51.3}$, are the same in the two sequences, and the variations in composition show no trends within the sequences or individual map units. Some of the variation in Wo content is related to the volume of cumulus plagioclase. The 100Mg/(Mg+Fe^{2+}+Mn+Ni) ratio in olivine ranges from 70.2 to 83.1. The NiO content of olivine is similar in both sequences and unrelated to 100Mg/(Mg+Fe^{2+}+Mn+Ni) ratio. In the layered sequence, the Fs content of clinopyroxene is inversely related to 100Mg/(Mg+Fe^{2+}+Mn+Ni) ratio, and increasing magnetite content correlates with an increase of this ratio in olivine. Similar relations, however, are not readily apparent in the intrusive sequence. Plagioclase composition ranges from about An_{62} to An_{94}. Hornblende content varies spatially in the pluton and is highest near the intrusive contact with the country rocks along the northern margin of the pluton.

Major-element chemistry of the rocks reflects the variations in mineral proportions; however, ultramafic rocks of the layered sequence are richer in TiO_2 than those of the intrusive sequence. In general, TiO_2, V, Co, Ni, and Cr contents tend to increase with increasing MgO content in both sequences, and Co, Ni, and Cr contents tend to increase in individual rock units from oldest to youngest in the order of emplacement for the intrusive sequence. The spatial distribution of copper (samples containing more than 150 ppm Cu) correlates with that of hornblende. Pt and Pd contents of the rocks range from less than 10 to 230 ppb and from less than 1 to 47 ppb, respectively. Rh content ranges from less than 1 to 13 ppb, and Ir and Ru contents are less than 20 and 100 ppb, respectively.

A reconnaissance soil geochemical survey, based on data from hand-augered holes, showed that Pt content ranges from 17 to 181 ppb and averages 70 ppb, with a standard deviation of 48 ppb. Pd content ranges from less than 1 to 33 ppb and averages about 3 ppb, with a standard deviation of 6 ppb. Both platinum and palladium are enriched in soils, on average, about twice over their protolith. Platinum is enriched as much as 7 times over its protolith, and palladium as much as 4 times.

Consideration of the platinum-group-element (PGE) geochemical surveys and the evidence for absence of sulfur saturation in the subalkaline to alkaline magmas from which

Manuscript approved for publication, November 6, 1991.

the Lower Coon Mountain pluton crystallized suggest a low probability for a large-tonnage, high-grade PGE deposit associated with the pluton.

INTRODUCTION

The Lower Coon Mountain pluton forms a sill-like mass consisting of mafic and ultramafic rocks that crop out over an area of about 8 to 9 km^2 at the west end of Lower Coon Mountain, approximately 6 km south of Gasquet in Del Norte County, northern California (fig. 1). Cater and Wells (1953) identified this mass as a wehrlite, described its sill-like characteristics, and separated it from other ultramafic rocks in the Gasquet quadrangle. Later mapping and reconnaissance petrologic studies by Harper (1980a, b) clarified the regional and contact relations of the pluton, described some of the petrologic variations, and identified the pluton as most similar to Alaskan-type or concentrically zoned ultramafic plutons. The report by Logan (1919) on platinum associated with gold placers in Tertiary and Holocene gravels on Lower Coon Mountain, in Coon Creek, and in Craigs Creek, in combination with the information generated by Harper (1980a, b), resulted in our initiation of a platinum-group-element (PGE) resource investigation of the pluton and adjacent country rocks. Earlier publications included a geologic map by Gray and Page (1985) and a geochemical map of the platinum and palladium contents of soils (Page and Gray, 1985). A brief overview of the PGE geochemistry of the pluton in comparison with that of other similar plutons in the Klamath Mountains was given by Gray and others (1986).

The purpose of this report is (1) to describe the geologic features, petrologic and mineralogic details, and geochemistry of the Lower Coon Mountain pluton; (2) to evaluate the potential for PGE resources; and (3) to compare the pluton with others of the same type. An aeromagnetic model for the pluton was constructed from the data of Griscom (1984).

Acknowledgments.—This study is based on more than a man-year of field mapping and sampling during 1981 to 1983, assisted by James B. Barnard in 1981, Lars D. Page in 1982, and Michael Grubensky in 1983.

REGIONAL GEOLOGIC SETTING

The Klamath Mountains province of northern California and southwestern Oregon is composed of accreted terranes that were divided by Irwin (1964, 1972) into four arcuate lithologic belts bounded by east-dipping faults (fig. 2); these belts are the eastern Klamath, central metamorphic, western Paleozoic and Triassic, and western Jurassic. Subsequently, the belts were subdivided by Blake and others (1982) into tectonostratigraphic terranes that record the development of oceanic crust and upper mantle and volcanic island arcs from Paleozoic through Jurassic time. Within the western Jurassic belt, the Smith River subterrane (Silberling and others, 1984) contains the Lower Coon Mountain pluton.

The Smith River terrane includes the Josephine ophiolite and conformably overlying chert, shale, argillite, flysch, and volcaniclastic rocks. The Smith River terrane was interpreted by Saleeby and others (1982) to represent the remnants of a marginal basin formed by backarc extension about 157 Ma. The Josephine ophiolite, which contains all the rock units of a complete ophiolite sequence, has been most recently investigated by Harper (1980a, b), Smith and others (1982), Evans (1984), and Gray and others (1986). The rocks overlying the ophiolite were regarded by Cater and Wells (1953) to be correlative with the Galice Formation of southwestern Oregon. Both contain the same bivalve fossils and are of a similar age (Harper, 1980b); however, the type Galice overlies a sequence of andesitic volcanic flows, tuff breccia, tuff, and volcaniclastic rocks, is overlain by a sequence of waterlain tuff and breccia, and is not physically and stratigraphically linked to the relatively younger shale, mudstone, and sandstone of the shale of Illinois Valley that are continuous with rocks overlying the Josephine ophiolite (Smith and others, 1982). The Lower Coon Mountain pluton intrudes rocks that overlie the ophiolite, and is, in turn, cut by dikes. The minimum age of the pluton is 142 Ma, based on a concordant U-Pb age on a crosscutting granodiorite dike (Saleeby and others, 1982).

The Lower Coon Mountain pluton occupies the central part of a syncline that plunges gently southeast, as defined by mapped patterns of contacts between sedimentary and volcanic country rocks. Evans (1984) stated that poles to bedding define a β axis that plunges 10° N., whereas poles to cleavage and axial planes of folds define a β axis plunging 20°, S. 10° E., that is similar to the mapped pattern of the rocks.

GEOLOGY

Shape, Size, and Contact Relations

In plan, outcrops of the Lower Coon Mountain pluton outline an irregular, rounded to subrounded, rectangular area with an arm-shaped segment to the south, pointing southwest (pl. 1). The rectangular area has maximum dimensions of 2.4 by 3.2 km, and the arm-shaped area of 1.3 by 0.3 km. Cross-section interpretations suggest a maximum thickness of 600 to 900 m for the rectangular, dish-shaped mass. This estimate for the thickness of the sheet is larger than both the 290 m reported by Cater and Wells (1953) and the 300 m suggested by Harper

(1980a). Aeromagnetic modeling studies imply that the pluton is as much as 610 m thick, but that most of it is quite thin

Two distinct sequences of rocks form the pluton: a layered sequence of ultramafic cumulates and an intrusive sequence of crosscutting mafic to ultramafic rocks. On the basis of this simplified petrologic subdivision and the faulting of the pluton, the pluton can be divided into four petrologic-structural segments (fig. 3): (1) a northern segment, (2) a southwestern segment, (3) a southeastern segment, and (4) a Haines Flat segment. These artificial subdivisions, in combination with the geologic map and cross sections (pl. 1), are used here to discuss the structural and spatial geometry of the pluton.

The northern segment consists predominantly of rocks of the intrusive sequence. Its south boundary is marked by a steeply dipping contact that crosscuts layering planes in ultramafic rocks of the layered sequence (pl. 1; fig. 3). The east boundary of this segment consists of a steeply west-dipping normal fault, with an overlying cover of Tertiary gravel deposits. Observed contacts between the pluton and country rocks on the north and northwest boundaries, and the intersection of the mapped contact and topography, demonstrate that the contact dips shallowly 20°–30°

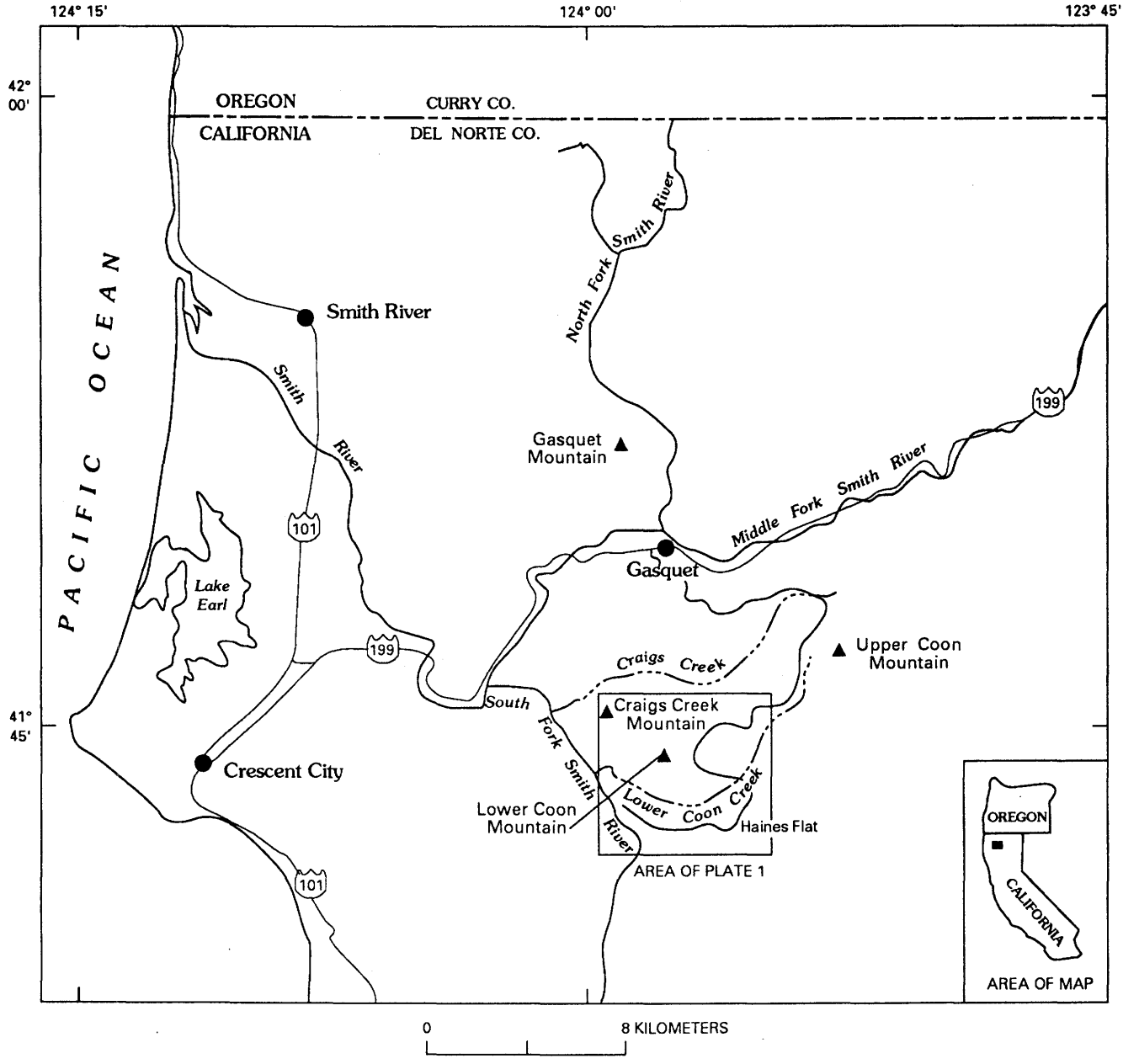

Figure 1. Index of map of northern California, showing location of the Lower Coon Mountain study area.

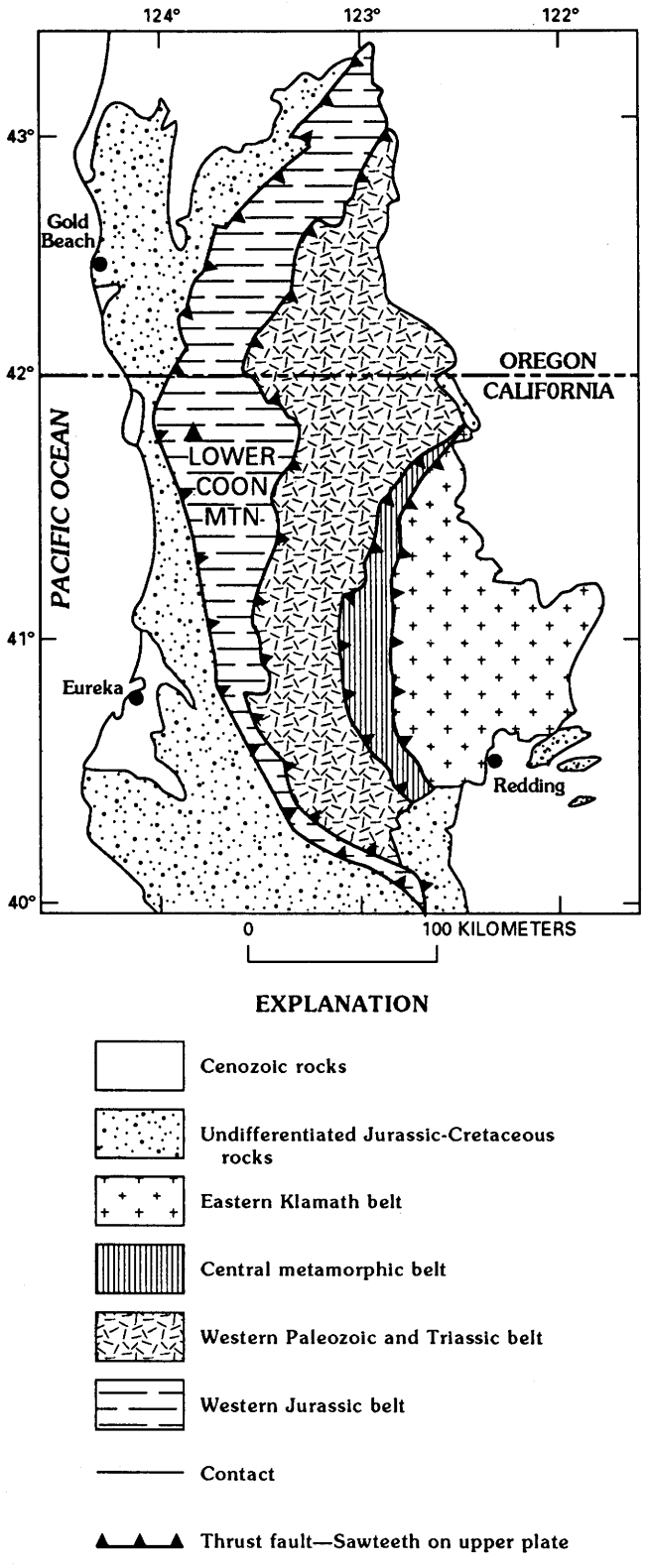

Figure 2. Schematic map of part of the Klamath Mountains province, Calif. (from Irwin, 1972), showing regional geologic and tectonic setting of the Lower Coon Mountain pluton.

inward, generally south and southeast, toward the center of the pluton. The rest of the north boundary is marked by a southwest-dipping fault. The external contact of the pluton appears to be semiconcordant with bedding in the sedimentary rocks. In the immediate vicinity of this contact, the sedimentary rocks have been metamorphosed to hornfels and amphibolite, and locally rocks of the intrusive sequence are fine grained near the margin. Within the northern segment are pendants(?) or inclusions of ultramafic rocks of the layered sequence.

The southwestern segment (fig. 3) consists of ultramafic rocks of the layered sequence, cut by a mass of the intrusive sequence (pl. 1). Its irregular north boundary is marked by a contact between the layered sequence and the intrusive sequence of the northern segment. A steeply dipping, northeast-trending fault marks the east or southeast boundary of this segment of the pluton, which on the southwest is in contact with shale and mudstone. On the basis of the map pattern, the southwest contact of the layered sequence dips 20°–30° NE., whereas the internal layering of this sequence strikes northwest and dips 50°–70° NE. The discordance between the attitude of internal layering and the external contact of the pluton suggests two alternative explanations. One explanation is that the southwest contact is a shallow, northwest-dipping fault, possibly formed by slippage along this incompetent plane during the development of the syncline. Another explanation is

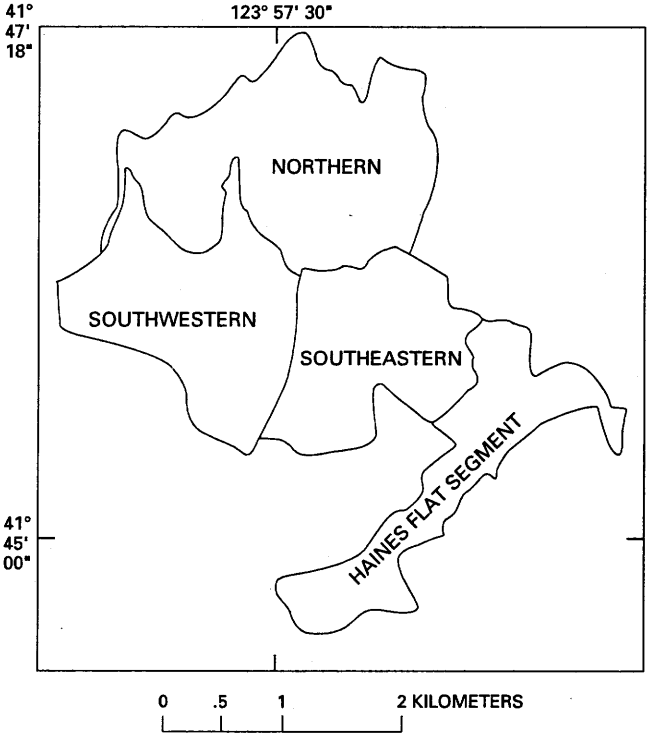

Figure 3. Sketch map showing petrologic-structural subdivisions of the Lower Coon Mountain pluton.

that the internal layering did not develop in a subhorizontal position. Absence of exposures, heavy brush in the area of the contact, and deep weathering of the shale have prevented a solution to this problem. The mass of the intrusive sequence exhibits a crosscutting, steeply dipping contact with the layered sequence and has a contact with country rocks that can be interpreted as steeply dipping.

The southeastern segment (fig. 3) consists of rocks of the layered sequence. It is bounded on the west and, in part, on the northeast by steeply dipping faults. Its north boundary is marked by a contact with the intrusive sequence. One part of the southeast boundary is marked by a steeply dipping contact with the intrusive sequence, and the other part by a contact between the intrusive sequence and country rocks. This contact dips shallowly (15°–30°) northwest, and internal layering of the pluton dips 15°–25° NW.; thus, no discordance exists between the pluton and bedding in the country rocks. Also, locally near this contact, hornfels and amphibolite are exposed.

The Haines Flat segment (fig. 3), an arm-shaped area, consists of rocks of the intrusive sequence. Its northwest boundary consists of two parts separated by a northwest-trending fault (pl. 1). The northeastern part of this boundary is marked by a relatively steeply northwest-dipping intrusive contact with the layered sequence; the southwestern part is marked by a southerly dipping contact between the pluton and country rocks. The northeast boundary is marked by a 20°–30° SW.-dipping contact between the pluton and country rocks. The west boundary is marked by a steeply east-dipping contact between the pluton and country rocks. The southwest boundary is marked by a similar contact that dips relatively steeply south, away from the pluton. Irregular apophyses of the intrusive sequence (gabbro) into metavolcanic country rocks form a complex, irregular contact along part of the southwest boundary. Cross-section interpretations (pl. 1) suggest that the Haines Flat segment does not extend southeastward under the country rocks any great distance, but that southwest and northwest contacts are connected in the subsurface. In general, the external contact of the Lower Coon Mountain pluton dips 15°–30° inward toward the pluton, except where it has been modified by faulting. Internal layering and contacts within the layered sequence dip shallowly and are generally concordant with this external contact. Contacts between the layered sequence and the intrusive sequence dip more steeply.

Composition by Unit and Stratigraphic Terminology

The subdivision of the Coon Mountain pluton into a layered sequence of ultramafic cumulates and an intrusive sequence of mafic to ultramafic rocks is further refined here, so that the bulk composition of the pluton by rock unit can be examined in some detail. The layered sequence consists of two units that are repetitively interlayered: clinopyroxene-olivine cumulate and plagioclase-rich clinopyroxene-olivine cumulate. Both units locally contain discontinuous, magnetite-rich cumulate layers. The intrusive sequence consists of five units, from oldest to youngest: layered olivine-clinopyroxene cumulate, olivine-clinopyroxene cumulate, intrusive feldspathic pyroxenite, olivine cumulate and dunite, and gabbro. Of the total area of outcrop of the Lower Coon Mountain pluton, about 52 percent is underlain by the layered sequence. The distribution of units in the outcrop area of the pluton is summarized in table 1.

The southeastern and southwestern segments, which consist of rocks of the layered sequence, are underlain by differing proportions of clinopyroxene-olivine cumulate and plagioclase-rich clinopyroxene-olivine cumulate. Although these two segments contain inverse amounts of the units, the overall outcrop area of clinopyroxene-olivine cumulate is about equal to that of plagioclase-rich clinopyroxene-olivine cumulate. Layered olivine-clinopyroxene cumulate of the intrusive sequence underlies the next largest area, and olivine-clinopyroxene cumulate is the next most abundant. All other rocks of the intrusive sequence, mostly gabbro, compose only 7.2 percent of the total outcrop area of the pluton.

Stratigraphy

Country Rocks

The Lower Coon Mountain pluton intrudes shale, mudstone, sandstone, and, locally, volcanic rocks, which are continuous with those of the shale of Illinois Valley of southwestern Oregon (Smith and others, 1982). Harper (1980a, b) described these rocks in some petrologic detail and believed that they were correlative with the Galice Formation. Near the immediate contact of the pluton, shale, mudstone, or sandstone protoliths were metamorphosed to phyllite, slaty shale, and hornfels. Locally, as shown on plate 1, the protoliths were andesitic to basaltic volcanic flows and breccias. Some of the more phyllitic shale near the contact contains biotite, chlorite, and epidote as metamorphic minerals, whereas the hornfels of both sedimentary and volcanic protoliths contains green-brown hornblende, epidote, plagioclase, quartz, chlorite, and tremolite-actinolite. Some of the chlorite and the tremolite-actinolite developed later than the other minerals. Locally, very near the contact, some of the hornfels contains a clear, untwinned clinopyroxene. Thus, the grade of contact metamorphism may have locally reached pyroxene hornfels facies but apparently is more commonly no higher than hornblende hornfels facies.

Table 1. Percentage of outcrop area by unit

Unit (fig. 4)	Number of points	Percentage of outcrop area	Outcrop area (km^2)
Intrusive sequence			
Jg	136	5.59	0.490
Jo	9	.37	.032
Ji	29	1.19	.104
Joc	415	17.05	1.494
Jl	584	23.99	2.102
Layered sequence			
Jp	629	25.84	2.264
Jc	625	25.68	2.250
Mt[1]	7	.29	.025
Total	2,434	100.00	8.761

[1]Magnetite layers.

Lower Coon Mountain Pluton

The rocks of the Lower Coon Mountain pluton are here discussed in two major sequences, layered and intrusive, and in relative age from oldest to youngest. The pluton is characterized by a general absence of orthopyroxene in the igneous rocks. Stratigraphic and intrusive relations in the pluton are illustrated in figure 4, where the diagrammatic section represents a combination of all cross sections and the geologic map (pl. 1), and the proportions of rock units are similar to those outlined in table 1. The following discussion focuses on the definition of units, their distribution, thickness, lithology, contact relations, and primary structures. Petrologic and chemical characteristics are described in later sections.

The Layered Sequence

Repetitive units of clinopyroxene-olivine and plagioclase-rich clinopyroxene-olivine cumulates form and define the layered sequence. The clinopyroxene-olivine cumulate contains less than 1 volume percent plagioclase and accessory amounts of hornblende and magnetite. Varying proportions of clinopyroxene, olivine, and magnetite form layers, 1 to 50 cm thick, that are locally characteristic of this unit (figs. 5*A*, 5*B*). The plagioclase-rich clinopyroxene-olivine cumulate contains more than 10 and as much as 40 volume percent plagioclase, as well as hornblende and magnetite as accessory minerals. Modal variations in the proportions of cumulus clinopyroxene, olivine, and plagioclase form layers from less than 1 to 50 cm thick (fig. 5*C*). Thin, discontinuous, and lenslike along strike, magnetite-rich layers occur in both cumulate units. Rocks of the layered sequence occur in all four segments of the pluton (pl. 1, fig. 3) but are most abundant in the southwestern and southeastern segments. Comparison of columnar sections constructed from the geologic map for the different segments shows variations in the thickness, proportion, and relative position of the repetitive units of clinopyroxene-olivine cumulate and plagioclase-rich clinopyroxene-olivine cumulate (fig. 6). Layers of clinopyroxene-olivine cumulate range in thickness from about 13 to as much as 625 m; layers of plagioclase-rich clinopyroxene-olivine cumulate range in thickness from about 13 to as much as 457 m, excluding the covered area in the southeastern segment. Evidently, the proportions of these two cumulates differ between segments, as do their relative positions. In two segments, the plagioclase-rich clinopyroxene-olivine cumulate has an external contact with the country rocks; and in the southwestern segment, where this contact could be a fault, the clinopyroxene-olivine cumulate is in contact with the country rocks. Within the layered sequence, contacts between the two cumulate units are defined by a rapid increase in the proportion of plagioclase mesoscopically visible in the rocks.

Primary structural features include modal layering, crystal-size layering, and relatively rare basinlike structures. Both the modal and crystal-size layering appear to be lensoidal, are discontinuous along strike, and are not traceable for distances of more than tens of meters. However, mostly poor outcrops may bias this observation.

The Intrusive Sequence

Ultramafic and mafic rocks of the intrusive sequence crosscut each other and the layered sequence (fig. 4). Crosscutting features include discordant contacts with layering, dikes and apophyses, fine-grained margins, xenoliths and pendants, and intrusive breccias. The oldest units are ultramafic, and the youngest unit is mafic.

Layered Olivine-Clinopyroxene Cumulate

Most exposures of the layered olivine-clinopyroxene cumulate occur in the northern and Haines Flat segments of the pluton, but an isolated large mass occurs in the southwestern segment. Besides its characteristic lithology, the unit displays a strong foliation, in part due to the proportions of olivine and clinopyroxene but also to the planar alignment of clinopyroxene (fig. 7*A*). The outcrop width of the unit, perpendicular to layering, is more than 457 m, but because of the generally steeply dipping foliation, outcrop patterns, and inferences from aeromagnetic models, a true thickness cannot be determined, and depending on the origin of the layered rock, such estimates

may be inappropriate. The layered olivine-clinopyroxene cumulate intrudes with angular discordance the layered sequence and contains pendants of clinopyroxene-olivine cumulate, the largest of which is in the northern segment (pl. 1). The layered olivine-clinopyroxene cumulate is, in turn, cut by all younger units of the intrusive sequence.

Olivine-Clinopyroxene Cumulate

The olivine-clinopyroxene cumulate is massive and exhibits only rare foliation; it varies only slightly in the proportion of olivine to clinopyroxene. The unit is most abundant in the northern and Haines Flat segments of the pluton (pl. 1). No thickness can be assigned to the unit, but it has an outcrop width of as much as 1,433 m in the Haines Flat segment. Locally, intrusion of the olivine-clinopyroxene cumulate into layered olivine-clinopyroxene cumulate has produced an intrusion breccia.

Intrusive Feldspathic Pyroxenite

The intrusive feldspathic pyroxenite has been mapped only in the northern segment of the pluton as one relatively small mass, but it may be more common than as mapped (pl. 1). The unit contains varying amounts of plagioclase, from 49 to as much as 81 volume percent, and

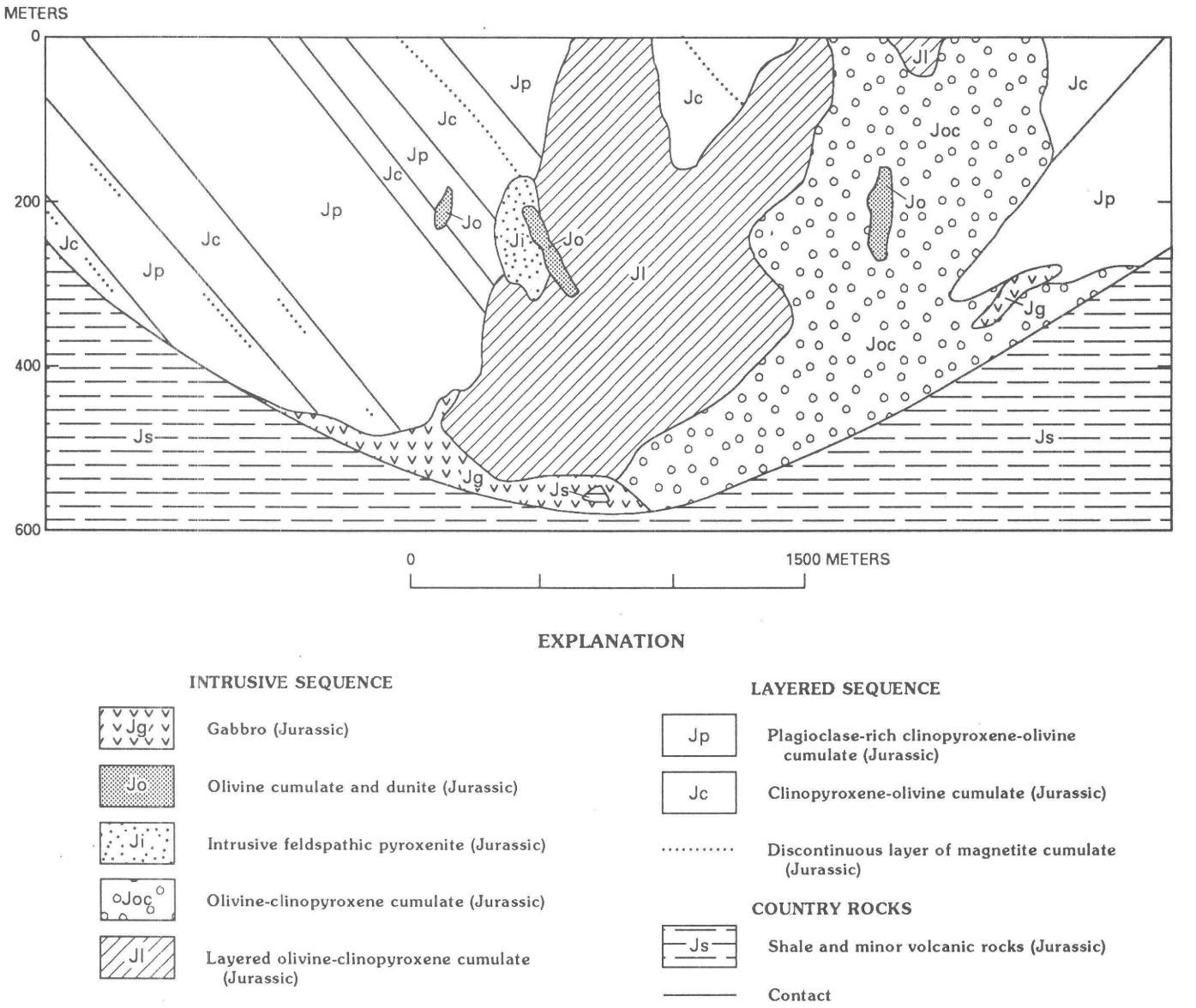

Figure 4. Diagrammatic reconstructed cross section showing stratigraphic and intrusive relations in the Lower Coon Mountain pluton.

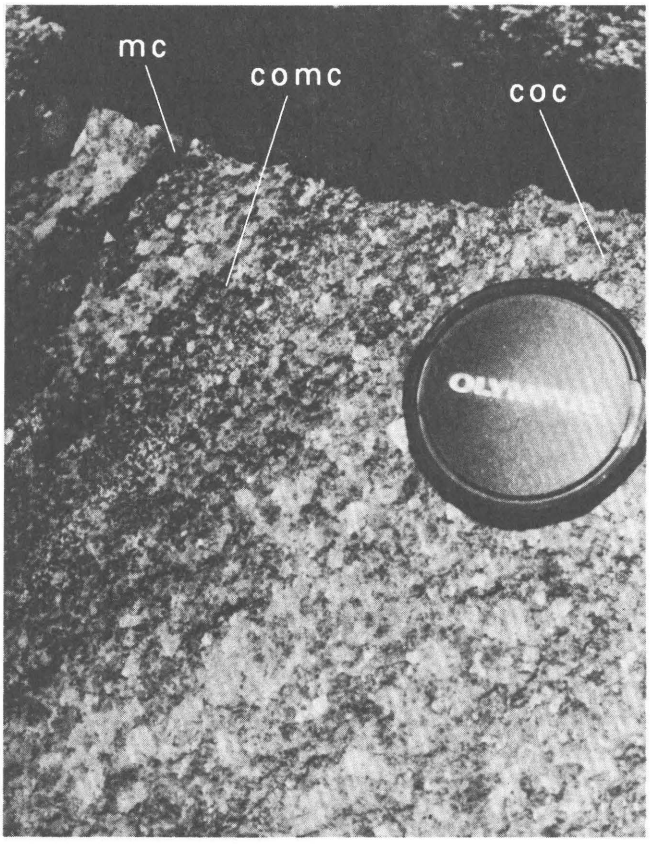

A

its texture and mineralogy vary rapidly over small areas. Some hand specimens resemble the plagioclase-rich clinopyroxene-olivine cumulate, whereas others are similar to the gabbro. Poor exposures in some areas prevent the identification of these rocks as a separately mappable unit. The intrusive feldspathic pyroxenite appears to intrude only the layered sequence (fig. 7*B*) and the layered olivine-clinopyroxene cumulate, and it is intruded only by olivine cumulate and dunite, and gabbro. Locally, its contacts, such as that with plagioclase-rich clinopyroxene cumulate, are gradational, and elsewhere against other units they are sharp.

Olivine Cumulate and Dunite

The olivine cumulate and dunite occur as irregular pods (fig. 7*C*) and lensoid and pipelike masses intruding all rock units except the gabbro, and in all segments of the pluton (pl. 1) except the southwestern segment. Masses range in size from centimeter scale to as large as 183 by 91 m; many are subrounded to rounded. Locally, the dunite contains xenoliths of pyroxenite in which the fragments are rounded (fig. 7*D*). The larger masses tend to be entirely olivine cumulate—that is, they contain large poikilitic clinopyroxene crystals and minor interstitial plagioclase—and the smaller masses to be entirely dunite that is clinopyroxene and plagioclase free.

B

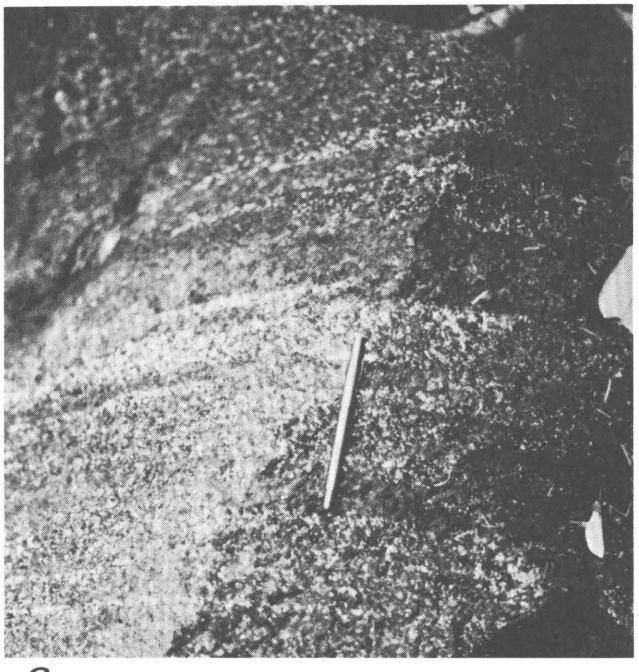

C

Figure 5. Features in rocks of the layered sequence. *A*, Layering formed by variation in proportions of clinopyroxene, olivine, and magnetite. Coc, clinopyroxene-olivine cumulate; comc, clinopyroxene-olivine-magnetite cumulate; mc, magnetite cumulate. Lens cap is 5 cm in diameter. *B*, Layer of olivine cumulate (oc) in clinopyroxene-olivine cumulate. Hammer is 38 cm long. *C*, Layering formed by variation in proportions of clinopyroxene (dark) and plagioclase (light). Pen is 14 cm long.

Gabbro

The gabbro is essentially confined to the margins of the pluton, except for two occurrences in the southeastern and Haines Flat segment in which the gabbro occurs between other units. The unit varies in texture, grain size, and mineral proportions, and it is locally layered or foliated. The fact that it exhibits contacts with all other units demonstrates that it is the youngest rock, except in one area in the northern segment (pl. 1) where poor outcrops and steep hillslopes make a contact with olivine cumulate and dunite equivocal. Where the gabbro intrudes clinopyroxene-olivine cumulate, it produces extensive intrusion breccias (fig. 8). In general, the gabbro appears to represent a relatively younger, marginal facies of the Lower Coon Mountain pluton.

Postplutonic Intrusive Rocks

Mineralogically, at least two rock types form dikes that intrude the Lower Coon Mountain pluton and adjacent country rocks but are not mapped separately on plate 1: hornblende diorite, and basalt to andesite. Both rock types locally contain xenoliths of mafic to ultramafic rocks of the pluton. The dikes tend to be discontinuous along strike and to strike northeast or northwest; they range from tens of centimeters to about 10 m in thickness.

The hornblende diorite dikes have an inequigranular to equigranular, fine- to medium-grained texture, although local variants are porphyritic. The rock consists of greenish-brown to brown, subhedral to euhedral hornblende and anhedral to subhedral, blocky to tabular plagioclase; locally, sphene, apatite, quartz, magnetite, and sulfide minerals are

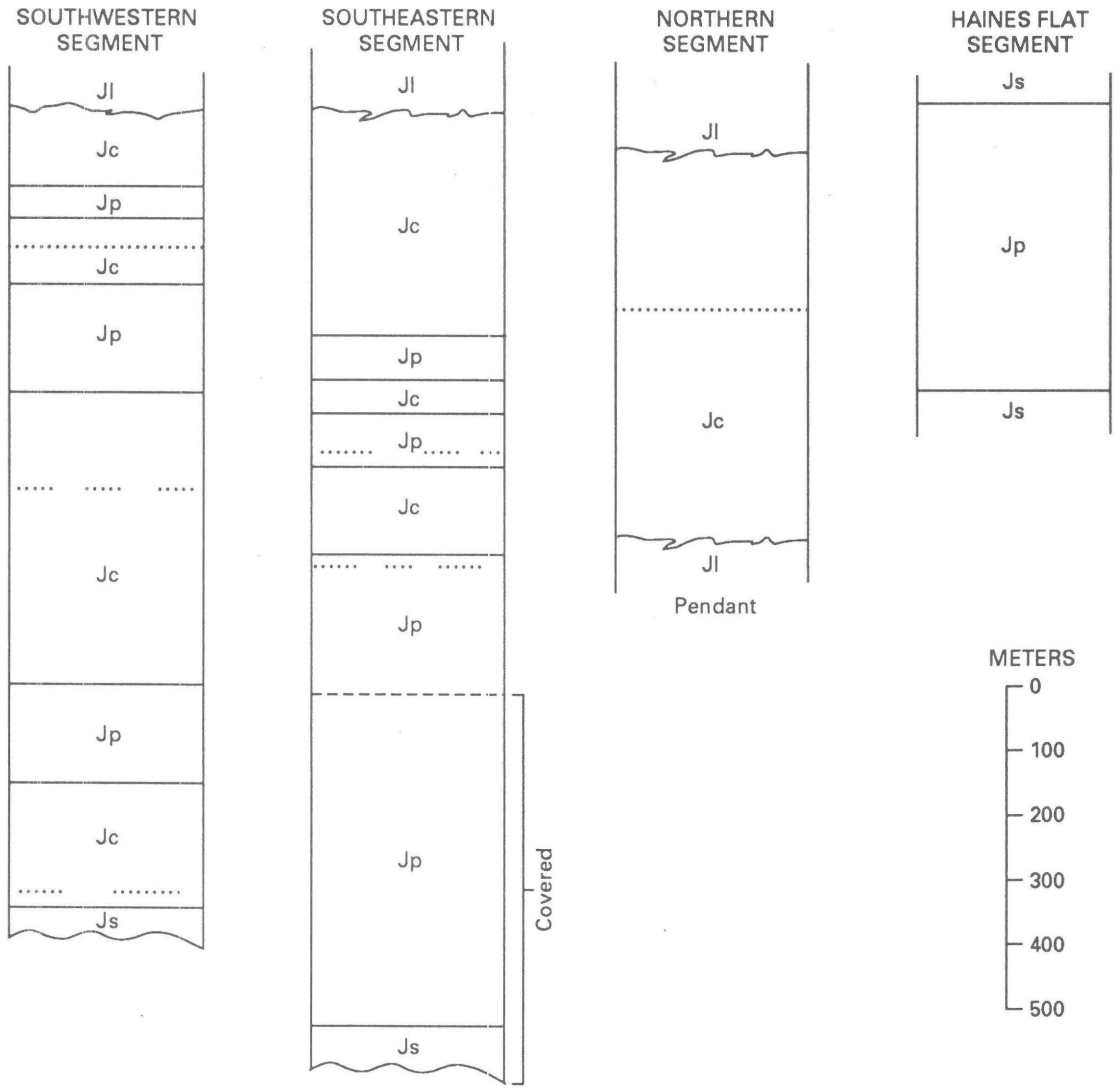

Figure 6. Columnar sections of the layered sequence of the Lower Coon Mountain pluton. Same symbols as in figure 4. Contact between units Jc and Jl is intrusive.

accessory minerals. One dike contained small clots (approx 1 mm diam) of sulfide minerals composed of pyrite, chalcopyrite, bornite, and chalcocite. Plagioclase is commonly altered to chlorite, epidote, and sericite; and brown hornblende is locally altered to bluish-green hornblende and actinolite-tremolite.

The basalt to andesite dikes consist of phenocrysts of clinopyroxene or of clinopyroxene and hornblende in a fine- to medium-grained groundmass of plagioclase and hornblende. The plagioclase generally is extremely altered to chlorite, sericite, and epidote-group minerals. In some samples, brown hornblende forms anhedral to subhedral crystals intergrown with plagioclase to form the groundmass. Clinopyroxene phenocrysts are twinned and zoned. Opaque minerals are accessory constituents of the rocks. Some of this rock in dikes that intruded the country rocks, shale, and hornfels resembles gabbroic rocks of the pluton and may be related to the magmas that formed part of it. However, the absence of exposures prevents a solution to the problem of their relation to the pluton, except where some variants cut parts of the pluton and contain xenoliths of rocks of the pluton.

Quaternary and Tertiary Deposits

Aside from a thin but extensive soil, broken weathered rock, and colluvium, parts of the pluton are covered by Tertiary gravel and Quaternary alluvial and landslide deposits (pl. 1). According to Cater and Wells (1953,

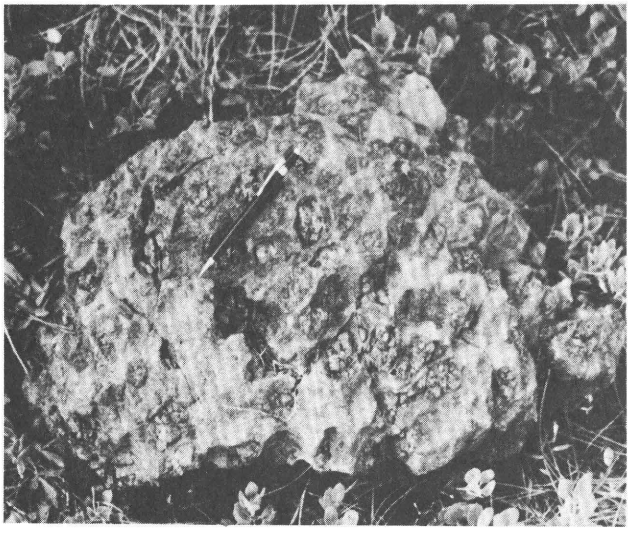

A

B

C

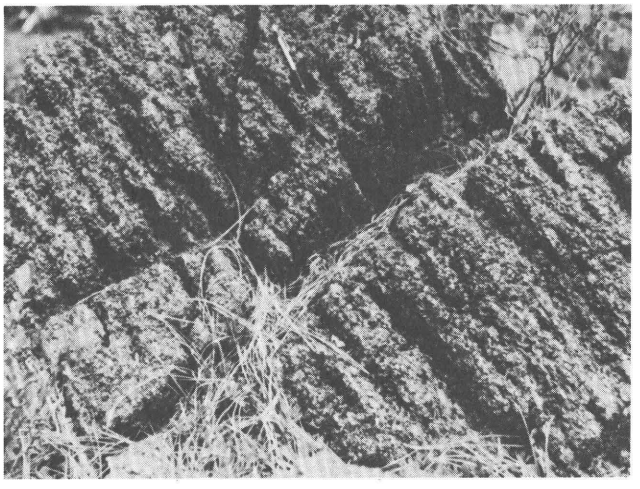

D

Figure 7. Features in rocks of the intrusive sequence. *A*, Modal layering in layered olivine-clinopyroxene cumulate; more deeply etched layers are olivine rich. *B*, Xenoliths of layered olivine-clinopyroxene cumulate (dark) in intrusive feldspathic pyroxenite. *C*, Dunite (du, outlined) pod crosscutting olivine-clinopyroxene cumulate. *D*, Intrusion breccia consisting of rounded clinopyroxene cumulate fragments in dunite. Pen is 14 cm long.

p. 104–105), the Tertiary gravel on Lower Coon Mountain (east side of the northern segment) and on Haines Flat (pl. 1) is post-late Miocene in age because, elsewhere, gravel-filled channels cut into upper Miocene sedimentary rocks. The gravel is poorly sorted, ranges in size from clay to boulders (max 0.3 m diam), and includes a wide variety of rock types. Quaternary alluvial deposits are of minor extent in the study area and have not been mapped. One large landslide deposit that occurs in the southeastern segment covers the contact of the pluton with country rocks.

Structure

Relatively steeply dipping faults are the major postintrusion features that were observed. Cater and Wells (1953) and Harper (1980a, b) both showed the Lower Coon Mountain pluton as a thin, rootless body. Evans (1984) mapped a thrust contact around the pluton; however, we observed little evidence for the existence of this fault in the immediate vicinity of the pluton. Some minor folds were reported by Harper (1980a) in the country rocks; crenulated, foliated, crinkled shale, and mudstone, were observed in float. There is little evidence, except for the semiconformable contacts of the pluton with country rocks, to relate the timing of emplacement of the pluton to the time of formation of the larger syncline that it intruded.

Faults

There are two sets of faults, one striking northeast and the other striking northwest (pl. 1). Dips on the northeast-striking set range from 55° SE. to 65° NW., and on the northwest-striking set from 50° SW. to 60° NE. Where determinable, offset on the faults appears to be as much as 100 m. The northeast-striking fault between the southwestern and southeastern segments (pl. 1; fig. 3) shows an offset of the contact between layered olivine-clinopyroxene cumulate and clinopyroxene-olivine cumulate of about 60 m. However, correlations between units of the layered sequence in these two segments are difficult on the basis of thickness or other characteristics. This fault may have been active before the emplacement of the intrusive sequence, and so the offset observed between the two sequences may result from reactivation along this fault.

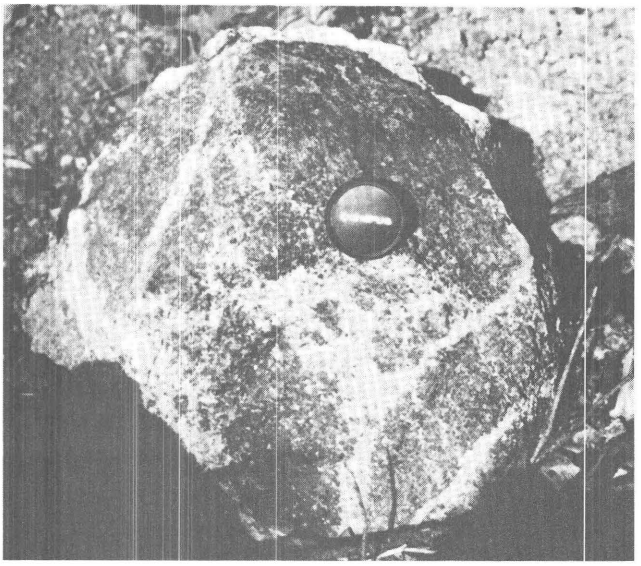

Figure 8. Gabbro (light) intruding and brecciating clinopyroxene-olivine cumulate (dark). Lens cap is 5 cm in diameter.

Aeromagnetic Model

An aeromagnetic map (fig. 9) encompassing the Lower Coon Mountain pluton is available from a 1977 survey (Griscom, 1984) at a scale of 1:62,500. Traverses were oriented east-west at a spacing of 0.8 km and were flown at an elevation of 1,200 m above sea level. This elevation was 305 to 800 m above the topography of the exposed part of the pluton. Contour intervals on the map are 25 and 100 nT. An average regional field of 53,038 nT plus a regional trend of 4.72 nT/km north and 2.78 nT/km east was removed from the data before contouring, on the basis of the International Geomagnetic Reference Field (IGRF) of 1975.

Magnetic-susceptibility measurements were made on a total of 22 rock samples collected from throughout the pluton, including all the major varieties of cumulate. Values ranged from 1×10^{-3} to 20×10^{-3} emu, with an average value of 6×10^{-3} emu (table 2). Multiplying this average by the local intensity of the Earth's main field (53,038 nT) gives an induced magnetization of 3.2×10^{-3} emu/cm^3. Remanent magnetizations were not measured on these samples, but data from similar rocks in California indicate that the remanent magnetization may be 25 to 50 percent of the induced magnetization. The total magnetization of these rocks (vector sum of the two magnetizations) thus may be approximately 4×10^{-3} to 5×10^{-3} emu/cm^3, assuming that the remanent component approximately parallels the Earth's present field. This large magnetization indicates that the pluton is highly magnetic because the sedimentary rocks surrounding the pluton are essentially nonmagnetic.

Examination of the aeromagnetic map shows a circular magnetic high, about 1.4 km in diameter and about 500 nT in amplitude, over the southwest quadrant of the pluton. A more important observation is that most of the pluton fails to display any substantial magnetic anomaly, even though the rocks are highly magnetic. We conclude that the pluton in the region of a negligible anomaly must generally be so extremely thin that it does not display a more extensive magnetic anomaly.

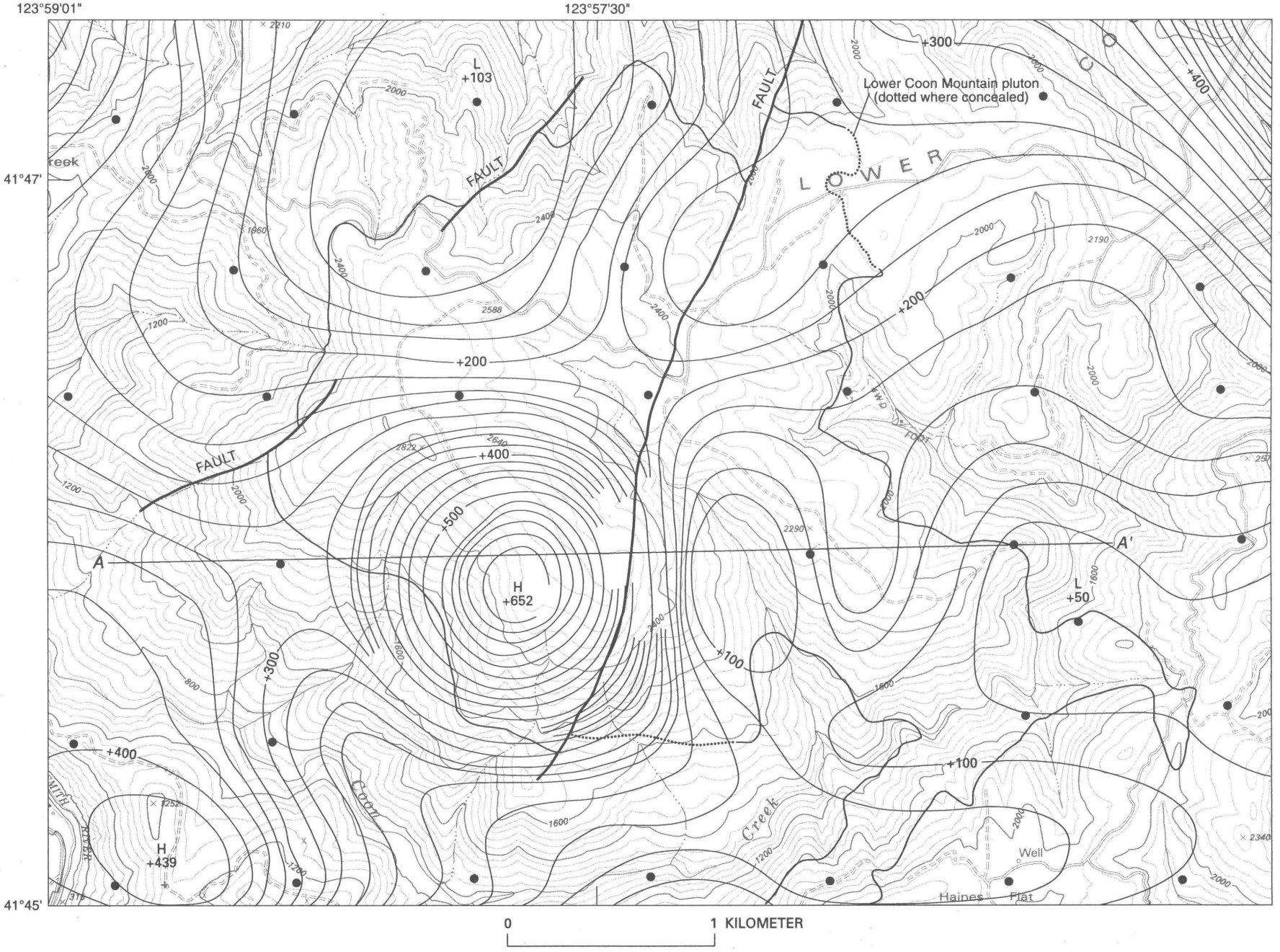

Figure 9. Aeromagnetic map of the Lower Coon Mountain pluton. Contours of total magnetic-field intensity in nanoteslas; contour interval, 25 nT. Dots, locations of east-west flightlines. Line *A*–*A*′ shows location of magnetic profile in figure 10. H, magnetic high; L, magnetic low. Base from U.S. Geological Survey 1:24,000–scale Gasquet (1981) quadrangle. Contour interval, 80 ft.

Table 2. Magnetic susceptibility of rock samples from the Lower Coon Mountain pluton

[Measured with a hand-held Scintrex SM—5 meter]

Sample	Susceptibility (10^{-3} cgs)		Comment
	Average	Range	
Layered olivine-clinopyroxene cumulate			
82CMG28	1.5	---	---
82CMG30	3.0	---	Small sample.
82CMG84	6.0	---	Small chip.
82CMG173	2.3	---	---
82CMG174	1.0	---	---
82CMG175	3.0	---	---
82CMG176	2.4	---	---
82CMG177	5.2	---	---
Clinopyroxene-olivine cumulate and plagioclase-rich clinopyroxene-olivine cumulate			
82CMP3	14	---	---
82CMP4	10	---	Small sample.
82CMP5	5.0	---	Small chip.
82CMP6	12	---	Small sample.
82CMP7	6.0	---	Small chip.
82CMP8	2.5	---	Small sample.
82CMP9	11	---	---
82CMG130	1.6	1.0–1.8	---
82CMG131	3.2	3.0–3.4	---
82CMG132	3.0	2.5–3.0	---
82CMG133	10.0	---	---
Olivine-clinopyroxene cumulate			
82CMP1	20	---	---
82CMP2	3.6	---	---
82CMP25	6.2	---	---
Average of 22 samples---	6.0	---	---

An east-west magnetic profile was selected that passes across the pluton through the crest of the magnetic high. The magnetic expression of a thin tabular model (fig. 10) lying beneath this profile was calculated by using program parameters that assumed the model to end 0.4 and 0.6 km to the north and south of the profile, respectively. These limiting distances are appropriate for the source of the circular magnetic high and do not significantly affect the calculation over the thinner parts of the model. It is additionally necessary to extract a reasonable residual profile from the original magnetic profile so as to isolate the magnetic effects of the Lower Coon Mountain pluton. In figure 10, there is a local magnetic anomaly that is caused by a nearby unrelated source body; this anomaly is then subtracted from the observed profile to produce the residual. This local unrelated anomaly is deduced from the contour map (fig. 9), where a linear, east-sloping, north-south-striking magnetic gradient can be observed through the west side of the circular magnetic high, both distorting the high and causing the saddle on the west edge of the high. The final datum for the residual profile is necessarily arbitrary and is reasonable, considering the form of the anomaly.

The model of the pluton (fig. 10) is mostly constructed within the geologic and topographic constraints. The upper surface of this model is the actual topography, and the bottom of the east half of the model is set at an elevation of 488 m, in agreement with the local elevations here of the external contact of the pluton. The bottom of the west tip of the model is set at an elevation of 610 m, also in agreement with the elevation of the contact of the pluton at this point. The model is thicker underneath the magnetic high over the west half of the model, to correspond to the magnetic high. A magnetization of 4.2×10^{-3} emu/cm^3 was used in the calculation, in accord with results from the sample measurements.

The general agreement between the model calculation and the observed magnetic profile is good, even including the small magnetic high over the east third of the model. Clearly, the pluton is very thin, and its contacts tend to follow the topographic contours because the pluton is relatively flat bottomed. The reality of the slightly thicker "root" beneath the magnetic high is less certain, although the vertical east boundary of this "root" at 2.6 km does correspond to a normal fault on the geologic map. Alternative explanations for that part of the magnetic high caused by the "root" could be that (1) the rocks are simply more magnetic beneath the high; or (2) the aircraft, unknown to us, flew somewhat lower as it went over the higher topography. The relatively complex structure and steep dips shown on the geologic map do not appear to agree with a very thin, flat-bottomed pluton and suggest that this flat bottom may be a later thrust fault at some depth from the surface of the pluton, although no evidence for this thrust has been observed in the field.

PETROLOGY

Most rocks of the Lower Coon Mountain pluton have cumulus textures and are dominated mineralogically by diopside-rich rocks. This section describes the petrography and mineralogy of these rocks by sequence and unit. Cumulus terminology is used to describe the rocks, but rock names using the classification of the International Union of Geological Sciences (IUGS Subcommission on the Systematics of Igneous Rocks, 1973) are included for comparative purposes. Some petrographic varieties, such as clinopyroxene-olivine cumulate, occur in both the layered and intrusive sequences but display different structures and textures.

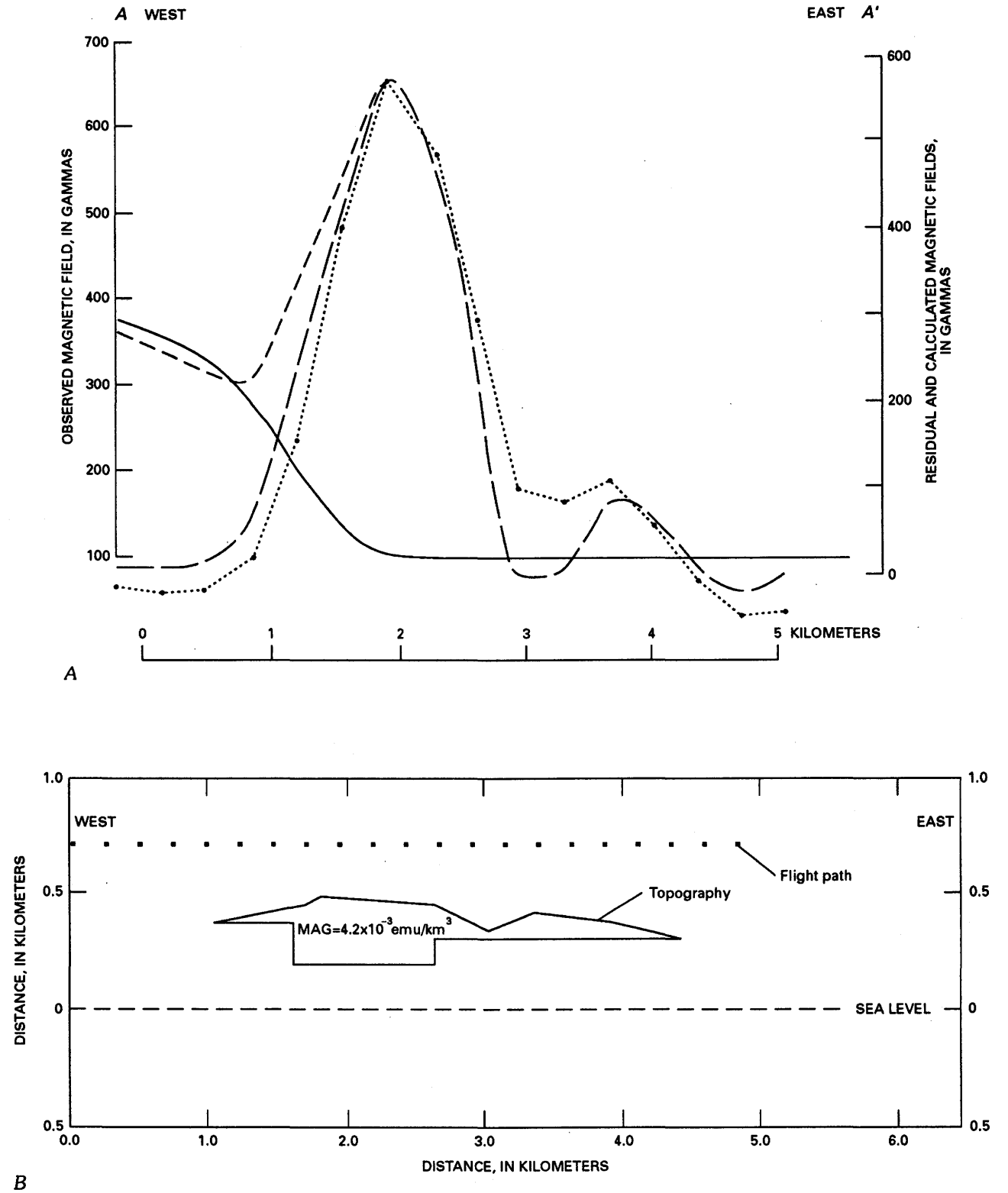

Figure 10. Calculated model for magnetic profile along line *A–A'* (fig. 9). *A*, Calculated and observed magnetic profiles. Short-dashed curve, observed magnetic field; long-dashed curve, residual magnetic field; dotted curve, calculated magnetic field; solid curve, local regional magnetic field. *B*, Magnetic model.

The Layered Sequence

Clinopyroxene-Olivine Cumulate

The clinopyroxene-olivine cumulate consists of both clinopyroxene-olivine cumulate and clinopyroxene-olivine-magnetite cumulate. Locally, the unit contains layers of clinopyroxene-magnetite cumulate and magnetite cumulate, both of which may locally contain traces of interstitial plagioclase (more than 0.5 volume percent) and minor to accessory amounts of brown hornblende. Modal data for samples of this unit are plotted in figure 11; figure 11*A* illustrates the absence of plagioclase in the unit. In the IUGS classification, samples of the clinopyroxene-olivine cumulate and the clinopyroxene-olivine-magnetite cumulate are mainly magnetite-bearing olivine clinopyroxenite; some samples are hornblende-bearing olivine-magnetite clinopyroxenite or olivine-magnetite-hornblende clinopyroxenite. The proportion of olivine to clinopyroxene ranges from about $Ol_{18}Cpx_{82}$ to $Ol_{40}Cpx_{60}$ and does not cluster around the proportion $Ol_{20}Cpx_{80}$ suggested by Irvine (1974) as the modal composition of cotectic precipitation for similar rocks in the Duke Island ultramafic complex, Alaska. Neither does the proportion of clinopyroxene to magnetite cluster near the proportion Cpx_{85} Mt_{15} suggested for coprecipitation, although the ratio of clinopyroxene plus olivine to magnetite ranges from about $(Cpx\text{-}Ol)_{85}$ Mt_{15} to $(Cpx\text{-}Ol)_{90}Mt_{10}$ and appears to be fairly constant for most samples of the clinopyroxene-olivine-magnetite cumulate.

Major minerals in the clinopyroxene-olivine cumulate are clinopyroxene (55–77 volume percent), olivine (15–38 volume percent), magnetite (0.2–15 volume percent), and brown hornblende (0.8–6 volume percent). Minor minerals are plagioclase, biotite, and pyrrhotite; secondary minerals include serpentine minerals, magnetite, tremolite-actinolite, epidote, chlorite, zeolite(?), and carbonates. Clinopyroxene texture ranges from anhedral, with interlocking grains forming mosaic-like patterns in some samples, to subhedral

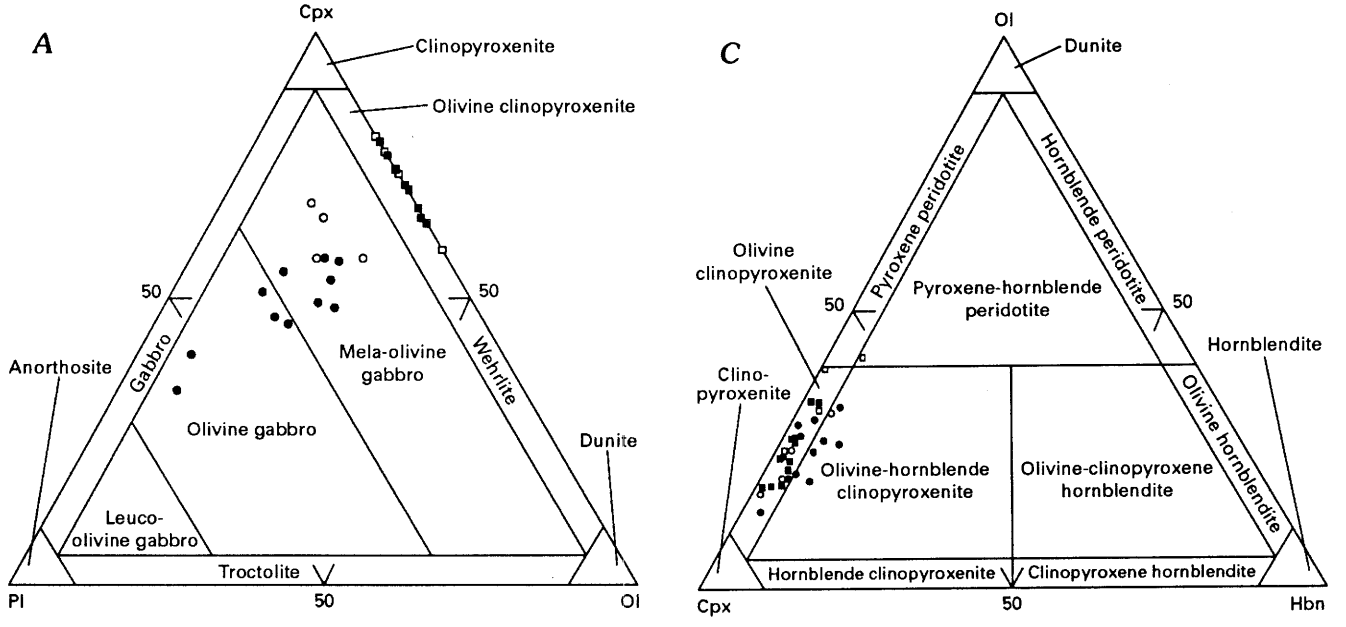

Figure 11. Modal compositions of rocks of the layered sequence. *A*, Modal plagioclase (Pl), olivine (Ol), and clinopyroxene (Cpx) contents. *B*, Modal magnetite (Mt), olivine (Ol), and clinopyroxene (Cpx) contents. *C*, Modal clinopyroxene (Cpx), hornblende (Hbn), and olivine (Ol) contents. Dots, cpx-pl-mt-pl cumulate of unit **Jp** (fig. 4); circles, cpx-ol-mt cumulate of unit **Jp**; solid boxes, cpx-ol-mt cumulate of unit **Jc**; open boxes, cpx-ol cumulate of unit **Jc**.

to euhedral, with locally laminated cumulus grains. Twinning, exsolution lamellae or blebs of spinel, and inclusions of olivine and magnetite in the clinopyroxene are common features. In some samples, clinopyroxene lacks olivine inclusions; in others, it lacks magnetite inclusions. Clinopyroxene grain size ranges from fine to coarse (max 2 cm across). Olivine generally forms subhedral to euhedral cumulus grains but also anhedral grains that in some samples make mosaic or adcumulate textures and in others fill interstitial spaces between clinopyroxene. In a few samples, olivine exhibits wavy or undulatory extinction.

Primary magnetite occurs as subhedral to euhedral crystals, singularly or in branching groups, in interstitial spaces and as inclusions in clinopyroxene. It exhibits varying amounts of exsolution of ilmenite and spinel, locally forming patchy areas in some crystals of a sample but not in other crystals of the same sample. In rocks containing less magnetite, its grain size tends to be smaller than in rocks containing abundant magnetite. Anhedral olive-brown to brown hornblende occurs as interstitial material, as material replacing clinopyroxene along cleavages, in patchy areas, and as rims on silicate minerals and magnetite. In a few samples containing much less than 1 volume percent hornblende, hornblende is associated with magnetite.

Biotite is an uncommon accessory mineral, occurring in 2 out of 29 thin sections; in both samples it forms anhedral grains associated with hornblende. In one thin section, it also forms patches in clinopyroxene. Plagioclase, or secondary minerals after it, occurs in about 15 percent of the samples. It forms blocky to irregular, anhedral crystals that are interstitial to clinopyroxene, olivine, and magnetite. Serpentine minerals and fine-grained, dusty magnetite, without exsolution lamellae, are alteration products of olivine; the degree of serpentinization varies. Brown hornblende, clinopyroxene, and, locally, olivine are replaced by tremolite-actinolite; plagioclase is replaced by epidote, chlorite, and zeolite(?). Some samples are cut by carbonate veins.

The order of crystallization, as implied by textures and inclusions of olivine and magnetite in clinopyroxene, is olivine and magnetite, followed by clinopyroxene, with continued crystallization of olivine and magnetite as cumulus crystals in the clinopyroxene-olivine-magnetite cumulate. Postcumulus crystallization must have included clinopyroxene and olivine to make adcumulate textures. Hornblende formed in interstices and by replacement of clinopyroxene. Traces of biotite, sulfide minerals, and plagioclase also crystallized as postcumulus material. At some point in the cooling history, spinel exsolved from clinopyroxene, and ilmenite from magnetite. Later alteration affected the olivine and plagioclase.

Plagioclase-Rich Clinopyroxene-Olivine Cumulate

The plagioclase-rich clinopyroxene-olivine cumulate consists predominantly of clinopyroxene-olivine-plagioclase-magnetite cumulate and minor amounts of clinopyroxene-olivine-magnetite cumulate. Both rock types contain more than 14 volume percent plagioclase; in the clinopyroxene-olivine-magnetite cumulate it is a postcumulus mineral. Locally, the unit contains thin, discontinuous layers of magnetite cumulate. Modal data, with the various rock names that would be applied in the IUGS classification, are plotted in figure 11. Most of the unit is a hornblende-bearing olivine-magnetite gabbro or hornblende-bearing mela-olivine gabbro. The proportions of olivine to clinopyroxene and of olivine plus clinopyroxene to magnetite are similar to those in the clinopyroxene-olivine cumulate. The proportions of plagioclase to olivine plus clinopyroxene vary widely (fig. 11*A*).

Major minerals in the plagioclase-bearing clinopyroxene-olivine cumulate are clinopyroxene (32–61 volume percent), olivine (7–15 volume percent), plagioclase (14–50 volume percent), magnetite (1–11 volume percent), and brown hornblende (0.8–6 volume percent). Minor minerals are biotite, pyrrhotite, and chalcopyrite; secondary minerals include serpentine minerals, magnetite, chlorite, sericite (muscovite?), epidote, tremolite-actinolite, and zeolite.

Clinopyroxene forms subhedral, locally euhedral cumulus crystals. In some thin sections, the crystal margins are embayed and appear ragged; in others, clinopyroxene crystals form interlocking textures. In one sample, some of the clinopyroxene grains have recrystallized to make finer grained mosaic necklaces on the margins of larger clinopyroxene crystals. Twinning is a common feature, and spinel exsolution is not as common as in the clinopyroxene-olivine cumulate. Four different combinations of inclusions are present in clinopyroxene in different thin sections. About 50 percent of the thin sections contain clinopyroxene with both magnetite and olivine inclusions; about 20 percent contain magnetite and plagioclase inclusions; about 25 percent contain olivine, magnetite, and plagioclase inclusions; and about 5 percent contain magnetite inclusions only. Clinopyroxene grain size ranges from fine to coarse (max 1 cm diam).

Olivine forms subhedral cumulus crystals, euhedral and anhedral in some thin sections. In some thin sections, anhedral olivine appears to have extensive overgrowths and fills interstitial spaces. Undulatory extinction is rare, and two thin sections contained vermiform olivine-magnetite intergrowths. Olivine contains inclusions of euhedral magnetite and, in a few thin sections, of euhedral plagioclase.

Plagioclase generally forms blocky and (or) tabular, subhedral cumulus crystals but in some thin sections is anhedral and interstitial. Locally, patchy zoning is common. Where plagioclase forms inclusions in clinopyroxene or olivine, it is euhedral and finer grained than elsewhere in the rock. A few samples contain a bimodal distribution of plagioclase grains consisting of a few larg-

er, more euhedral crystals associated with more abundant, blocky, subhedral, finer-grained crystals.

Primary magnetite occurs as subhedral to euhedral crystals either singularly or in branching groups in interstitial spaces and generally is finer grained than clinopyroxene and olivine. Exsolution lamellae of ilmenite and spinel are irregularly distributed; some crystals in the same thin section are exsolved, whereas others are not. Magnetite inclusions in olivine generally do not contain exsolution lamellae. Anhedral greenish-brown to brown hornblende occurs as interstitial space-filling crystals, replacement of clinopyroxene in patches or along cleavages, and rims on clinopyroxene, olivine, and magnetite. One thin section contained veinlets of brown hornblende in olivine, and another vermiform intergrowths of hornblende with magnetite.

Biotite, an uncommon accessory mineral, was observed as interstitial anhedral grains or in association with hornblende in olivine crystals. Pyrrhotite crystals (10–15 μm) form inclusions in silicates and oxides, slightly larger (30–50 μm) at grain boundaries. Chalcopyrite occurs as inclusions in clinopyroxene and, less commonly, with pyrrhotite as inclusions in clinopyroxene. Olivine is altered to varying amounts of serpentine minerals and dusty magnetite, whereas much of the plagioclase is altered to varying proportions of epidote, chlorite, sericite, and zeolite.

The fine-grained euhedral inclusions in clinopyroxene suggest that olivine, magnetite, and, in some rocks, plagioclase began crystallizing before clinopyroxene. The presence of magnetite inclusions in olivine is evidence that magnetite began crystallizing before olivine. Olivine, magnetite, and plagioclase continued to crystallize along with clinopyroxene to form the cumulus framework of the rocks. Ragged, embayed clinopyroxene suggests some period of clinopyroxene resorption during crystallization. The occurrence of sulfide minerals as inclusions in silicate and oxide minerals implies that they crystallized from an immiscible sulfide liquid which was present early in the crystallization history. Hornblende crystallized in part by reaction with clinopyroxene and in part as interstitial space-filling material. Later serpentinization and alteration affected olivine and plagioclase.

The Intrusive Sequence

Layered Olivine-Clinopyroxene Cumulate

The layered olivine-clinopyroxene cumulate consists predominantly of clinopyroxene-olivine cumulate and rare clinopyroxene-olivine-magnetite cumulate. In contrast to most of the layered sequence, these cumulates are characterized by lower magnetite and plagioclase contents. Modal data, with the various rock names that would be applied in the IUGS classification, are plotted in figure 12. The proportion of olivine to clinopyroxene varies and thus forms the basis for the modal layering observed in this unit.

Major minerals in the layered olivine-clinopyroxene cumulate are clinopyroxene (50–80 volume percent) and olivine (6–39 volume percent). Minor minerals are hornblende (0.2–11 volume percent), magnetite (0.3–10.8 volume percent), plagioclase (0–4 volume percent), pyrrhotite,

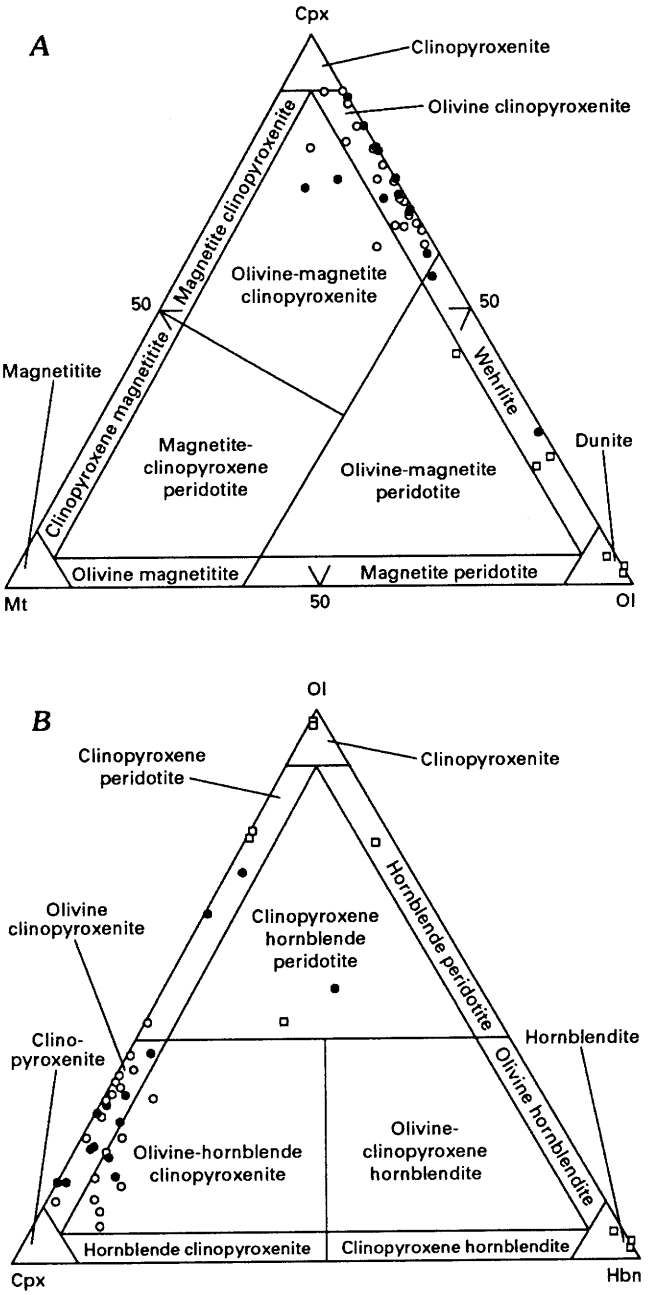

Figure 12. Modal compositions of the ultramafic rocks of the intrusive sequence. *A*, Modal magnetite (Mt), olivine (Ol), and clinopyroxene (Cpx) contents. *B*, Modal clinopyroxene (Cpx), hornblende (Hbn), and olivine (Ol) contents. Dots, olivine-clinopyroxene cumulate; circles, layered olivine-clinopyroxene cumulate; boxes, olivine cumulate.

and chalcopyrite; secondary minerals include serpentine minerals, magnetite, chlorite, epidote, sericite, hydrogrossular, and tremolite-actinolite.

Within the unit, clinopyroxene texture ranges from anhedral to subhedral, with interlocking cumulus crystals locally making a coarsely crystalline rock in some samples, to subhedral to euhedral, with locally elongate cumulus crystals in others. Exceptions occur in the layers of olivine cumulate within which clinopyroxene forms anhedral poikilitic crystals. Twinning, spinel exsolution, and olivine and magnetite inclusions are common features; one sample contained zoned clinopyroxene.

Olivine forms subhedral to euhedral cumulus crystals, locally elongate. Undulatory extinction and kink bands are relatively common in comparison with other units.

Greenish-brown to brown hornblende occurs as anhedral crystals in interstitial spaces and as replacement of clinopyroxene on the margins of crystals, along cleavages, and in patches. In some samples it forms poikilitic crystals, and in others veins crosscutting olivine and clinopyroxene. Plagioclase fills interstitial spaces as blocky, anhedral to subhedral crystals but commonly is completely altered to combinations of secondary minerals. Magnetite, with two sets of exsolution lamellae, occurs in interstitial spaces, as inclusions locally associated with brown hornblende, and at triple junctions of grains in rocks with interlocking textures. Some sections contain single grains of exsolved ilmenite associated with magnetite. Traces of pyrrhotite associated with serpentine minerals, and even rarer chalcopyrite as inclusions in clinopyroxene, complete the list of primary minerals. Serpentine minerals and fine-grained, dusty magnetite without exsolution lamellae replace olivine. Combinations of epidote, chlorite, hydrogrossular, and sericite replace plagioclase. Tremolite-actinolite replaces hornblende locally.

The crystallization order was olivine, locally with magnetite, followed by clinopyroxene. Olivine continued to crystallize as a cumulus mineral during the crystallization of clinopyroxene. Hornblende, both as poikilitic crystals and interstitial space filling, and plagioclase, as interstitial space filling, form postcumulus material. Hornblende also formed by reaction with clinopyroxene. Later alteration produced the secondary minerals.

Olivine-Clinopyroxene Cumulate

The olivine-clinopyroxene cumulate consists of olivine-clinopyroxene cumulate and clinopyroxene-olivine-magnetite cumulate that contain less magnetite and plagioclase than does the layered sequence. Modal compositions are similar to those of the layered olivine-clinopyroxene cumulate but include more olivine-rich variations (fig. 12), including some dunite that was not point-counted because of the complete alteration of those rocks.

Major minerals in the olivine-clinopyroxene cumulate are clinopyroxene (26–75 volume percent) and olivine (9–70 volume percent). Minor minerals are magnetite (0.3–16 volume percent), hornblende (0.3–2.7 volume percent), plagioclase (0–0.5 volume percent), rare biotite, and pyrrhotite; secondary minerals include serpentine minerals, magnetite, chlorite, epidote, sericite, pyrite, tremolite-actinolite, and carbonates.

Twinned cumulus clinopyroxene forms ragged, interlocking, anhedral to euhedral, predominantly subhedral, crystals containing subhedral to euhedral inclusions of olivine and magnetite. Olivine occurs as subhedral cumulus crystals, locally with subhedral to euhedral magnetite inclusions. Magnetite forms inclusions and subhedral to euhedral clusters filling interstitial spaces and contains (111) exsolution lamellae of ilmenite.

Greenish-brown to brown hornblende, locally as poikilitic crystals, forms anhedral crystals that fill interstitial spaces, replaces clinopyroxene at rims and cleavages and as patches, and occurs as veins. Some of the hornblende replacing clinopyroxene as patches extinguishes as single hornblende crystals in single clinopyroxene crystals. Plagioclase fills interstitial spaces and generally is completely replaced by combinations of chlorite, epidote, and sericite. Pyrrhotite occurs as inclusions in magnetite, interstitial to clinopyroxene, and in association with serpentine. Serpentine minerals and dusty veinlets and spongy-appearing areas of magnetite replace olivine. Pyrite occurs as cubes (max 0.01 mm) in serpentine-mineral veinlets. Tremolite-actinolite replaces hornblende and, locally, clinopyroxene. Carbonates and serpentine minerals form the latest veinlet system in the rocks.

Inclusions of olivine and magnetite within cumulus clinopyroxene and of magnetite within cumulus olivine suggest that magnetite crystallized first or at the same time as olivine, followed by clinopyroxene. Plagioclase crystallized as postcumulus material, as did hornblende, but the hornblende crystallized in part as a reaction between clinopyroxene and the trapped or remaining magma.

Intrusive Feldspathic Pyroxenite

The intrusive feldspathic pyroxenite consists of plagioclase-clinopyroxene-olivine-magnetite cumulate and ranges in modal composition from leuco-olivine-magnetite gabbro to olivine gabbro in the IUGS classification (fig. 13). This unit contains the most plagioclase rich rocks in the Lower Coon Mountain pluton.

Major minerals in the intrusive feldspathic pyroxenite are plagioclase (49–81 volume percent), clinopyroxene (9–30 volume percent) and olivine (5–16 volume percent). Minor minerals are hornblende (0.1–1 volume percent) and magnetite (1–6 volume percent); secondary minerals are serpentine minerals, magnetite, epidote, chlorite, sericite, and tremolite. Plagioclase forms blocky, anhedral to subhe-

dral cumulus crystals that exhibit some overgrowths and are locally replaced by epidote, chlorite, and sericite. Clinopyroxene occurs as subhedral to euhedral, twinned cumulus crystals with spinel exsolution lamellae and subhedral to euhedral inclusions of magnetite, olivine, and plagioclase. Olivine forms subhedral to euhedral cumulus crystals, generally in clusters. Magnetite fills interstitial spaces and occurs as a secondary mineral associated with serpentine minerals after olivine. Brown hornblende fills interstial spaces and occurs as patchy replacements in clinopyroxene.

Olivine Cumulate and Dunite

The olivine cumulate and dunite range in modal composition from clinopyroxene peridotite, through dunite and clinopyroxene-hornblende peridotite, to hornblende peridotite (fig. 12*B*) in the IUGS classification. The unit contains relatively small amounts of magnetite (fig. 12*A*).

The major mineral in the olivine cumulate and dunite is cumulus, subhedral to euhedral olivine (41–93 volume percent). Minor minerals are clinopyroxene (1–33 volume percent), hornblende (0.3–21 volume percent), magnetite (0.1–5 volume percent), pyrrhotite, and serpentine minerals; secondary minerals are tremolite-actinolite, epidote, chlorite, and hydrogrossular. Olivine locally contains vermiform masses of magnetite, commonly near the margins of crystals. Clinopyroxene forms anhedral, untwinned, poikilitic and interstitial-space-filling crystals that are partly replaced by brown hornblende in patches and along cleavages. Elsewhere, brown hornblende forms poikilitic crystals, fills interstitial spaces, and occurs as veins crosscutting olivine and clinopyroxene. Magnetite occurs as subhedral to euhedral crystals and groups of crystals filling interstitial spaces with (111) and (100) exsolution lamellae of ilmenite, and as dusty, feathery masses with serpentine minerals replacing olivine. Pyrrhotite occurs in serpentinized olivine and in association with primary magnetite. Chlorite, epidote, and hydrogarnet fill interstitial spaces and completely replace plagioclase (0–5.9 volume percent), and tremolite-actinolite replaces clinopyroxene and brown hornblende.

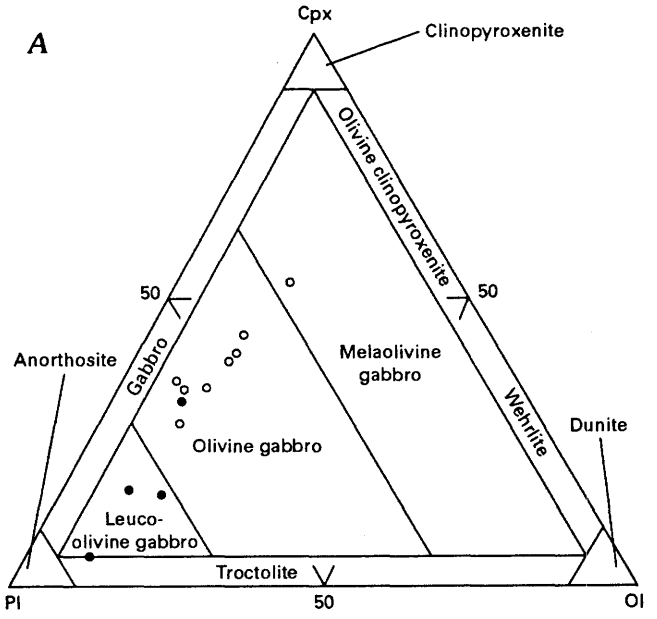

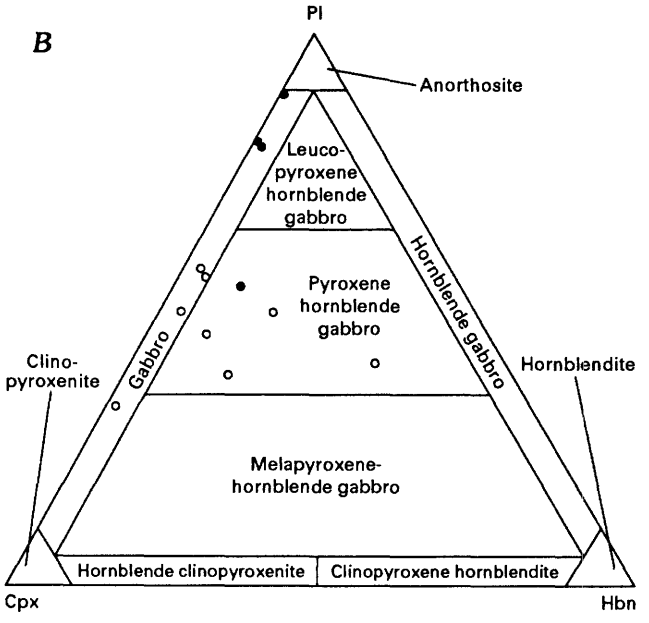

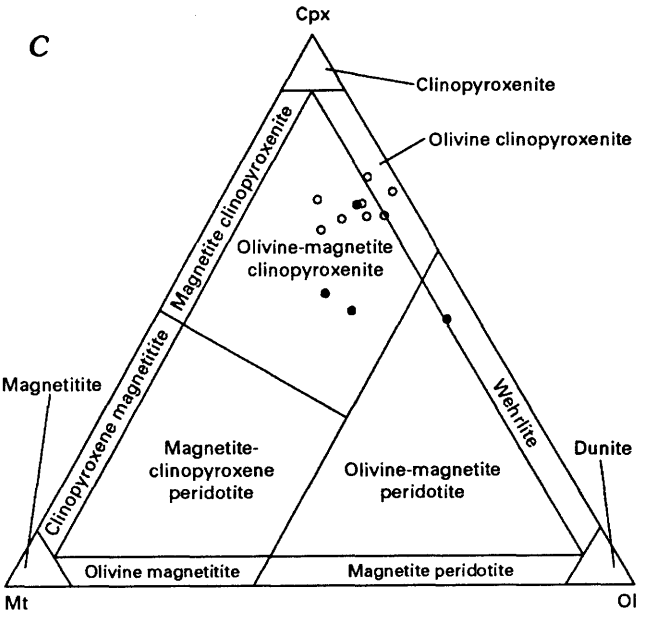

Figure 13. Modal compositions of mafic rocks of the intrusive sequence. *A*, Modal plagioclase (Pl), olivine (Ol), and clinopyroxene (Cpx) contents. *B*, Modal clinopyroxene (Cpx), hornblende (Hbn), and plagioclase (Pl) contents. *C*, Modal magnetite (Mt), olivine (Ol), and clinopyroxene (Cpx) contents. Dots, intrusive feldspathic pyroxenite; circles, gabbro.

Gabbro

The gabbro consists of plagioclase-clinopyroxene-olivine-magnetite cumulate, which in the IUGS classification is best described as olivine-magnetite gabbro, olivine-hornblende-magnetite gabbro, and mela-olivine-magnetite gabbro (fig. 13). The proportion of olivine to clinopyroxene plus plagioclase is fairly constant (fig. 13*A*); the contents of other minerals vary.

Major minerals in the gabbro are plagioclase (24–48 volume percent), clinopyroxene (15–49 volume percent), olivine (7–16 volume percent), hornblende (1–35 volume percent), and magnetite (0.9–9 volume percent). Minor and secondary minerals are biotite, serpentine minerals, magnetite, epidote, chlorite, sericite, tremolite-actinolite, and hydrogarnet. Plagioclase forms blocky to elongate, subhedral cumulus crystals with local patchy zoning; in some samples it occurs as anhedral interstitial-space-filling material, and in others as poikilitic crystals. Clinopyroxene occurs as subhedral to euhedral cumulus crystals but in some thin sections is anhedral, embayed, with a ragged appearance. Twinning and spinel exsolution are common features. Near contacts with the country rocks, clinopyroxene is strongly zoned and, locally elsewhere, less strongly zoned. In thin sections, combinations of olivine, plagioclase, and magnetite form inclusions in clinopyroxene; magnetite and olivine, and plagioclase and magnetite, are the most abundant combinations. Olivine forms subhedral to euhedral cumulus crystals or crystal clusters. Subhedral to euhedral magnetite forms crystals filling interstitial spaces and occurs as inclusions. Brown anhedral hornblende occurs interstitially, as rims, as replacement of clinopyroxene, as large poikilitic crystals, and in minor veins. Pale-yellow-brown biotite is an uncommon accessory mineral. Olivine generally is highly altered to serpentine minerals and dusty magnetite, as is plagioclase to combinations of epidote, chlorite, sericite, and, locally, hydrogarnet. In a few thin sections, alteration of hornblende and clinopyroxene to tremolite-actinolite is common.

From the inclusions in clinopyroxene, magnetite was probably the first mineral to begin crystallizing in most of the rocks, followed rapidly by olivine and plagioclase. These minerals continued to crystallize as cumulus minerals while clinopyroxene crystallized. Postcumulus processes controlled the crystallization of hornblende.

Mineral Compositions

Analyses of minerals were done on an ARL EMX–SM electron-probe microanalyzer at the U.S. Geological Survey laboratory in Menlo Park, Calif., using a series of natural and synthetic standards. Operating conditions for the instrument were an excitation potential of 15 kV and an aperture current of 25 to 30 mA. The raw data were corrected for dead time and background; corrections for mass absorption and fluorescence were made by the procedure of Bence and Albee (1968), using the correction factors of Albee and Ray (1970). Each analysis represents the mean of seven to nine analyzed points in each of at least four grains. Fe^{3+} content of clinopyroxene was calculated by the charge-balance method of Papike et al. (1974).

Clinopyroxene

All the clinopyroxene compositions determined in the Lower Coon Mountain pluton are diopsidic, according to

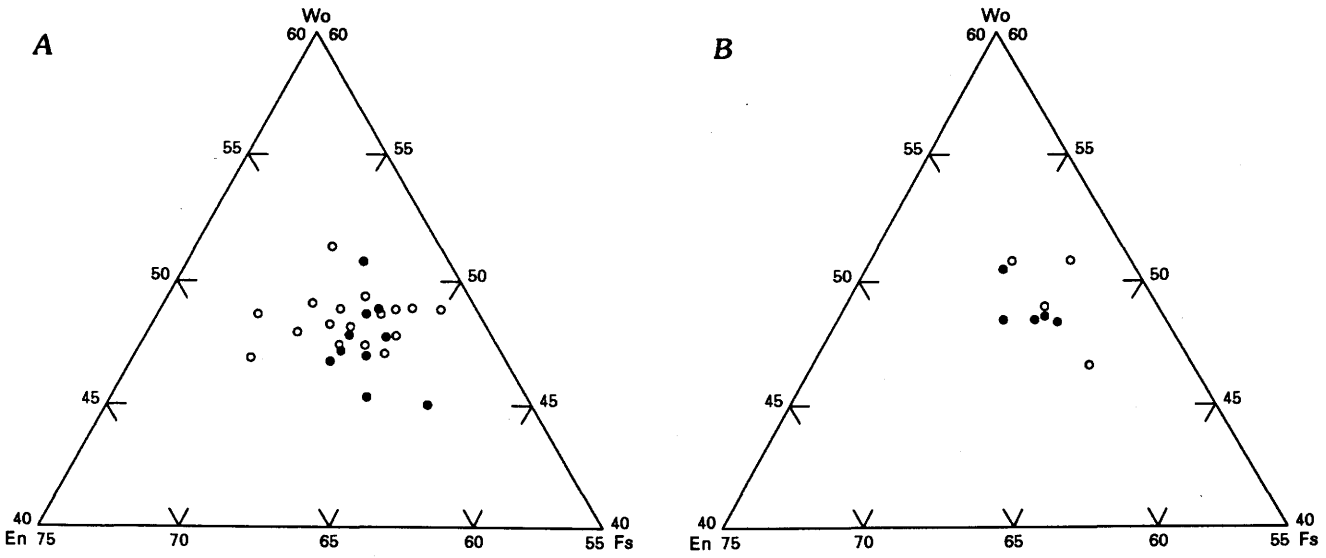

Figure 14. Enstatite (En), ferrosilite (Fs), and wollastonite (Wo) contents of clinopyroxene in diopside of rocks of the layered (*A*) and intrusive (*B*) sequences. Dots, plagioclase-rich clinopyroxene-olivine cumulate; circles, clinopyroxene-olivine cumulate.

the nomenclature of Poldevaart and Hess (1951). Selected electron-microprobe analyses of diopside, with calculated mineral formulas for comparison among the various map units, are listed in table 3. The diopside compositions in the layered sequence (fig. 14*A*) are indistinguishable from those in the intrusive sequence (fig. 14*B*), and within the two sequences the small variations in diopside composition do not seem to form trends within individual map units. Within individual samples the variations in the Wo, En, and Fs contents of diopside are less than ±1.5 percent. In the clinopyroxene-olivine-plagioclase-magnetite cumulates, the Wo content of diopside partly appears to be directly related to the content of cumulus plagioclase (fig. 15). However, the Fs content of diopside does not appear to be systematically related to olivine content (fig. 16).

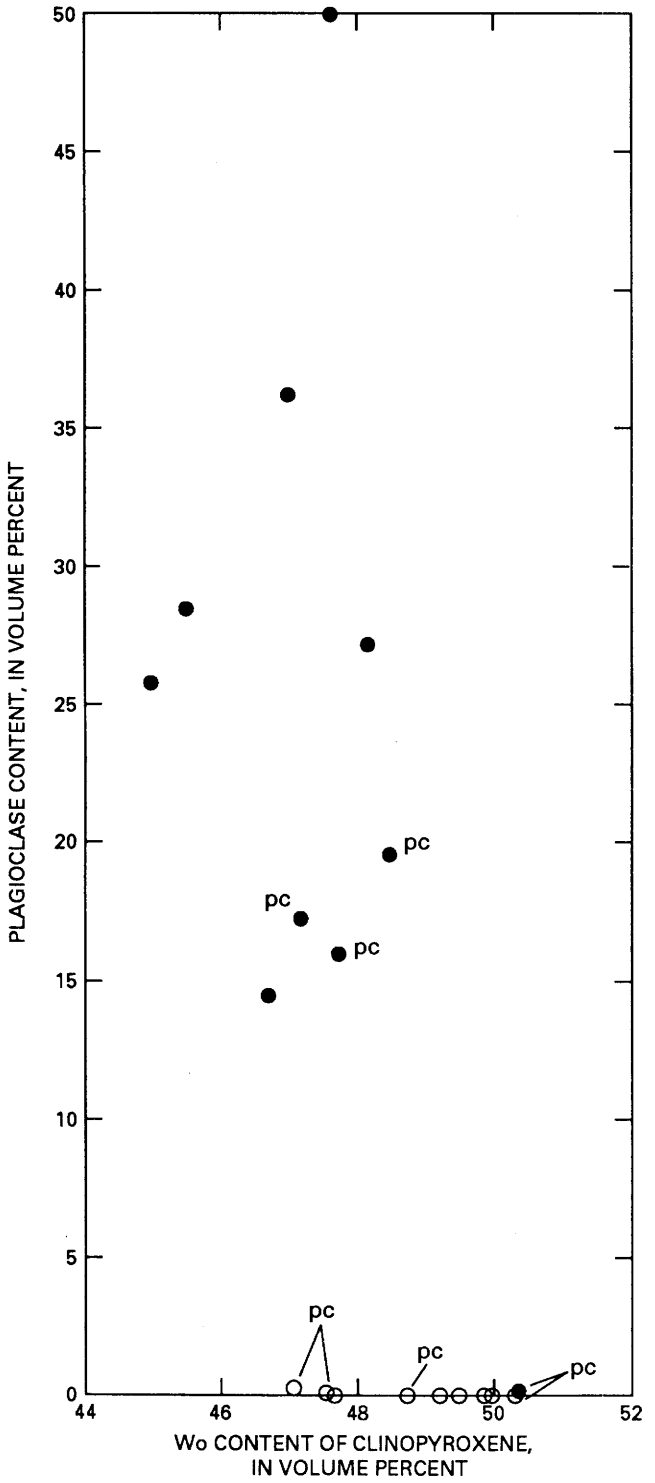

Figure 15. Plagioclase content versus wollastonite (Wo) content of clinopyroxene in rocks of the layered sequence. Dots, plagioclase-rich clinopyroxene-olivine cumulate; circles, clinopyroxene-olivine cumulate; pc, postcumulus plagioclase.

Olivine

Olivine composition, as $100Mg/(Mg+Fe^{2+}+Mn+Ni)$ ratio, ranges from 70.3 to 82 in the Lower Coon Mountain pluton, and in individual samples the variation is less than ±1.0 unit. Selected electron-microprobe analyses, with calculated mineral formulas of olivine for comparison among the various map units, are listed in table 4. The NiO content of olivine in relation to $100Mg/(Mg+Fe^{2+}+Mn+Ni)$

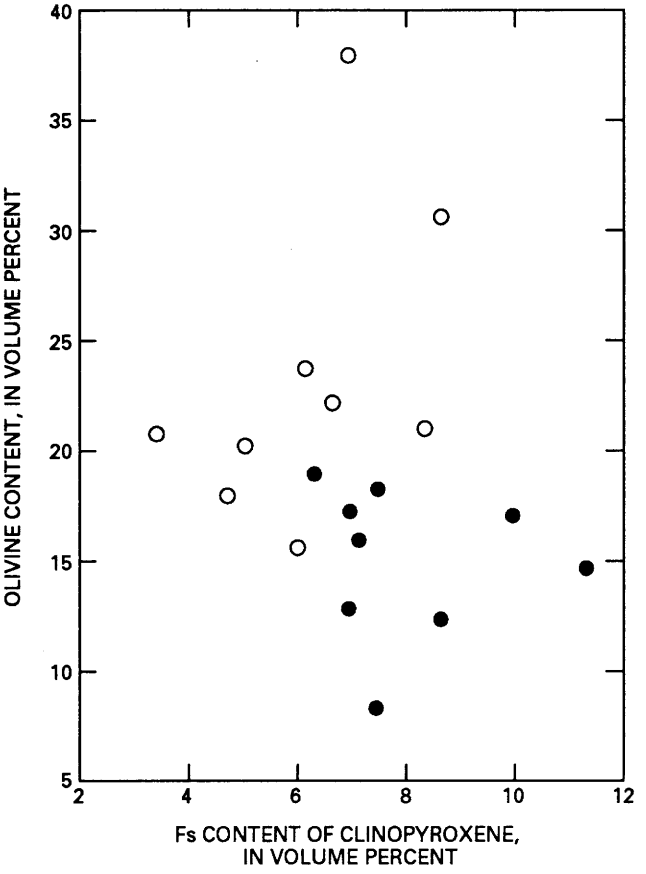

Figure 16. Olivine content versus ferrosilite (Fs) content of clinopyroxene in rocks of the layered sequence. Dots, plagioclase-rich clinopyroxene-olivine cumulate; circles, clinopyroxene-olivine cumulate.

ratio for the layered and intrusive sequences is plotted in figure 17. The variation in the NiO content of olivine appears to be similar in both sequences and is apparently correlated with 100Mg/(Mg+Fe^{2+}+Mn+Ni) ratio. The Fs content of diopside and the 100Mg/(Mg+Fe^{2+}+Mn+Ni) ratio in rocks of the layered sequence (fig. 18) appear to be inversely related; however, the Fs content and modal composition of olivine are unrelated (fig. 16). Because of the limited number of data, a similar relation in the intrusive sequence is not readily apparent (fig. 18*B*); however, there may be weak correlations between units of the layered sequence. The relation between magnetite content and 100Mg/(Mg+Fe^{2+}+Mn+Ni) ratio in rocks of the layered and intrusive sequences is plotted in figure 19. The limited number of data preclude discussing the intrusive sequence. In the layered sequence, there are two groups of samples: those containing less than 5 volume percent magnetite and those containing more than 6 volume percent. The occurrence of magnetite as inclusions in clinopyroxene in both groups indicates that the magnetite is a cumulus mineral; those rocks without magnetite inclusions fall outside both groups. In both groups, 100Mg/(Mg+Fe^{2+}+Mn+Ni) ratio is directly related to magnetite content, particularly for the plagioclase-rich clinopyroxene-olivine cumulate.

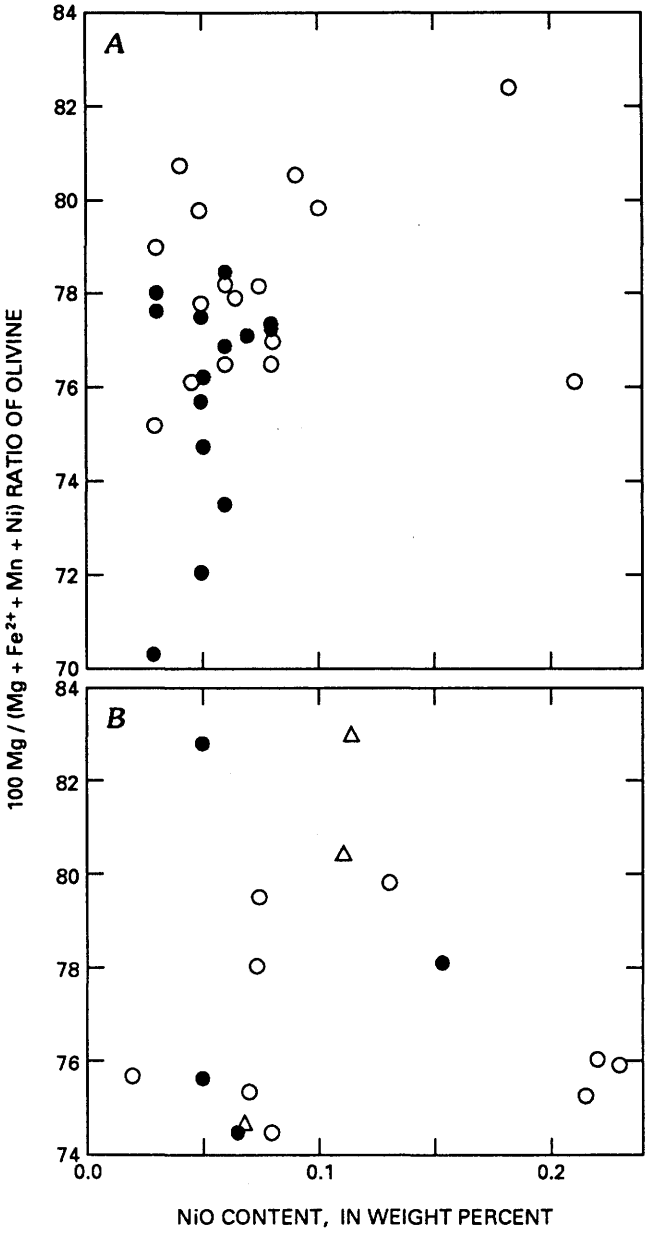

Figure 17. 100Mg/(Mg+Fe^{2+}+Ni+ Mn) ratio versus NiO content of olivine in rocks of the layered (*A*) and intrusive (*B*) sequences. Dots, plagioclase-rich clinopyroxene-olivine cumulate; circles, clinopyroxene-olivine cumulate; triangles, olivine cumulate.

Plagioclase

Selected analyses of plagioclase and their mineral formulas are listed in table 5. Within most rocks containing

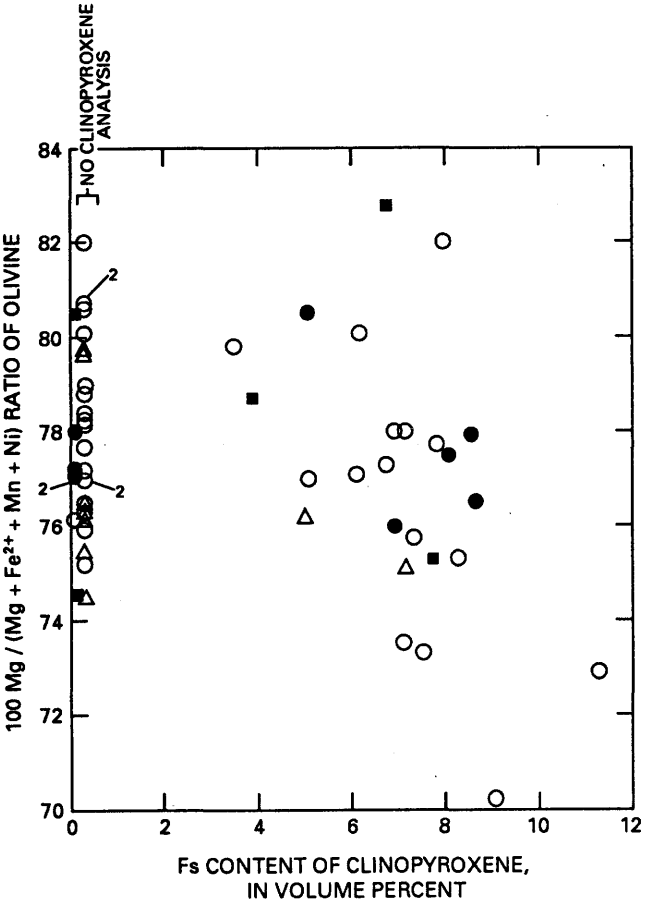

Figure 18. 100Mg/(Mg+Fe^{2+}+Mn+Ni) ratio of olivine versus ferrosilite (Fs) content of clinopyroxene in rocks of the layered and intrusive sequences. Dots, plagioclase-rich clinopyroxene-olivine cumulate; circles, clinopyroxene-olivine cumulate; boxes, layered olivine-clinopyroxenite cumulate; triangles, olivine-clinopyroxene cumulate; 2, two analyses.

olivine, the high degree of alteration of plagioclase limits the potential for analysis. Patchy zoning and grain-to-grain variation produce a maximum variation of 11 mol percent in An content, but most samples show a variation of less than 2 mol percent An. Plagioclase content ranges from about An_{62} to An_{94}, and Or content is low (fig. 20). Because the cumulus plagioclase content is related to the Wo content of diopside (fig. 15), the An content of plagioclase may be similarly related (fig. 21).

Interpretation of Mineralogic Relations

The observed relations between the Wo content of clinopyroxene and the modal amount of cumulus plagioclase, the Fs content of clinopyroxene, the 100Mg/(Mg+Fe^{2+}+Mn+Ni) ratio of olivine, and the modal amount of magnetite all indicate parts of processes of crystallization. For example, the relation between the modal amount of magnetite and the 100Mg/(Mg+Fe^{2+}+Mn+Ni) ratio of olivine suggests that the activity of FeO in the magma was controlled by the fayalite-magnetite buffer system during cumulus crystallization. In general, the limited variations in composition of clinopyroxene, olivine, and plagioclase also imply constraints on the processes of crystallization. In the following discussion of vertical variations in the composition of cumulus minerals, these processes are more constrained.

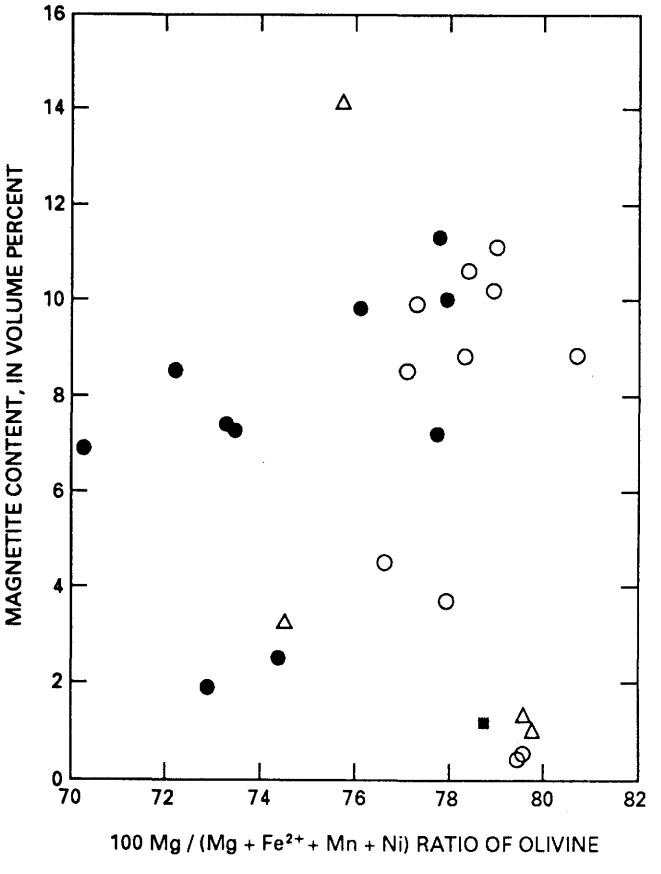

Figure 19. Magnetite content versus 100Mg/(Mg+Fe^{2+}+Mn+Ni) ratio of olivine in rocks of layered and intrusive sequences. Dots, plagioclase-rich clinopyroxene-olivine cumulate; circles, clinopyroxene-olivine cumulate; boxes, layered olivine-clinopyroxenite cumulate; triangles, olivine-clinopyroxene cumulate.

Variations in Mineral Composition with Stratigraphic Position

As demonstrated in the subsection above entitled "Mineral Compositions," the compositions of diopside, olivine, and plagioclase in the layered sequence overlap those in the intrusive sequence. Units within both sequences also exhibit overlapping mineral compositions, some of which may be due to differentiation of repeated influxes of new batches of magma of similar composition. Within the layered sequence, two stratigraphic columns were constructed by projecting samples onto two traverses, one in the southwestern and the other in the southeastern segment. Figure 22 compares the variations in the compositions of diopside, olivine, and plagioclase between these two segments and correlates these variations with stratigraphic position within each column.

Examination of figure 22 suggests little overall regular variation in the compositions of diopside, olivine, and plagioclase with stratigraphic position. Individual units of clinopyroxene-olivine cumulate and plagioclase-rich clinopyroxene-olivine cumulate show both increases and decreases in Fs, Fo, and An contents. Where sufficient

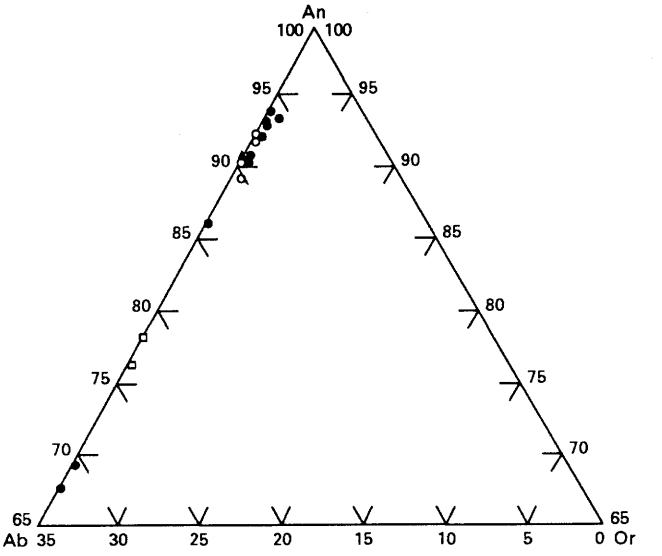

Figure 20. Albite (Ab), orthoclase (Or), and anorthite (An) contents of plagioclase in rocks of the Lower Coon Mountain pluton. Dots, plagioclase-rich clinopyroxene-olivine cumulate; circles, clinopyroxene-olivine cumulate; boxes, layered olivine-clinopyroxenite cumulate; triangles, olivine cumulate.

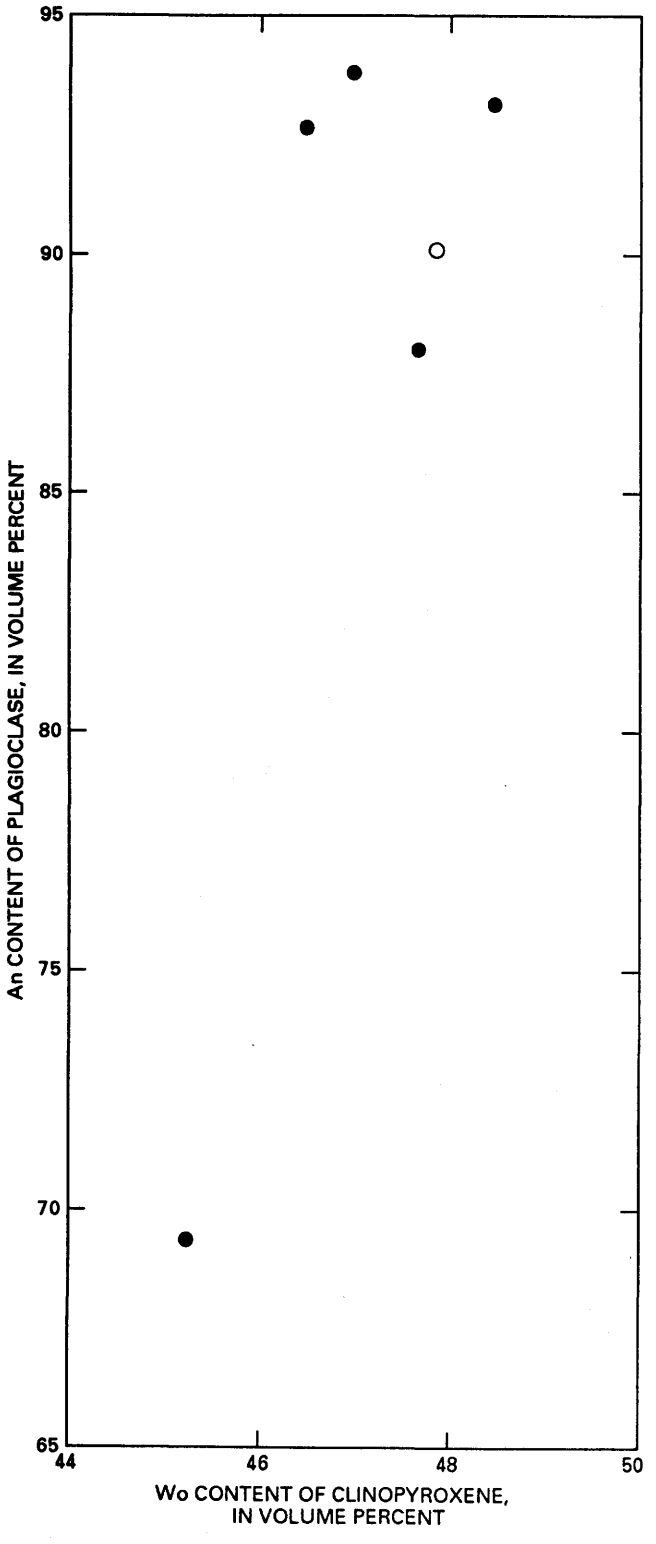

Figure 21. Anorthite (An) content of plagioclase versus wollastonite (Wo) content of clinopyroxene in rocks of the layered sequence. Dots, plagioclase-rich clinopyroxene-olivine cumulate; circles, clinopyroxene-olivine cumulate.

data are available, there appear to be breaks in composition across rock-unit boundaries. There is no overall trend in compositional variations in the minerals within the southwestern segment. In the southeastern segment, however, the Fs content of diopside tends to decrease, and the Fo content of olivine to increase, overall from the top to the bottom of the section. Thus, there is a weak suggestion of an Mg enrichment in mafic minerals upward in the southwestern segment but little evidence for it in the southeastern segment. If the more extreme maximums and minimums for Fs, Fo, and An contents are excluded, mineral composition remains fairly constant with stratigraphic position.

Lateral Variation in Modal Hornblende

The range in hornblende content from a few tenths of a volume percent to more than 35 volume percent in rocks of the Lower Coon Mountain pluton does not seem to be a property of individual rock units alone. Hornblende contents of a few tenths to 2–3 volume percent, texturally in the cumulate rocks, represent interstitial-space-filling materials, poikilitic hornblende crystals, and minor patchy replacements of diopside. As the hornblende content increases, the diopside content decreases until much of it is replaced by brown hornblende. In the more hornblende rich samples, crosscutting of olivine and diopside by veinlets of brown hornblende suggests a very late stage process in the crystallization history of the rocks. The distribution of hornblende in the pluton is illustrated in figure 23 by contours of greater than 4 volume percent and greater than 10 volume percent hornblende. Two major areas, one in the northern segment and the other in the southeastern segment, are richest in hornblende. The contact of the pluton with country rocks along this part of the northern segment is predominantly intrusive, as is the contact along the hornblende-rich part of the southeastern segment.

GEOCHEMISTRY

Selected rock, soil, and stream-sediment samples from the Lower Coon Mountain pluton were analyzed for major, trace, and platinum-group elements (PGE's) to characterize the geochemical environment of the pluton. Most of the trace-element and PGE analyses were performed to evaluate the potential for a precious-metal deposit within or on the margins of the pluton. Major-element analyses of rock samples, in combination with Cross-Iddings-Pirsson-Washington (CIPW) norms and modal data, were done to trace the petrologic and geochemical development of the pluton and to allow comparisons with other similar plutons.

Analytical Techniques and Calculation Methods

Major elements were analyzed by X-ray-fluorescence (XRF) methods at U.S. Geological Survey laboratories, using a variation of the borate-flux method of Fabbi (1972); FeO, H_2O+, H_2O-, and CO_2 content were determined by conventional methods, as described by Shapiro (1975). Trace elements were analyzed by direct-read quantitative emission-spectrographic or visual six-step semiquantitative emission-spectrographic techniques, as indicated in tables 13 and 14. Elements not found above the detection limits (in parentheses) are Ag (0.5 ppm), As (1,000 ppm), Au (20 ppm), Be (1 ppm), Bi (10 ppm), Cd (50 ppm), Mo (3 ppm), Sb (150 ppm), Sn (10 ppm), Te (2,000 ppm), U (500 ppm), W (100 ppm), Ge (10 ppm), Hf (100 ppm), In (10 ppm), Li (100 ppm), Re (50 ppm), Ta (500 ppm), Th (200 ppm), and Tl (50 ppm). Pt, Pd, and Rh contents were determined by fire-assay/atomic-absorption techniques, as described by Haffty and others (1977), Simon and others (1978), and Page and others (1980). Ir and Ru contents were determined by fire-assay and emission-spectrographic techniques (Haffty and others, 1980).

CIPW norms were calculated by using a version of the PETCAL program (Bingler and others, 1976). The extensive development of secondary magnetite due to serpentinization makes it difficult to reconstruct the original FeO and

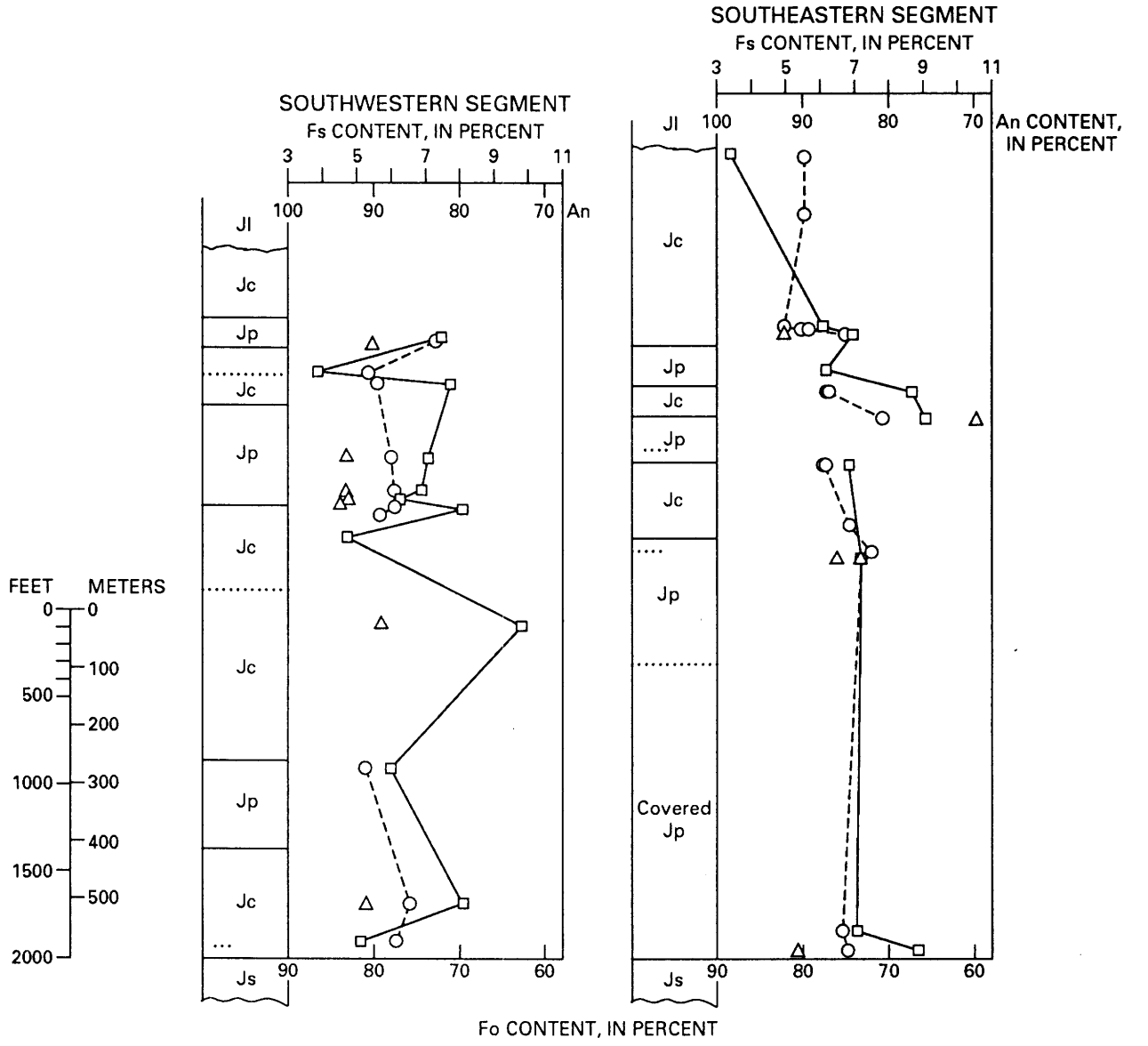

Figure 22. Anorthite (An), forsterite (Fo), and ferrosilite (Fs) contents of clinopyroxene (box), olivine (triangle), and plagioclase (circle) in rocks of the layered sequence in relation to stratigraphic position in the southwestern and southeastern segments. Same unit symbols as in figure 4.

Fe_2O_3 contents before serpentinization, and the proportions of these constituents severely affect normative calculations. The variation in Fe_2TO_3 content with loss on ignition (LOI), which is an approximation of the H_2O and CO_2 contents of the ultramafic-rock samples and thus of the degree of alteration, is plotted in figure 24. The relation of Fe_2TO_3 content to LOI demonstrates the problem in correcting for secondary magnetite. Samples of clinopyroxene-olivine cumulate are richer in magnetite than those of other rocks but also show an increase in Fe_2TO_3 content caused by serpentinization. Several different approaches were tried to adjust these values so as to make the CIPW norms and mineral compositions approach the modal data and the analyzed olivine and clinopyroxene compositions. For some

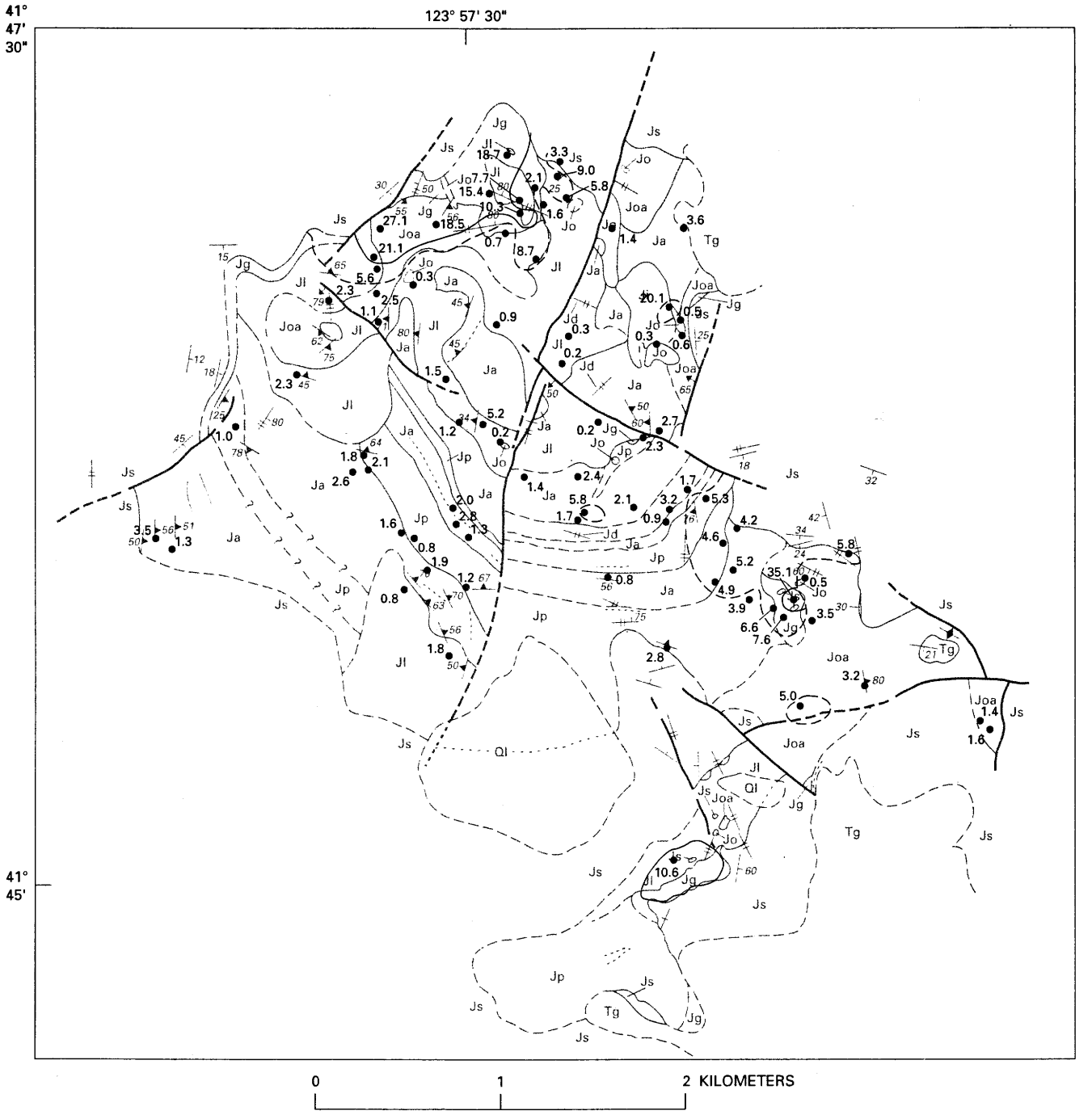

Figure 23. Geologic sketch map of the Lower Coon Mountain pluton, showing distribution of brown hornblende (in volume percent). Solid line encompasses area of greater than 10 volume percent hornblende; dashed line encompasses area of greater than 4 volume percent hornblende. See plate 1 for explanation.

units, the determined FeO and Fe_2O_3 contents appear to provide the more realistic CIPW norms, for others setting Fe_2O_3 content equal to 0.5 weight percent, and for others using the correction of Irvine and Baragar (1971). The Na_2O and K_2O contents of many samples are below the detection limits of 0.15 and 0.02 weight percent, respectively. For CIPW norm calculations, Na_2O and K_2O contents were set at the detection limit or above, as measured. This setting introduces trace amounts of leucite or orthoclase and nepheline or albite that are too large, and these normative components may be absent in some samples. However, the FeO/Fe_2O_3 ratio much more widely affects whether the rock is nepheline or hypersthene normative. The presence of hornblende and nonquadrilateral clinopyroxene in diopside also affects the CIPW–norm calculations, tending to increase the contents of normative albite, hypersthene, magnetite, and nepheline. The presence of apatite in the norm for most samples results from using the detection limit of P_2O_5 in the calculations.

The modal data were based on thin sections, and 800 or more points were counted. Alteration products were counted as primary minerals where textural relations allowed interpretation.

Rock Geochemistry

Country Rocks

Analyses of shale, volcaniclastic rocks, hornfels, and amphibolite from the adjacent country rocks are listed in table 6, and the locations of samples are shown on plate 1. The major element composition of the shale samples are similar to the composition of average shales reported by Pettijohn (1957, p. 344) and do not appear unusual, nor do the trace-element compositions. However, the presence of parts per billion of palladium and platinum in the shale samples is unusual. The volcaniclastic-rock sample has a bulk composition approaching that of a basalt, suggesting that it was derived from the weathering of mafic volcanic rocks. Both the shales and volcaniclastic rocks have been contact metamorphosed to hornfels and amphibolite. Major changes in CaO, Na_2O, and K_2O contents appear to result from the metamorphism of shale to hornfels (compare the shale analysis with that of sample 82CMG100). Thus, the hornfels has higher CaO and Na_2O contents than its protolith.

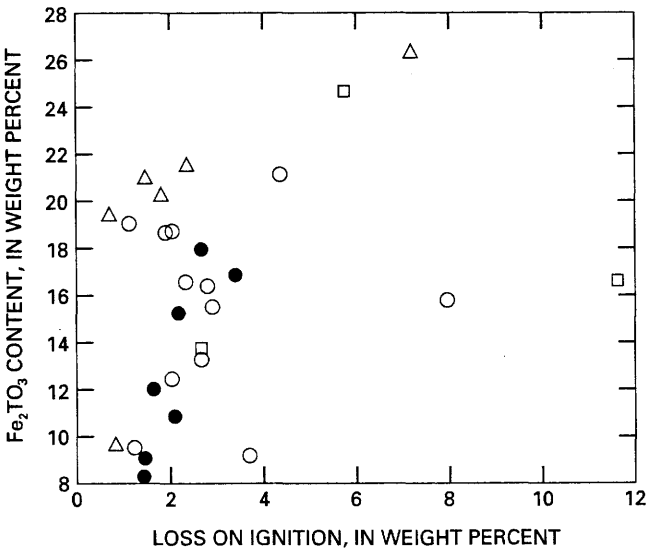

Figure 24. Fe_2TO_3 content versus loss on ignition in ultramafic rocks of the layered and intrusive sequences. Dots, layered olivine-clinopyroxenite cumulate; circles, olivine-clinopyroxene cumulate; boxes, olivine cumulate; triangles, clinopyroxene-olivine cumulate.

The Layered Sequence

The bulk compositions of the two units in the layered sequence are similar except for higher Na_2O, K_2O, Al_2O_3, and Sr contents in the plagioclase-rich clinopyroxene-olivine cumulate (table 7). This difference reflects the plagioclase content of the unit. The average compositions of units in the layered sequence are listed in table 8, and the locations of samples are shown in plate 1. Trace-element contents are also similar, except for the Cu- and Cr-rich samples of the plagioclase-rich clinopyroxene-olivine cumulate. Sample 84CM81 has visible secondary Cu minerals developed along fractures and is enriched in Pd and Pt relative to the other samples.

CIPW norms, in both the selected Fe_2O_3-adjusted and nonadjusted calculations, approach the observed modal data and agree favorably if the mode is converted to weight percent. The content of normative magnetite is generally higher than that of modal magnetite and reflects the nonquadrilateral Fe_2O_3 component in diopside, as does part of the contents of normative anorthite and hypersthene. The normative-mineral compositions also approach the analytical compositions of diopside (table 3) and olivine (table 4). Plots of normative Di, Fo, and An, which show a compositional overlap between the two units and an enrichment in plagioclase (fig. 25), demonstrate that the samples analyzed approach eutectoid compositions.

The Intrusive Sequence

Chemical analyses, CIPW norms, and modal data for rock samples from the intrusive sequence are listed in tables 9 and 10. Compositions of the layered olivine-clinopyroxene cumulate and the olivine-clinopyroxene cumulate are similar but differ from that of the olivine cumulate and dunite in higher CaO and lower MgO contents, on average (table 11). The gabbro, as would be expected, is enriched in plagioclase-forming components. In comparison with the

layered sequence, ultramafic rocks of the intrusive sequence have lower TiO_2 and higher MgO contents (compare tables 8, 11). More than half the samples from the intrusive sequence are nepheline normative, and the CIPW norms compare well with the modal data. Figure 26 compares the CIPW norms for the intrusive sequence, showing the difference in plagioclase contents between the gabbro and the ultramafic rocks.

Postplutonic Intrusive Rocks

The compositions of four dikes are listed in table 12. Samples 82CMG137 and 82CMG138 represent the clinopyroxene phenocryst-rich basalt to andesite dikes; the other two samples are from hornblende diorite dikes. Sample 82CMG138 contains xenoliths of shale. Normative-mineral data for the dikes plot in the diopside field on Di-Fo-An diagrams (fig. 25), showing that their compositions differ from those of other rocks of the pluton, as does a comparison of CIPW norms.

Comparison of Compositions of the Layered and Intrusive Sequences

MgO, TiO_2, Co, Cr, Ni, V, Pt, and Pd contents were selected for comparison of the two sequences and of the units within each sequence. The TiO_2 and MgO contents of rocks of the pluton are listed in tables 7, 9, and 10 and plotted in figure 27. For each sequence, the variation in TiO_2 content with MgO content is about the same; the TiO_2 content of the rocks, in general, is inversely related to MgO content. However, all but one sample from the layered sequence plots at the higher end of the range in TiO_2 content. Each rock unit, as illustrated by the average content (tables 8, 11), is more heavily represented in a particular segment of the total range in TiO_2 content. Co, Cr, and Ni contents tend to increase with increasing MgO content (fig. 28), and, as with the variation in TiO_2 content with MgO content, the sequences and rock units vary over particular segments of the total range in their Co, Cr, and Ni contents. Individual rock units in each sequence, on average, tend to increase in Co, Ni, and Cr contents from oldest to youngest in the order of emplacement, except for the gabbro, which has the lowest Co, Ni, and Cr contents. The intrusive sequence is, in general, enriched in these elements relative to the layered sequence. The pattern of variation in V content (fig. 28*D*) is similar to that in TiO_2 content; rocks of the layered sequence tend to be V rich in comparison with those of the intrusive sequence. Other trace elements do not show such simple variations in relation to magnesium and appear to be more irregularly distributed. Pd content (fig. 29*A*) shows no correlation, and Pt content (fig. 29*B*) relatively little correlation, with MgO content.

Spatial Distribution of Selected Trace Elements

On the basis of the summary of chemical data listed in tables 8 and 11 and plotted in figure 28, Ni, Cr, and V were

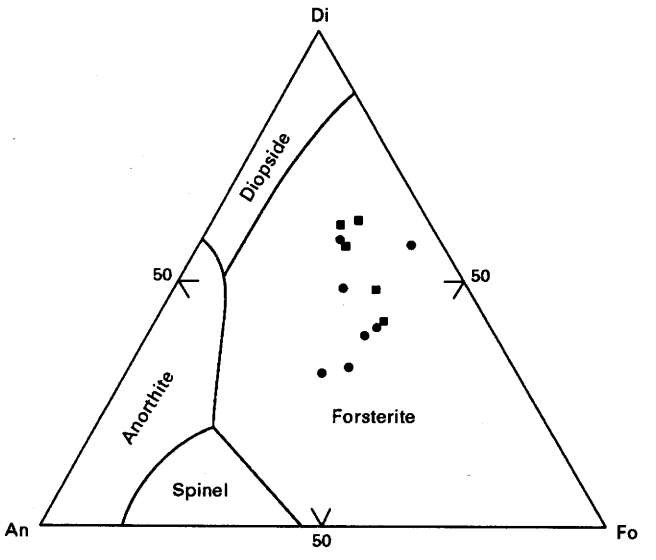

Figure 25. Normative anorthite (An), forsterite (Fo), and diopside (Di) contents of rocks of the layered sequence, with An-Fo-Di system of Osborn and Tait (1952) superimposed. Dots, plagioclase-rich clinopyroxene-olivine cumulate; boxes, clinopyroxene-olivine cumulate.

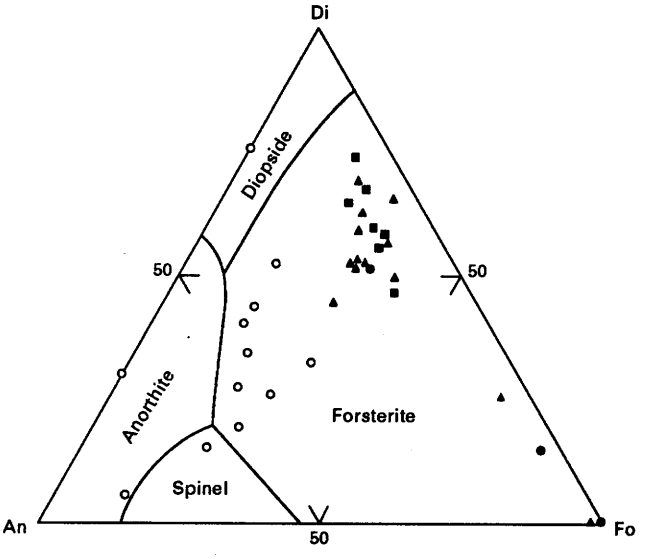

Figure 26. Normative anorthite (An), forsterite (Fo), and diopside (Di) contents of rocks of the intrusive sequence, with An-Fo-Di system of Osborn and Tait (1952) superimposed. Dots, olivine cumulate; circles, gabbro; boxes, layered olivine-clinopyroxenite cumulate; triangles, olivine-clinopyroxene cumulate.

selected to show the spatial distribution of trace elements. The analytical data plotted in figures 30 through 36 are listed in table 13. Figure 30 shows that most of the Ni contents higher than 300 ppm in rocks occur in the olivine-clinopyroxene and the olivine cumulate and dunite; thus, higher Ni content predominantly reflects a higher olivine content in these units. This result, in combination with the data plotted in figure 17, implies that nickel occurs in olivine because anomalous Ni contents are always associated with olivine-rich rocks. Thus, nickel occurs predominantly in olivine and not in a sulfide phase. Ni contents of less than 100 ppm occur in the clinopyroxene-olivine cumulate, the plagioclase-rich clinopyroxene-olivine cumulate, and the gabbro; intermediate Ni contents occur in the layered olivine-clinopyroxene cumulate. Each unit appears to have a relatively restricted range of Ni content. Comparison of the modal composition of olivine in the various units suggests that the olivine content of many of these rocks

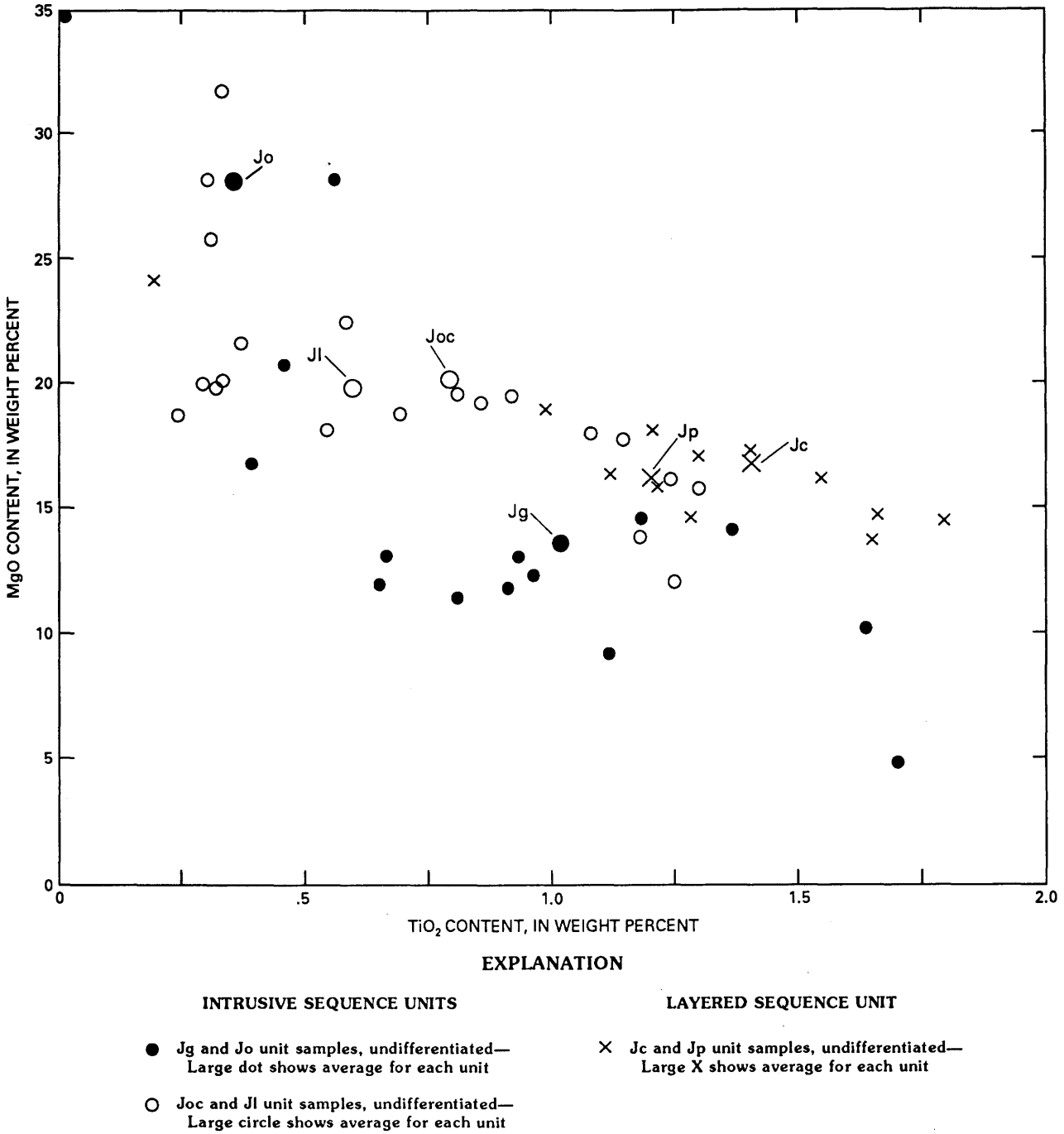

Figure 27. MgO versus TiO_2 content in rocks of the layered and intrusive sequences. Same unit symbols as in figure 4.

(compare figs. 11, 12) is nearly identical. Therefore, the distribution of nickel in the rocks not only reflects the proportion of olivine but also different Ni contents of olivine in the various units, such that Ni content is higher in the intrusive sequence than in the layered sequence.

The lowest Cr contents were measured in samples of the clinopyroxene-olivine cumulate and the gabbro of the intrusive sequence (fig. 31). In the layered olivine-clinopyroxene cumulate, olivine cumulate and dunite, and olivine-clinopyroxene cumulate, most Cr contents are higher than 800 ppm. The distribution of chromium within the various units is overall similar to that of nickel; however, the variation in Cr content is greater than in Ni content within the same units.

The spatial distribution of vanadium in rocks of the pluton is plotted in figure 32. All except one V content greater than 500 ppm were measured in samples from the southwestern and eastern parts of the northern segment. Rock samples from the layered sequence also have more V contents above 350 ppm, in addition to those above 500 ppm, whereas those from the intrusive sequence have lower V contents. The distribution of vanadium between the two sequences correlates with that of magnetite, such that the layered sequence is richer in magnetite than is the intrusive sequence.

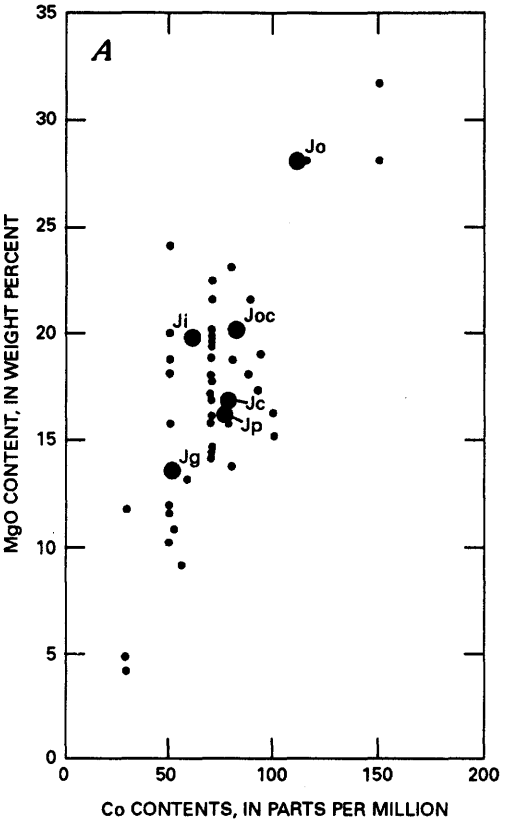

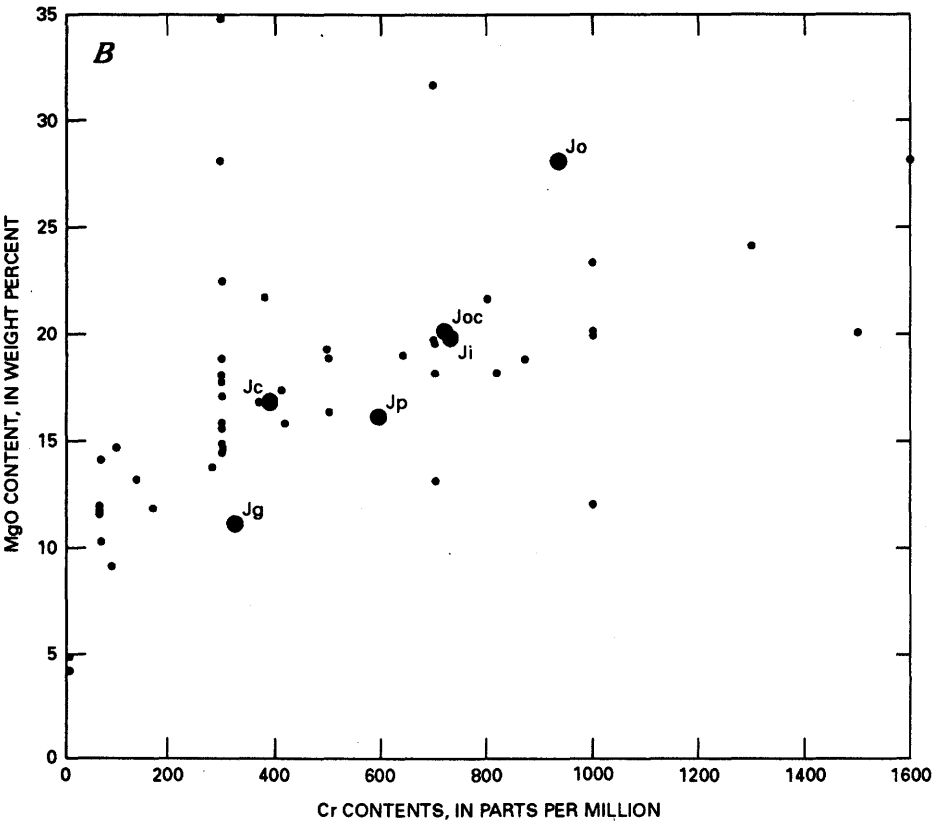

Figure 28. Mg content versus contents of selected trace elements in rocks of the layered and intrusive sequences, based on MgO versus V content. Same unit symbols as in figure 4. Small dots, individual sample from units Jg, Jo, Joc, Ji, Jp, and Jc,

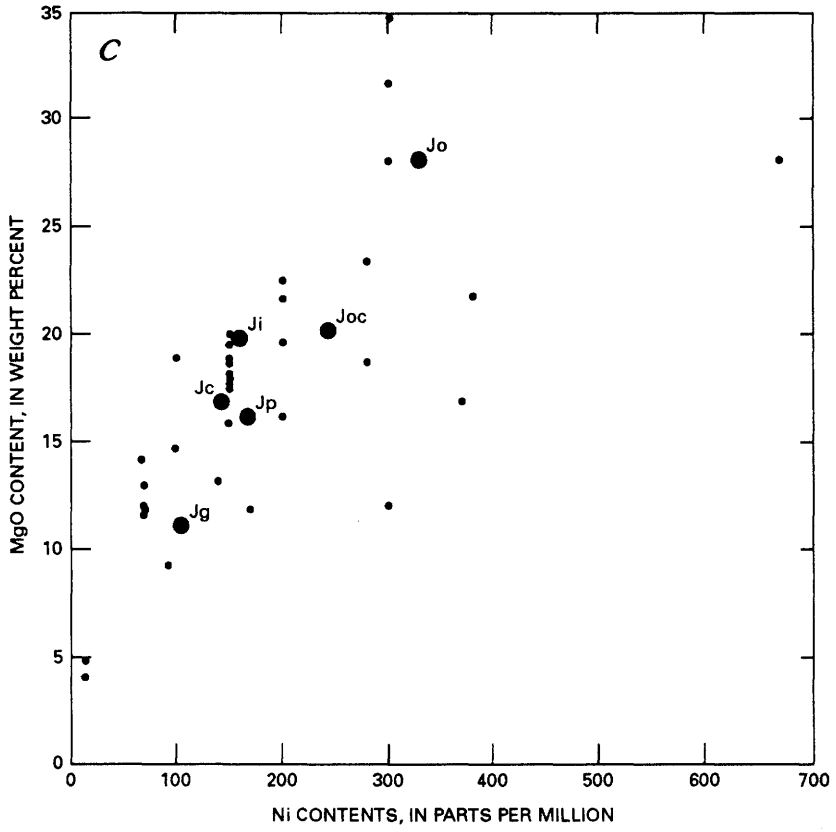

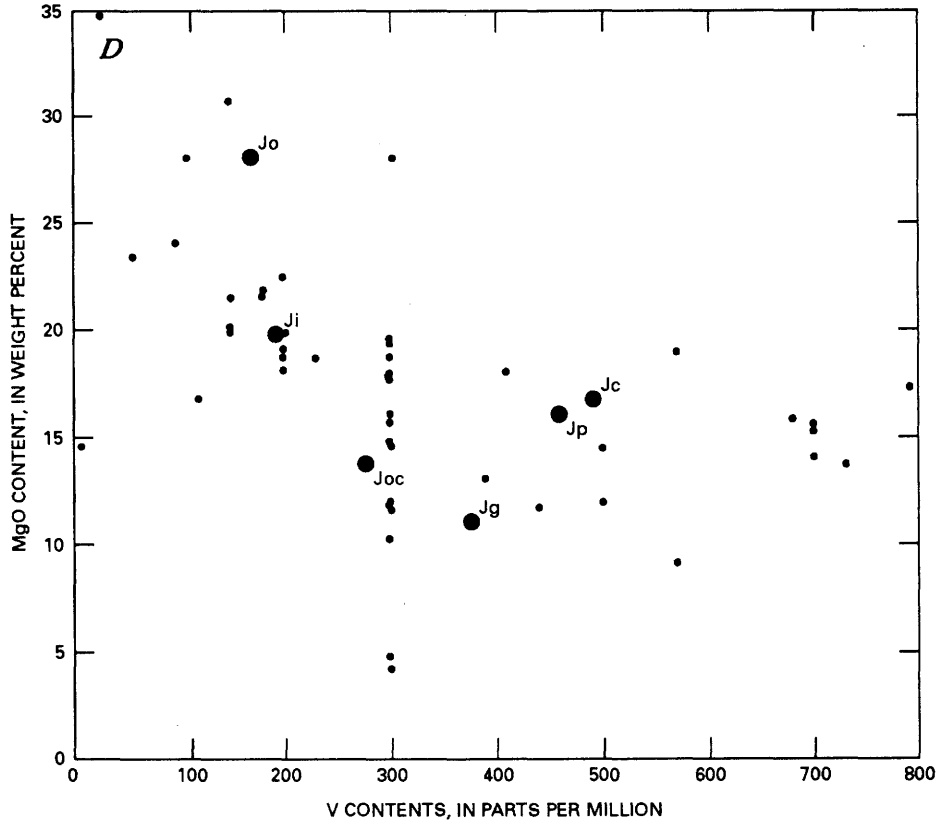

analyses listed in tables 7, 9, and 10. *A*, MgO versus Co content. *B*, MgO versus Cr content. *C*, MgO versus Ni content. *D*, undifferentiated; large dots, averages for each respective unit.

Copper substitutes in olivine, diopside, and plagioclase at very low levels, and relatively high Cu contents indicate that sulfide minerals are present in the rocks. The Cu contents summarized in tables 8 and 11 suggest that the distribution of copper in the rocks is unrelated to the mappable units and sequences of the pluton; figure 33 also supports this conclusion. All but one sample (pyritiferous shale) with a Cu content equal to or higher than 150 ppm occur in the northern segment of the pluton. Many high Cu contents in this segment occur near the margins of the pluton; figure 33 shows the distribution of modal hornblende, which demonstrates that high Cu contents are associated with the hornblende-rich areas. Cu contents between 70 and 149 ppm are scattered through the pluton; some are related to margins or faults, others to the hornblende-rich areas, and still others to no obvious feature. The association of Cu-rich areas with hornblende-rich areas may imply that the development of minor amounts of copper sulfide minerals is related to the timing and crystallization of magmatic hornblende and may not represent an immiscible-sulfide-melt event in the crystallization history of the pluton.

The distributions of platinum and palladium in rocks of the pluton are plotted in figure 34 and listed in table 13. There appears to be no correlation of Pt or Pd content with spatial position in the pluton, or with rock type or the intrusive sequence.

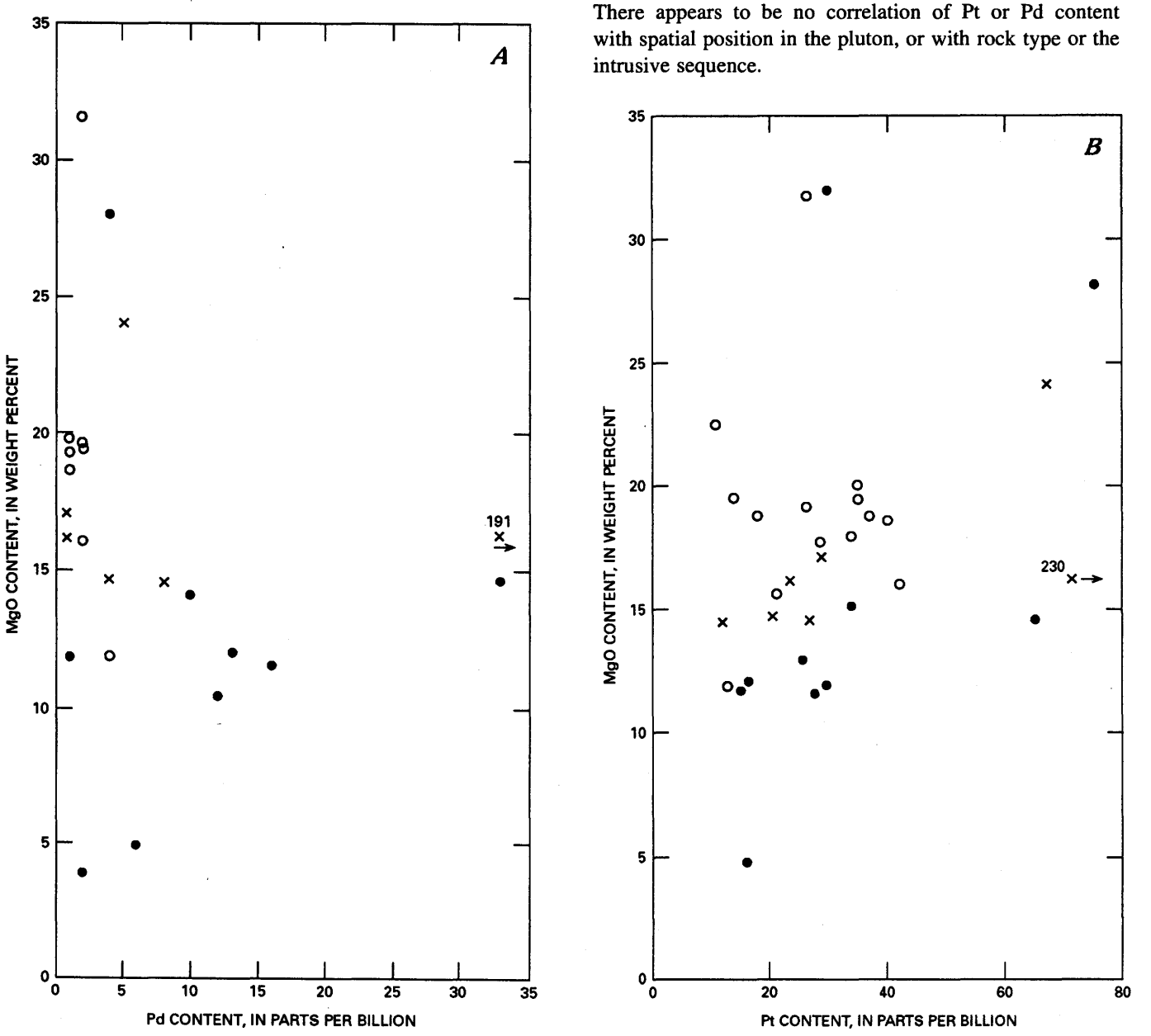

Figure 29. MgO versus Pd (*A*) and Pt (*B*) contents in rocks of the layered and intrusive sequences, based on analyses listed in tables 7, 9, and 10. Dots, gabbro and olivine cumulate units, undifferentiated; circles, olivine-clinopyroxene cumulate and layered olivine-clinopyroxene cumulate units, undifferentiated; x's, clinopyroxene-olivine cumulate and plagioclase-rich clinopyroxene-olivine cumulate, undifferentiated.

Soil Geochemistry

A reconnaissance soil geochemical survey, based on samples from hand-augered holes, was done to explore the feasibility of using soil samples to search for PGE-rich areas. Samples were collected at measured intervals downhole and analyzed by a six-step spectrographic method. Platinum, palladium, and rhodium were determined by fire-assay/atomic-absorption techniques, and selected samples were analyzed for gold and silver. The results are listed in table 14 for selected trace- and platinum-group elements by soil-sample interval and protolith. The distribution of platinum in soils is plotted in figure 35, and the locations of soil samples are listed in table 14. Samples used to represent the protolith are from the nearest outcrop of the appropriate rock type on which the soil was developed. Elements not found above the detection limits (in parentheses) include Ag (<0.05 ppm), As (1,000 ppm), Au (20 ppm), B 20 ppm), Be (1 ppm), Bi (20 ppm), Cd 150 ppm), La 30 ppm), Mo (3 ppm), Nb (10 ppm), Pb 10 ppm), Sb (150 ppm), Sn (10

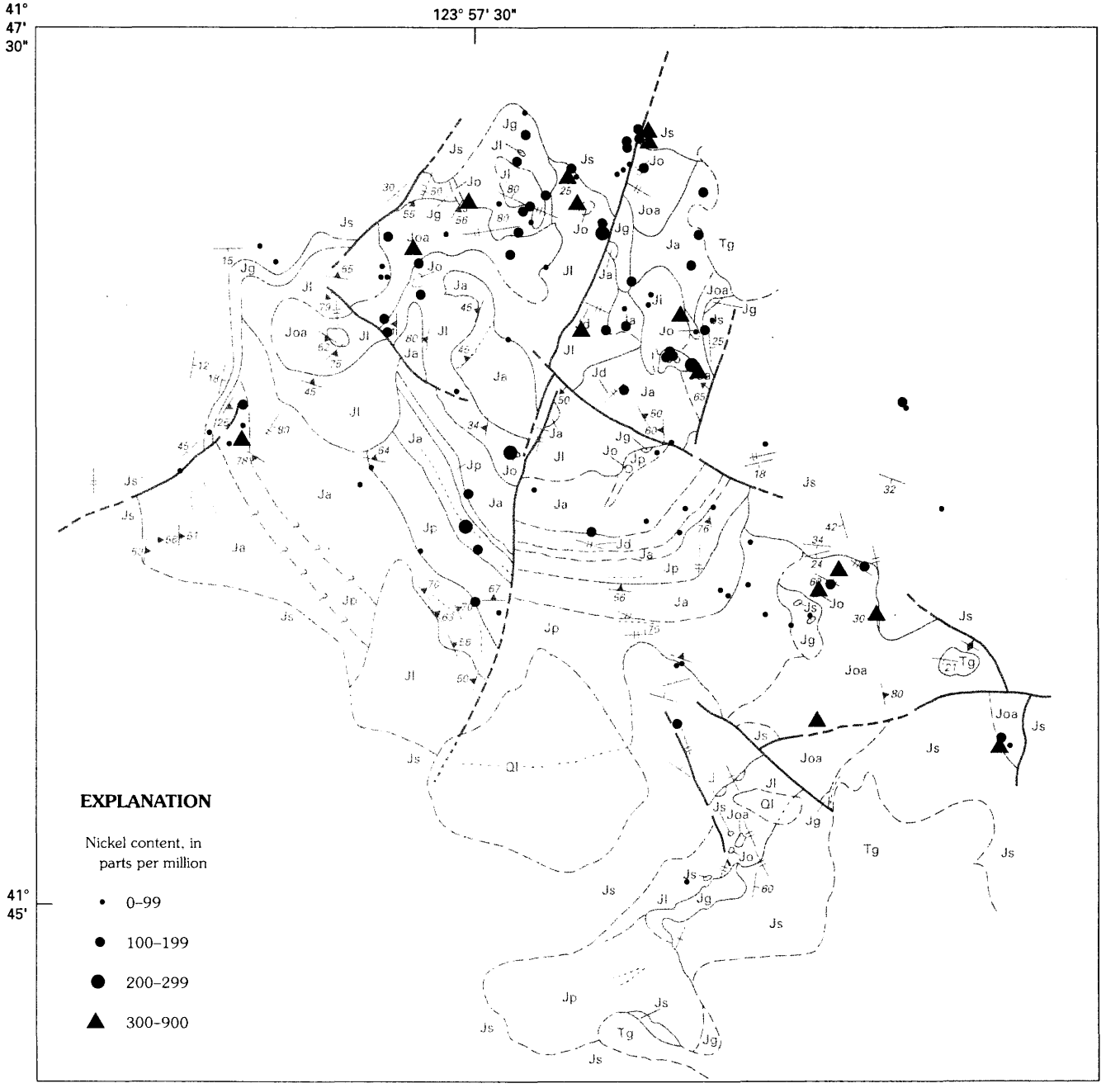

Figure 30. Geologic sketch map of the Lower Coon Mountain pluton, showing distribution of nickel in rock samples. See plate 1 for explanation.

ppm), Te (1,000 ppm), V (500 ppm), W (100 ppm), Zn (300 ppm), Ce (200 ppm), K (0.7 weight percent), and P (0.2 weight percent). Ba, Se, Sr, Na, and Ga were detected in the soil samples but are not listed in table 14.

Pd content in the soil samples ranges from less than 1 to 33 ppb and averages about 3 ppb, with a standard deviation of 6 ppb. Pt content ranges widely from 17 to 181 ppb and averages about 70 ppb, with a standard deviation of 48 ppb. In 1985, the Polar Resources Co. completed a soil-sample survey over the Lower Coon Mountain pluton (C.W. Hunt, written commun., 1985) that consisted of 408 samples collected on a grid system. The samples were analyzed by fire-assay/atomic-absorption techniques for platinum. Pt contents ranged from 1 to 337 ppb and averaged 51.4 ppb, with a standard deviation of 59.9 ppb; two maximums were 225 and 425 ppb. Thus, the results from this larger survey are compatible with those of the reconnaissance survey.

Profiles for the distribution of platinum in selected auger holes (fig. 36) indicate that in 6 of the 12 profiles, Pt content is highest in the lowest interval sampled, and in 4 of the 12 profiles, in the middle interval sampled. This re-

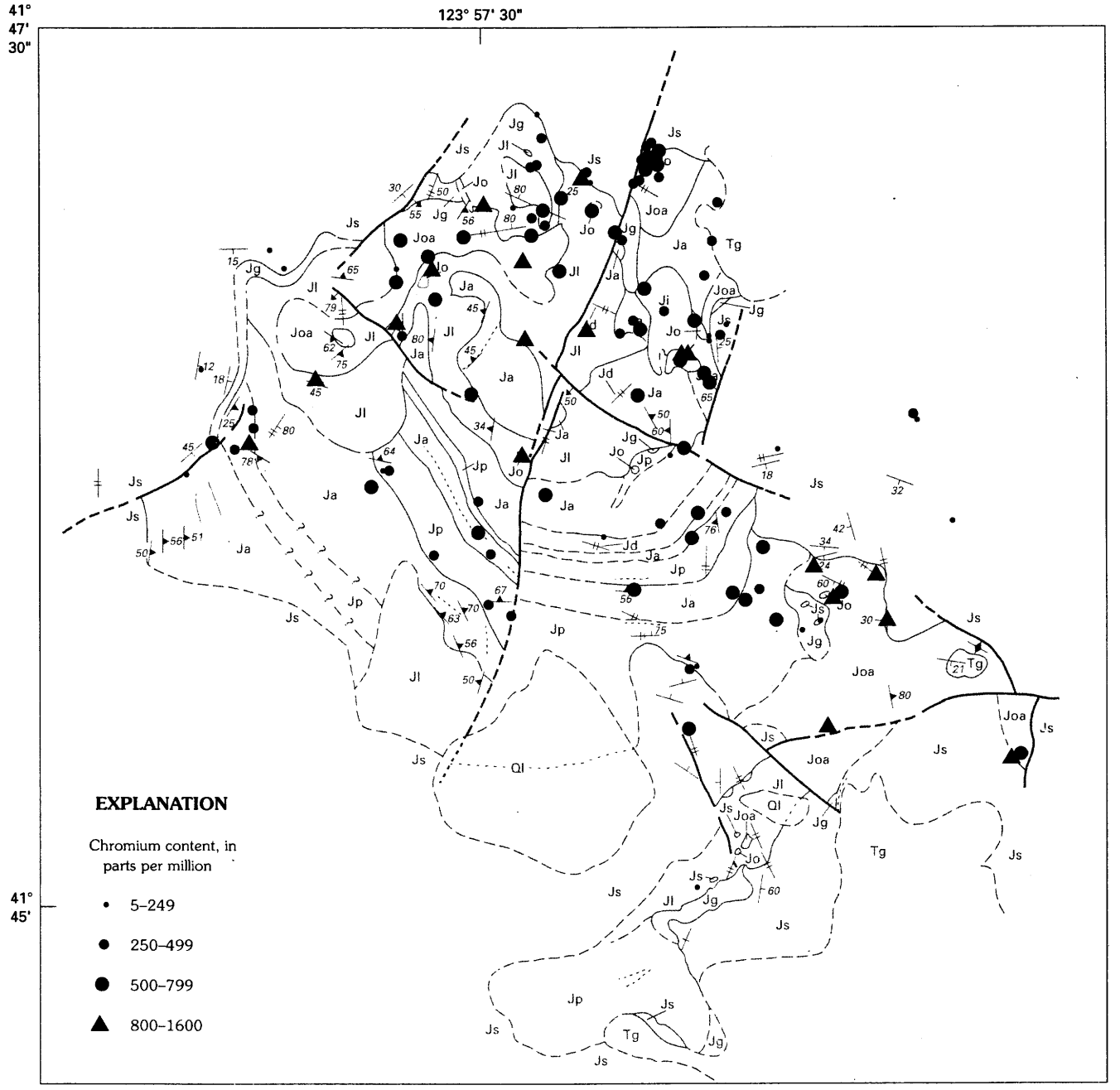

Figure 31. Geologic sketch map of the Lower Coon Mountain pluton, showing distribution of chromium in rock samples. See plate 1 for explanation.

connaissance study suggests that the lower to middle intervals of the profiles are Pt rich; however, analyses of other selected trace elements suggest that they have not been enriched in the lower intervals. The top parts of the soil profiles consist of dark-reddish-brown laterite except for samples 22CM81, 31CM81, and 62CM81, which contain abundant organic material. Locally, some of the soils contain iron oxide pellets, which were excluded from the sample. The lower parts of soil are light-tan to brown laterite containing semidecomposed pieces of protolith in their lowest parts. Generally, the hand-augered holes were not continued into soil containing semidecomposed protolith. The highest Pt content in a single auger hole is plotted in figure 35. No spatial-distribution patterns are discernible for platinum in the soils, owing to the limited number of samples collected in the reconnaissance study.

The Pt and Pd contents of rock samples from the pluton (fig. 34) range from less than 10 to 230 ppb and from less than 1 to 47 ppb, respectively. Most Pt contents range from less than 10 to 30 ppb, and most Pd contents from less

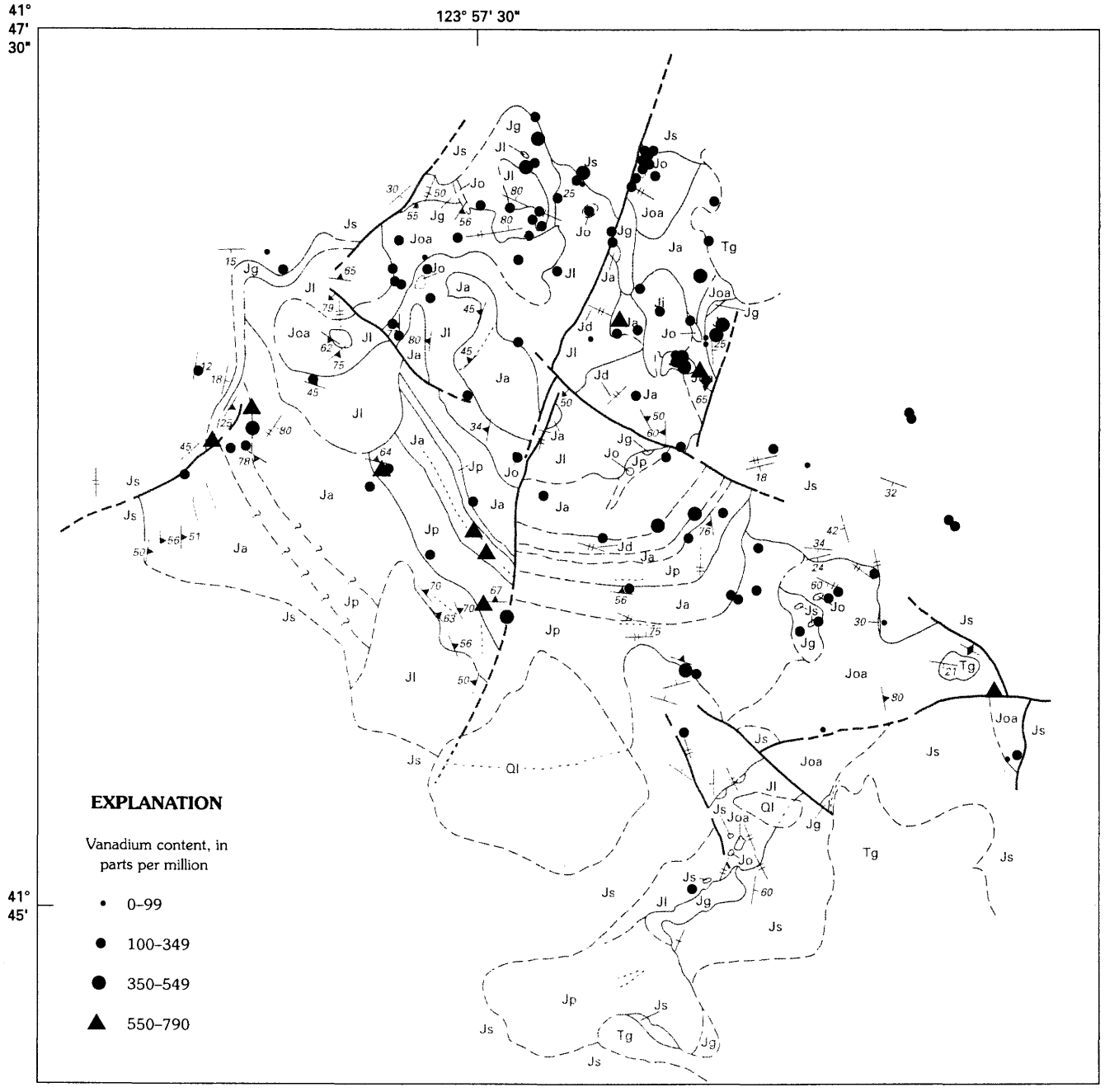

Figure 32. Geologic sketch map of the Lower Coon Mountain pluton, showing distribution of vanadium in rock samples. See plate 1 for explanation.

than 1 to 10 ppb. The immediate protoliths of the soil samples (table 14) reflect these ranges in Pt and Pd contents. Calculated ratios of Pt and Pd contents in soils versus the protoliths (table 14) demonstrate that both elements tend to be concentrated in the soils with respect to the protoliths. Platinum is enriched in soils as much as 7 times, and palladium as much 4 times, above the protoliths. On the average, both elements are enriched about twice as much in the soils as in the protolith. Other trace elements, such as Co, Cr, V, Ni, and Cu, are enriched in the soils by about the same factor as, or more than, the protoliths. Copper generally is the most enriched trace element in the soils.

PETROGENETIC DISCUSSION AND CONCLUSIONS

Field, petrologic, and geochemical evidence indicates that the Lower Coon Mountain pluton was formed by fractional crystallization from at least two magmas and thus pro-

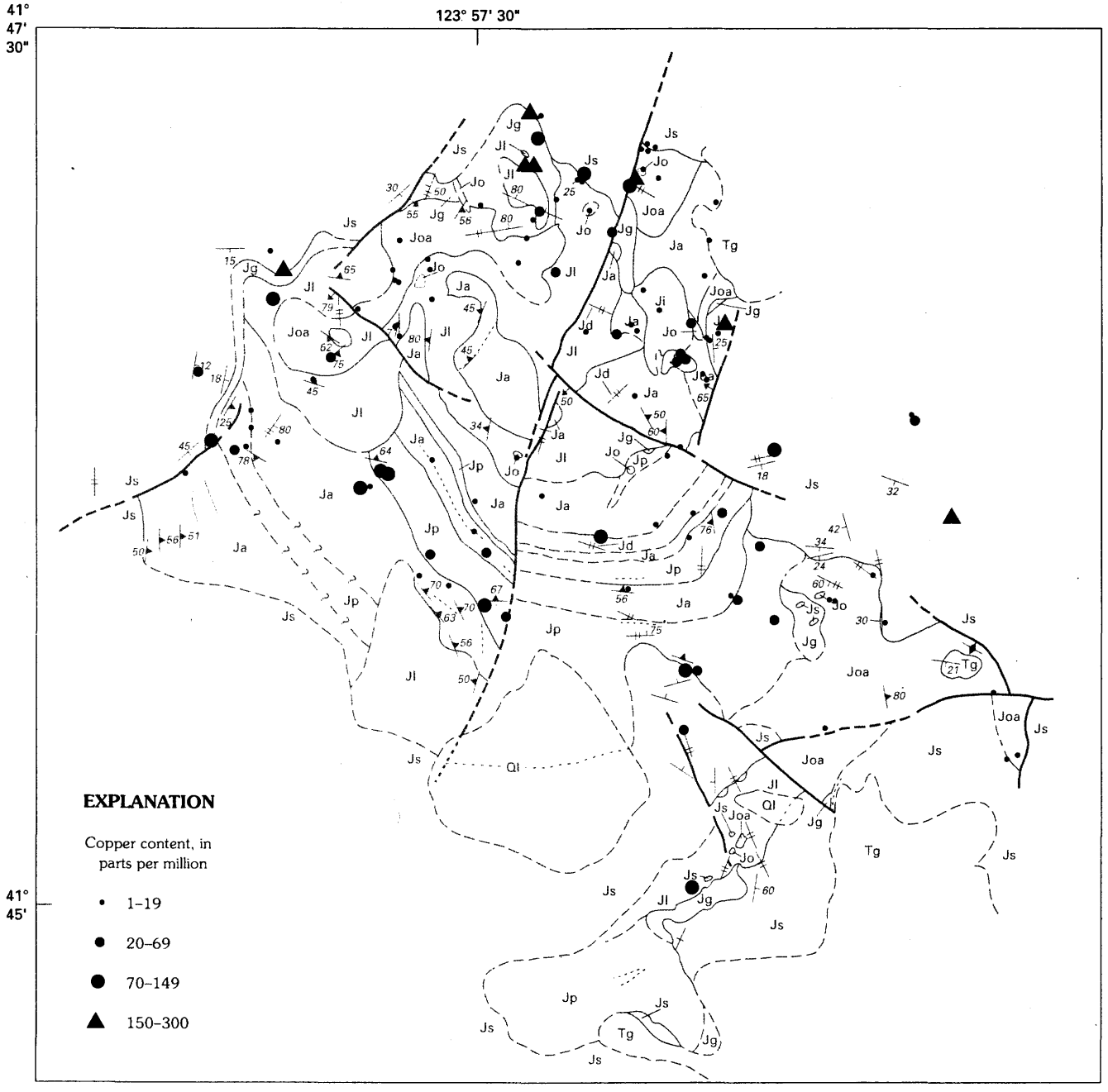

Figure 33. Geologic sketch map of the Lower Coon Mountain pluton, showing distribution of copper in rock samples. See plate 1 for explanation.

duced cumulates of clinopyroxene, olivine, magnetite, and plagioclase in various proportions. Increases in Ni, Cr, and Co contents relative to MgO content in rock units from youngest to oldest of both the layered and intrusive sequences are strong evidence for fractional crystallization. Limited variations in major-element composition of the minerals in both sequences suggest complexities to a simple process. Various questions need to be addressed to attempt to resolve some of the apparent conflicts: (1) What was the composition of the magma(s) involved? (2) What were the processes of crystallization? and (3) Were the magmas saturated with sulfur, so that they could have produced PGE concentrations? In this section, these questions are addressed and evaluated with respect to the potential for a PGE deposit associated with the Lower Coon Mountain pluton.

Consideration of Magma Compositions

Geologic, petrologic, and geochemical evidence indicates at least two major introductions of magma to form the

Figure 34. Geologic sketch map of the Lower Coon Mountain pluton, showing distribution of platinum and palladium in rock samples. See plate 1 for explanation.

Lower Coon Mountain pluton. No fine-grained marginal rocks with the appropriate geologic relations to the pluton have been identified that might represent these magma compositions. Because the rocks are cumulates, no individual rock type represents a liquid composition. If we assume that all the introduced magma crystallized by fractional crystallization and remained where it was emplaced—that is, a totally closed system—then an average composition of the pluton could represent a parental liquid. If we assume, however, that the introduced magma produced the cumulus products observed and extrusive volcanic products not observed—that is, an open system—then an average composition of the pluton will not represent a parental liquid. In the layered sequence, repetitive cycles and the absence of extreme variation in mineral composition between or within cycles suggest either the introduction of an extremely large volume of magma at one time, with a convection process to produce the cycles and a large volume of magma to keep compositions similar; or multiple introduction of smaller batches of magma with closely similar compositions. The

Figure 34.—Continued.

excess magma from cumulates of the layered sequence is absent in the intrusion, most likely removed as extrusive volcanic products. The intrusive sequence also contains cumulates that, as evidenced by crosscutting relations, imply the introduction of a sequence of magmas whose total products as rocks are absent in the pluton. Therefore, the combined geologic and chemical evidence strongly suggests that the Lower Coon Mountain pluton represents the cumulus products from an open system in which part of the products are missing.

Nevertheless, average compositions of the sequences and pluton were calculated for comparison with the Duke Island ultramafic complex, Alaska (Irvine, 1974). Besides the above considerations, the extent to which these averages represent initial magmas depends on the mechanics of the computations, the representativeness of rock analyses of a unit, and assumptions that the outcrop areas of units represent the composition of the intrusion. The average compositions of the layered and intrusive sequences (cols. 1, 2, table 15) emphasize the differences in major-element

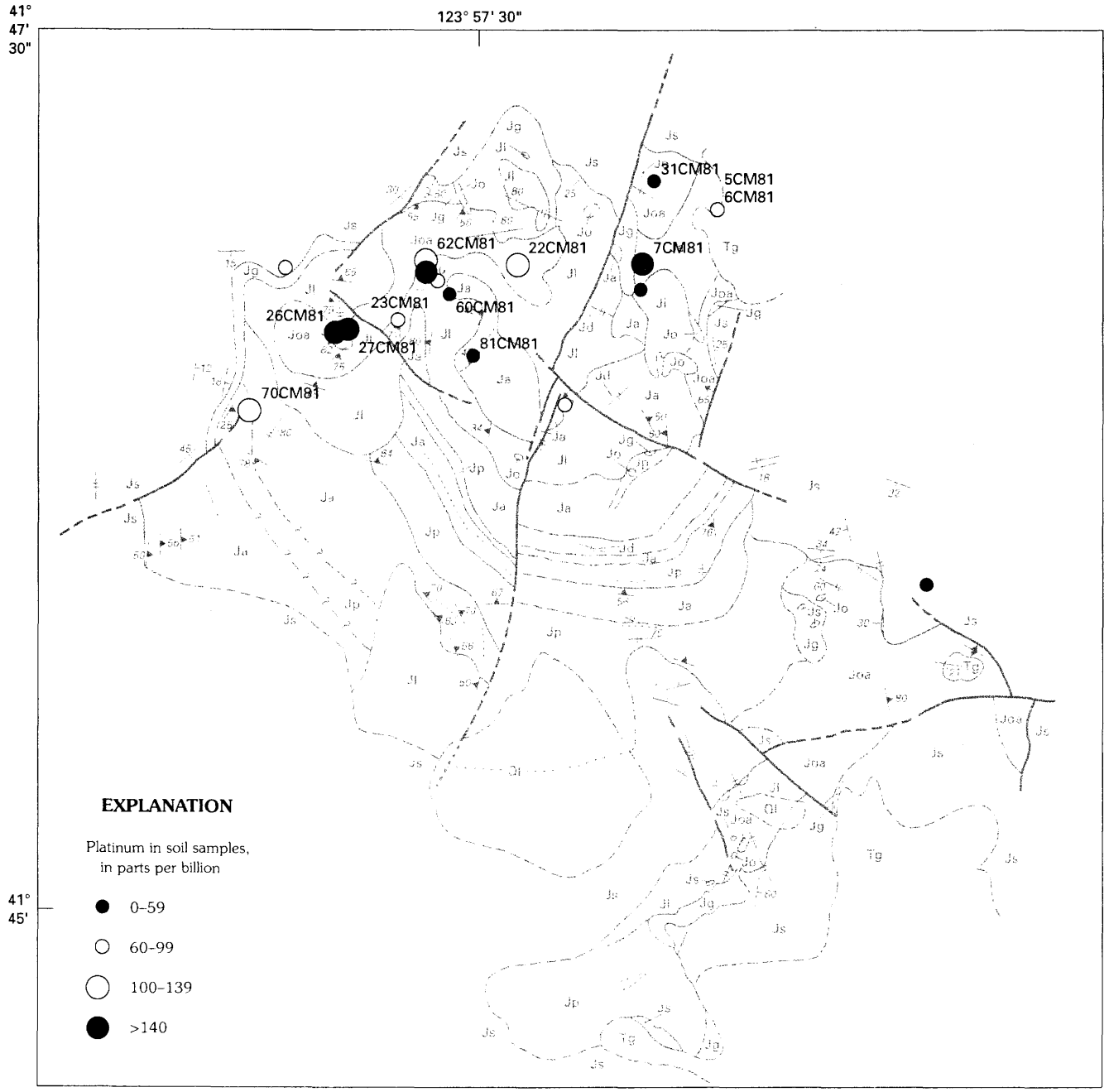

Figure 35. Geologic sketch map of the Lower Coon Mountain pluton, showing distribution of platinum in soil samples. See plate 1 for explanation and figure 36 for platinum data for selected samples (numbered).

contents between the two sequences. The layered sequence has higher total Fe and TiO_2 contents than the intrusive sequence, as reflected in the modal data by higher magnetite contents; it also has higher total Al_2O_3 contents. In comparison with the Duke Island ultramafic complex (col. 4, table 15), the Lower Coon Mountain pluton (col. 3, table 15) has, on average, slightly lower SiO_2 contents and higher total Fe and TiO_2 contents, but nearly the same composition within the errors of the calculations.

Recalculated analyses (cols. 5–9, table 15) demonstrate that similar statements or arguments about the crystallization of ultrabasic magmas made by Irvine (1963, 1974) and Presnall (1966) for the Duke Island ultramafic complex, Alaska, could be made for the Lower Coon Mountain pluton: (1) fractional crystallization of olivine, rich in magnesium, at the liquidus temperature, later joined by diopside, and still later by diopside and spinel (Presnall, 1966); (2) potential cotectic precipitation of olivine and diopside (Irvine, 1963, 1974; Presnall, 1966); (3) low SiO_2 activities (Irvine, 1974); (4) high Fe_2O_3 activities (Irvine, 1974); (5) a maximum formation temperature of olivine-clinopyroxene cumulate of 1,389°C (Irvine, 1974); and (6) possible buffering of oxygen fugacity by water (Presnall, 1966; Irvine, 1974). Although, in general, all of these statements are probably applicable, without the rest of the magma system they are impossible to document

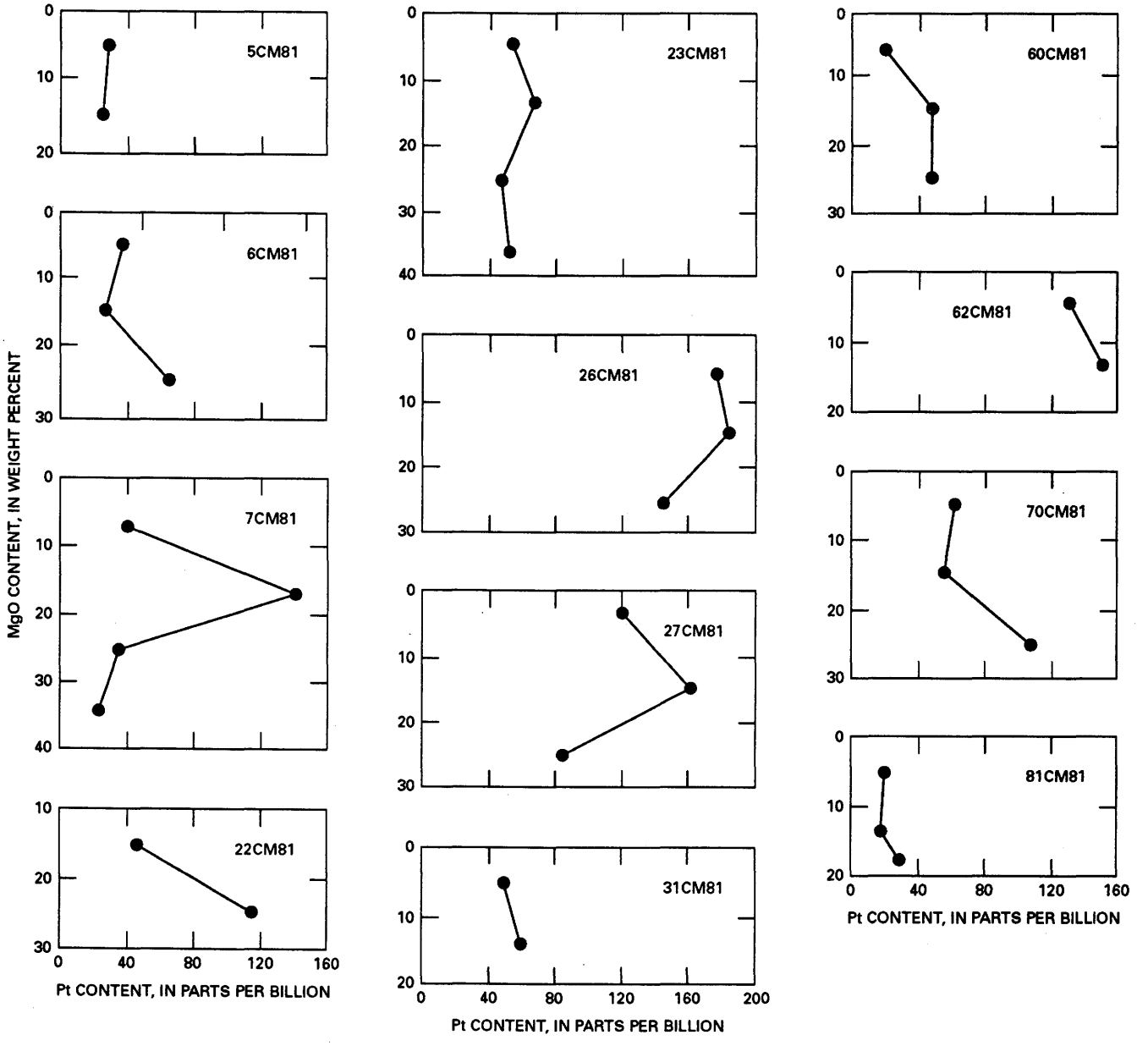

Figure 36. Profiles of selected auger holes in soils of the Lower Coon Mountain pluton, showing distribution of platinum in soil samples. See figure 35 for locations of samples.

in detail. More recent interpretations of the petrogenesis of Alaskan-type complexes involve crystallization differentiation of basaltic magmas to produce the observed cumulates (Murray, 1972; Irvine, 1974; Himmelberg and others, 1986). The exact composition of such magmas remains obscure and under debate.

Other evidence concerning the composition of the magmas involved in the Lower Coon Mountain pluton may be inferred from clinopyroxene compositions. LeBas (1962) and Leterrier and others (1982) appear to have successfully discriminated clinopyroxenes that crystallized from subalkaline, peralkaline, and normal alkaline magmas. Higher Ca, Ti, and Al contents tend to characterize those clinopyroxenes that crystallized from alkaline magmas, whereas lower contents tend to characterize those that crystallized from subalkaline magmas. LeBas (1962) showed that the Al and Ti contents of clinopyroxene increase as the composition of the magma changes from peralkaline through alkaline to subalkaline. The similar compositions of clinopyroxene with respect to Al_2O_3 content (fig. 37*A*) and TiO_2 and Al^{IV} contents (fig. 37*B*) in both the layered and intrusive sequences indicate that the parental magmas were subalkaline to alkaline in composition. Clinopyroxenes in the Duke Island ultramafic complex (Irvine, 1974) and in the Blashke Islands, Alaska (Himmelberg and others, 1986), are also plotted in figure 37 for comparison. Clinopyroxenes in the Duke Island ultramafic complex are nearly identical in composition to those in the Lower Coon Mountain pluton, whereas those

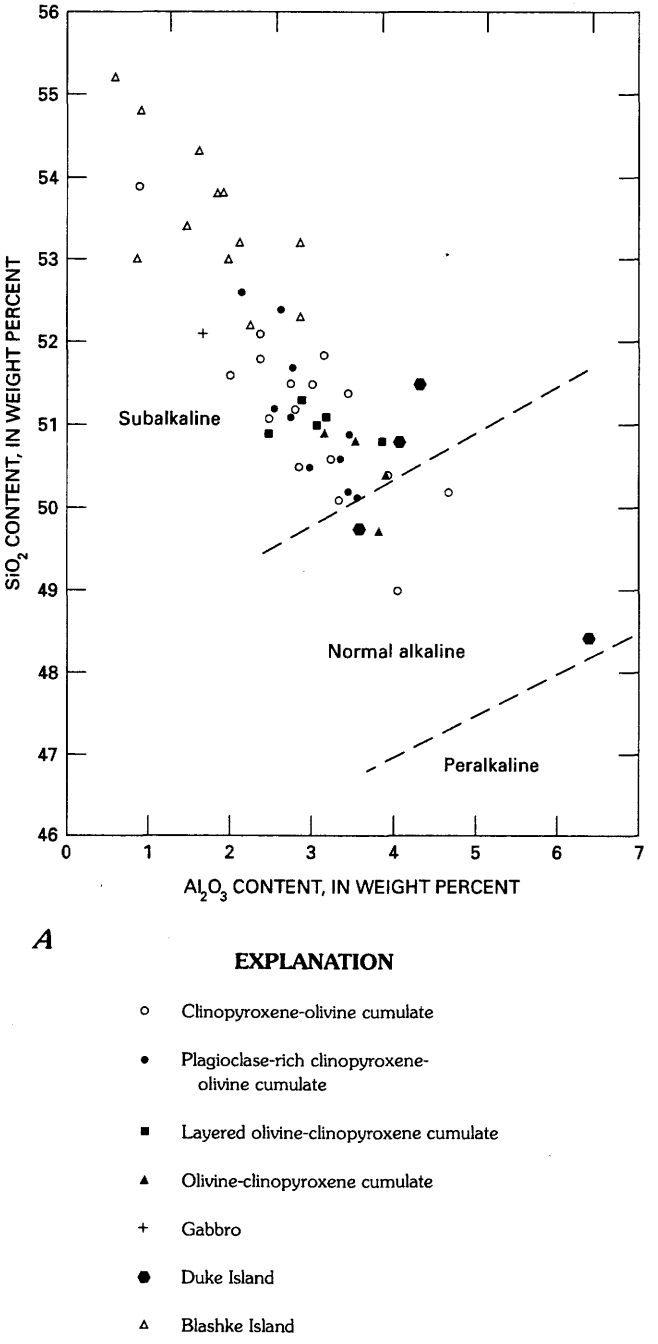

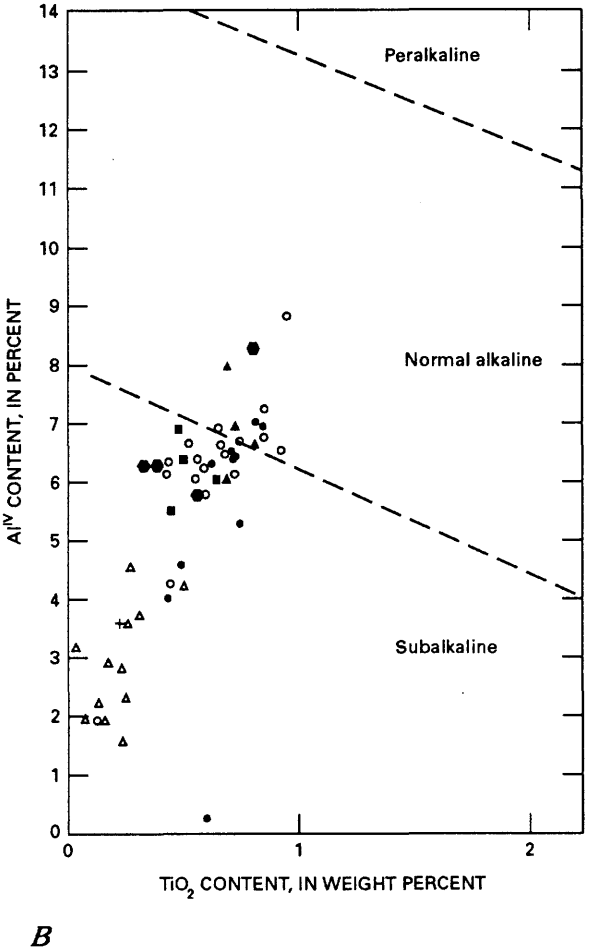

Figure 37. Modal compositions of clinopyroxene in rocks of the Lower Coon Mountain pluton, Duke Island, and Blashke Island. *A*, SiO_2 versus Al_2O_3 content. *B*, Proportion of tetrahedral Al^{IV} versus TiO_2 content. For comparison, Duke Island data from Irvine (1974), Blashke Island data from Himmelberg and others (1986), and boundaries between compositional fields from LeBas (1962).

in the Blashke Islands have lower Al_2O_3, TiO_2, and Al^{IV}-contents and thus crystallized from less alkaline magmas than those in the Lower Coon Mountain pluton.

Crystallization of the Magmas

The subalkaline magmas that formed all the rock units of both the layered and intrusive sequences of the Lower Coon Mountain pluton crystallized magnetite first, as evidenced by its occurrence as inclusions in all other cumulus phases. In most of the units, magnetite was closely followed by olivine, or olivine and magnetite were the first products of crystallization. Except in the gabbro, clinopyroxene was next to crystallize as a cumulus mineral, and, apparently, olivine and magnetite continued to crystallize with clinopyroxene. In the gabbro, plagioclase preceded clinopyroxene and continued to crystallize with clinopyroxene, as did olivine and magnetite. Minor variations on these general sequences of crystallization are found in the plagioclase-rich clinopyroxene-olivine cumulate of the layered sequence, where in some rocks plagioclase crystallized before clinopyroxene, and in other rocks clinopyroxene appears to have been resorbed sometime after its initial crystallization. In the cumulus rocks, plagioclase, hornblende, and other accessory minerals are postcumulus and partly crystallized in the interstices between the cumulus minerals. Clinopyroxene, olivine, and plagioclase also crystallized as overgrowths on the cumulus minerals. Hornblende formed partly by replacement of clinopyroxene and, where abundant, appears to have formed by a very late stage process, as evidenced by its spatial concentration in areas near contacts, without regard to rock type.

Sulfur Saturation in the Magmas

Very few of the rock samples from all units of the layered and intrusive sequences seem to have been saturated in sulfur when the cumulus minerals crystallized. If the subalkaline magmas had been so saturated, an immiscible sulfide liquid would have been produced, some of which would probably have been trapped as inclusions in the cumulus minerals. A few samples of the plagioclase-rich clinopyroxene-olivine cumulate contain inclusions of chalcopyrite and pyrrhotite in clinopyroxene, an observation suggesting that the magma forming this unit may have been saturated in sulfur. Rocks of the other units contain sulfide minerals, but only at grain boundaries and in interstices. In summary, the rocks of the Lower Coon Mountain pluton show little evidence for sulfide saturation early in the crystallization history of the magmas that produced the rocks.

Potential for Platinum-Group-Element Deposits

The rock and soil geochemical surveys suggest that the potential for a large-tonnage, high-grade PGE deposit associated with the Lower Coon Mountain pluton is small. Consideration of the absence of evidence for sulfide saturation before or during crystallization of the pluton also suggests the absence of this magma-concentration process to form such a deposit.

REFERENCES CITED

Albee, A.L., and Ray, Lily, 1970, Correction factors for electron probe microanalysis of silicates, oxides, carbonates, phosphates, and sulfates: Analytical Chemistry, v. 42, no. 12, p. 1408–1414.

Bence, A.E., and Albee, A.L., 1968, Empirical correction factors for the electron microanalysis of silicates and oxides: Journal of Geology, v. 76, no. 4, p. 382–403.

Bingler, E.C., Trexler, D.J., Kemp, W.R., and Bonham, H.F., Jr., 1976, PETCAL: A *BASIC* language computer program for petrologic calculations: Nevada Bureau of Mines and Geology Report 28, 27 p.

Blake, M.C., Jr., Howell, D.G., and Jones, D.L., 1982, Preliminary tectonostratigraphic terrane map of California: U.S. Geological Survey Open-File Report 82–593, 9 p., scale 1:750,000, 3 sheets.

Cater, F.W., Jr., and Wells, F.C., 1953, Geology and mineral resources of the Gasquet quadrangle, California-Oregon: U.S. Geological Survey Bulletin 995–C, p. 79–133.

Evans, J.G., 1984, Structure of part of the Josephine Peridotite, northwestern California and southwestern Oregon, *in* Geological and geophysical studies of chromite deposits in the Josephine Peridotite, northwestern California and southwestern Oregon: U.S. Geological Survey Bulletin 1546–A, p. 7–37.

Fabbi, B.P., 1972, A refined fusion X-ray fluorescence technique, and determination of major and minor elements in silicate standards: American Mineralogist, v. 57, no. 1–2, p. 237–245.

Gray, Floyd, and Page, N.J, 1985, Geologic map of the Lower Coon Mountain pluton, Del Norte County, California: U.S. Geological Survey Open-File Report 85–148, scale 1:24,000.

Gray, Floyd, Page, N.J, Carlson, C.A., Wilson, S.A., and Carlson, R.R., 1986, Platinum-group element geochemistry of zoned ultramafic intrusive suites, Klamath Mountains, California and Oregon: Economic Geology, v. 81, no. 5, p. 1252–1260.

Griscom, Andrew, 1984, A magnetic interpretation of the Josephine Periodotite, Del Norte County, California, *in* Geological and geophysical studies of chromite deposits in the Josephine Peridotite, northwestern California and southwestern Oregon: U.S. Geological Survey Bulletin 1546–D, p. 53–63.

Haffty, Joseph, Haubert, A.W., and Page, N.J, 1980, Determination of iridium and ruthenium in geological samples by fire

assay and emission spectrography: U.S. Geological Survey Professional Paper 1129–G, p. G1–G4.

Haffty, Joseph, Riley, L.B., and Goss, W.D., 1977, A manual on fire assaying and determination of the noble metals in geological materials: U.S. Geological Survey Bulletin 1445, 58 p.

Harper, G.D., 1980a, Structure and petrology of the Josephine ophiolite and overlying metasedimentary rocks, northwestern California: Berkeley, University of California, Ph.D. thesis, 260 p.

———1980b, The Josephine ophiolite—remains of a Late Jurassic marginal basin in northwestern California: Geology, v. 8, no. 7, p. 333–337.

Himmelberg, G.R., Loney, R.A., and Craig, J.T., 1986, Petrogenesis of the ultramafic complex at the Blashke Islands, southeastern Alaska: U.S. Geological Survey Bulletin 1662, 14 p.

Irvine, T.N., 1963, Origin of the ultramafic complex at Duke Island, southeastern Alaska, *in* Fisher, D.J., Frueh, A.J., Jr., Hurlbut, C.J., Jr., and Tilley, C.E., eds., International Mineralogical Association General Meeting, 3d, Washington, 1962, Papers and Proceedings: Mineralogical Society of America Special Paper 1, p. 36–45.

———1974, Petrology of Duke Island ultramafic complex, southeastern Alaska: Geological Society of America Memoir 138, 240 p.

Irvine, T.N., and Baragar, W.R.A., 1971, A guide to the chemical classification of the common volcanic rocks: Canadian Journal of Earth Sciences, v. 8, no. 5, p. 523–548.

Irwin, W.P., 1964, Late Mesozoic orogenies in the ultramafic belts of northwestern California and southwestern Oregon, *in* Geological Survey research, 1964: U.S. Geological Survey Professional Paper 501–C, p. C1–C9.

———1972, Terranes of the western Paleozoic and Triassic belt in the southern Klamath Mountains, California, *in* Geological Survey research, 1972: U.S. Geological Survey Professional Paper 800–C, p. C103–C111.

IUGS Subcommission on the Systematics of Igneous Rocks, 1973, Classification and nomenclature of plutonic rocks: Recommendation: Neues Jahrbuch für Mineralogie Monatshefte 1973, no. 4, p. 149–164.

LeBas, N.H., 1962, The role of aluminum in igneous clinopyroxenes with relation to their parentage: American Journal of Science, v. 260, no. 4, p. 267–288.

Leterrier, Jacques, Maury, R.C., Thonon, Pierre, Girard, Danielle, and Marchal, Michele, 1982, Clinopyroxene as a method of identification of the magmatic affinities of paleovolcanic series: Earth and Planetary Science Letters, v. 59, no. 1, p. 139–154.

Logan, C.A., 1919, Platinum and allied metals in California: California Mining Bureau Bulletin 85, 120 p.

Murray, C.G., 1972, Zoned ultramafic complexes of the Alaskan type: Feeder pipes of andesitic volcanoes, *in* Shagam, R.E., Hargraves, R.B., Morgan, W.J., Van Houten, F.B., Burk, C.A., Holland, H.D., and Hollister, L.C., eds., Studies in earth and space sciences (Hess volume): Geological Society of America Memoir 132, p. 313–335.

Osborn, E.F., and Tait, D.B., 1952, The system diopside-forsterite-anorthite: America Journal of Science (Bowen volume), v. 258–A, p. 413–433.

Page, N.J, Myers, J.S., Haffty, Joseph, Simon, F.O., and Aruscavage, P.J., 1980, Platinum, palladium, and rhodium in the Fiskenaesset Complex, southwestern Greenland: Economic Geology, v. 75, no. 6, p. 907–915.

Page, N.J, and Gray, Floyd, 1985, Platinum in soils and rocks from the Lower Coon Mountain pluton, Del Norte County, California: U.S. Geological Survey Open-File Report 85–149, scale 1:24,000.

Papike, J.J., Cameron, K.L., and Baldwin, K., 1974, Amphiboles and pyroxenes: Characterization of *other* than quadrilateral components and estimates of ferric iron from microprobe data [abs.]: Geological Society of America Abstracts with Programs, v. 6, no. 7, p. 1053–1054.

Poldervaart, Arie, and Hess, H.H., 1951, Pyroxenes in the crystallization of basaltic magmas: Journal of Geology, v. 59, no. 5, p. 472–489.

Presnall, D.C., 1966, The join fosterite-diopside-iron oxide and its bearing on the crystallization of basaltic and ultramafic magmas: American Journal of Science, v. 264, no. 10, p. 753–809.

Saleeby, J.B., Harper, G.D., Snoke, A.W., and Sharp, W.D., 1982, Time relations and structural-stratigraphic patterns in ophiolitic accretion, west central Klamath Mountains, California: Journal of Geophysical Research, v. 87, no. B5, p. 3831–3848.

Shapiro, Leonard, 1975, Rapid analysis of silicate, carbonate, and phosphate rocks—revised edition: U.S. Geological Survey Bulletin 1401, 76 p.

Silberling, N.J., Jones, D.L., Blake, M.C., Jr., and Howell, D.G., 1984, Lithotectonic terrane map of the western conterminous United States, pt. C *of* Silberling, N.J., and Jones, D.L., eds., Lithotectonic terrane maps of the North American Cordillera: U.S. Geological Survey Open-File Report 84–523, p. C1–C43.

Simon, F.O., Aruscavage, P.J., and Moore, R., 1978, Determination of platinum, palladium, and rhodium in geologic materials by fire-assay and atomic absorption spectroscopy using electrothermal atomization [abs.]: American Chemical Society National Meeting, 176th, Miami Beach, Fla., 1978.

Smith, J.G., Page, N.J, Johnson, M.G., Moring, B.C., and Gray, Floyd, 1982, Preliminary geologic map of the Medford 1°×2° quadrangle, Oregon and California: U.S. Geological Survey Open-File Report 82–955, scale 1:250,000.

TABLES 3–15

Table 3. Chemical compositions and structural formulas of selected samples of clinopyroxenes from rocks of the Lower Coon Mountain pluton

[Major-element-oxide analyses in weight percent.Iron determined as FeO; Fe_2O_3, FeO, Fe^{3+}, and Fe^{2+} calculated from assumed stoichiometry, using the program of Papike and others (1974). —, not detected; ±. standard deviation. Number in parentheses after unit symbol indicates number of analyses of sample averaged to give values reported]

Sample	82CMG15	82CMG19	82CMG21	82CMG37	82CMG43	82CMG45	82CMG64	82CMG75	82CMG78	82CMG82	82CMG96	82CMG110
Unit (fig. 4)	Jp(3)	Jp	Jc(2)	Jl(4)	Jl(5)	Jc	Jg	Jp	Jc(3)	Jc	Jl	Jc
Major-element oxides												
SiO_2	51.7±1.5	50.2	53.9	51.3±0.1	50.8±0.8	51.8	52.1	52.6	50.6	51.0	51.0	51.6
Al_2O_3	2.77±1.19	3.44	.90	2.88±0.16	3.86±0.63	3.15	1.66	2.14	3.22	2.46	3.07	2.00
TiO_2	.49±0.19	.83	.12	.46±0.03	.67±0.06	.67	.22	.60	.84	.37	.63	.54
Cr_2O_3	.02±0.02	.02	.52	.08±0.07	.05±0.05	.05	.02	.02	.02	.02	.27	.04
Fe_2O_3	1.84±1.06	3.71	.69	3.47±0.25	2.26±0.3	2.34	2.46	.88	1.96	3.34	2.08	1.96
FeO	4.93±0.64	4.45	2.51	2.94±0.24	4.05±0.23	4.85	3.18	7.00	5.18	2.13	4.66	4.12
MnO	.13±0.01	.25	.11	.11±0.01	.17±0.02	.25	.24	.27	.21	.17	.18	.19
MgO	15.4±0.4	14.5	17.9	15.3±1	15.1±0.3	15.3	16.4	15.2	15.0	16.4	15.2	15.7
CaO	22.4±0.9	22.5	23.7	23.9±1	22.9±0.7	22.6	23.7	21.7	22.1	23.2	22.2	22.7
Na_2O	.21+0.10	.32	.10	.19±0.01	.19±0.03	.21	.12	.29	.21	.15	.26	.17
Total	99.89	100.22	100.45	100.63	99.95	101.35	100.11	100.70	99.34	99.28	99.55	99.08
Formula per four cations												
Si	1.908	1.861	1.955	1.882	1.874	1.890	1.919	1.935	1.885	1.888	1.892	1.919
Al^{IV}	.092	.139	.038	.118	.126	.110	.072	.005	.115	.107	.108	.081
Al^{VI}	.029	.011	.000	.006	.042	.026	.000	.028	.027	.000	.026	.007
Ti	.014	.023	.003	.013	.019	.018	.006	.017	.023	.010	.017	.015
Cr	.001	.001	.015	.002	.001	.001	.000	.001	.001	.005	.008	.001
Fe^{3+}	.050	.103	.024	.098	.059	.064	.068	.024	.055	.093	.058	.055
Fe^{2+}	.153	.138	.071	.088	.129	.148	.098	.215	.162	.066	.145	.128
Mn	.006	.008	.003	.003	.005	.008	.007	.008	.007	.005	.006	.006
Mg	.847	.789	.986	.836	.830	.823	.898	.833	.831	.903	.839	.871
Ca	.886	.895	.921	.939	.901	.884	.932	.854	.880	.918	.883	.905
Na	.015	.023	.007	.014	.014	.018	.009	.020	.015	.011	.018	.012
Wo	46.97	48.89	47.00	50.40	48.45	47.42	48.34	44.91	47.01	48.65	47.28	47.54
En	44.91	43.58	49.38	44.87	44.63	44.65	46.58	43.77	44.36	47.86	44.98	45.73
Fs	8.12	7.53	3.62	4.73	6.92	7.93	5.07	11.32	8.63	3.49	7.74	6.73

Table 3. Chemical compositions and structural formulas of selected samples of clinopyroxenes from rocks of the Lower Coon Mountain pluton—Continued

Sample	82CMP6	82CMP8	82CMP9	82CMP10	82CMP11	82CMP34	82CMP35	41CM81	83CMG4	83CMG8	83CMG10	82CMP1	82CMP3
Unit (fig. 4)	Jc	Jc	Jp	Jc	Jc	Jc	Jl	Joc	Jc	Joc (3)	Joc (3)	Joc	Jc
Major-element oxides													
SiO_2	50.2	51.4	50.9	51.5	51.3	50.5	51.9	50.6	50.4	50.9±0.2	50.8±0.7	49.7	50.5
Al_2O_3	4.68	3.45	3.47	3.00	2.74	3.60	2.44	3.99	3.91	3.13±0.28	3.52±0.74	3.80	3.73
TiO_2	.84	.51	.70	.65	.55	.64	.44	.80	.92	.67±0.08	.71±0.17	.67	.74
Cr_2O_3	.02	.05	.01	.02	.16	.04	.27	.07	.06	.02±0.01	.11±0.07	—	.14
Fe_2O_3	1.99	3.63	3.33	2.93	2.75	3.61	2.08	1.87	.85	2.92±0.24	2.43±0.79	4.62	2.82
FeO	5.10	2.90	3.80	5.02	3.67	3.69	3.48	4.88	5.88	4.26±0.10	4.27±0.52	2.92	4.25
MnO	.19	.15	.23	.24	.17	.19	.12	.18	.16	.17±0.01	.17±0.01	.14	.21
MgO	14.2	15.1	15.1	15.1	15.6	15.0	15.8	14.7	14.5	14.3±0.02	14.9±0.4	14.7	15.1
CaO	22.8	24.5	22.9	22.3	22.9	22.8	23.2	22.8	21.6	23.9±0.02	22.6±0.03	23.3	22.2
Na_2O	.21	.14	.27	.30	.21	.24	.20	.15	.33	.21+0.02	.23+0.04	.20	.26
Total	100.23	101.83	100.71	101.06	100.05	100.31	99.93	100.04	98.61	100.48	99.74	100.05	99.95
Formula per four cations													
Si	1.855	1.867	1.869	1.887	1.892	1.862	1.909	1.887	1.869	1.879	1.882	1.841	1.866
Al^{IV}	.145	.133	.131	.113	.108	.138	.091	.113	.131	.121	.118	.159	.134
Al^{VI}	.058	.015	.019	.017	.011	.018	.015	.060	.043	.015	.036	.007	.029
Ti	.023	.014	.019	.018	.015	.018	.012	.026	.022	.019	.020	.019	.021
Cr	.001	.002	—	—	.005	.001	.008	.002	.002	.001	.003	.000	.004
Fe^{3+}	.055	.099	.092	.081	.076	.100	.087	.024	.052	.083	.056	.129	.078
Fe^{2+}	.157	.088	.117	.154	.113	.114	.107	.184	.151	.130	.144	.090	.131
Mn	.006	.004	.007	.007	.005	.006	.004	.005	.006	.005	.005	.004	.007
Mg	.784	.816	.826	.825	.854	.826	.868	.810	.811	.787	.823	.812	.832
Ca	.901	.952	.899	.876	.906	.900	.914	.866	.903	.945	.897	.925	.880
Na	.015	.010	.020	.021	.015	.017	.014	.024	.011	.015	.017	.014	.018
Wo	48.91	51.30	48.83	47.24	48.35	48.92	48.37	46.56	48.44	50.77	48.15	50.63	47.75
En	42.54	43.94	44.84	44.47	45.61	44.90	45.96	43.55	43.47	42.25	44.15	44.43	45.12
Fs	8.55	4.76	6.34	8.29	6.03	6.19	5.67	9.89	8.09	6.99	7.71	4.94	7.13

Table 3. Chemical compositions and structural formulas of selected samples of clinopyroxenes from rocks of the Lower Coon Mountain pluton—Continued

Sample	82CMP4	82CMP5	82CMG126	82CMG131	82CMG133	82CMG134	82CMG146	82CMG150	82CMG152	82CMG166	82CMG172	82CMG173	4CM81
Unit (fig. 4)	Jp	Jc	Jc(4)	Jp	Jc	Jp	Jp	Jp	Jp	Jc	Jc	Jl	Jc
Major-element oxides													
SiO_2	52.4	50.1	5.2±1.2	50.5	51.8	50.6	51.2	51.1	50.1	49.0	52.2	51.1	51.5
Al_2O_3	2.61	3.33	2.80±0.23	2.98	2.38	3.37	2.53	2.74	3.54	4.04	2.38	3.19	2.73
TiO_2	.43	.72	.41±0.06	.72	.44	.71	.62	.73	.80	.83	.57	.49	.58
Cr_2O_3	.30	.02	.25±0.02	.02	.10	.03	.09	.06	.04	.04	.01	.15	.03
Fe_2O_3	1.15	2.80	2.57±0.81	3.77	1.69	3.19	3.05	2.73	3.28	5.22	1.85	2.11	1.80
FeO	4.81	4.42	3.04±0.79	4.14	4.23	4.37	4.34	5.37	3.64	2.96	6.11	4.55	5.28
MnO	.13	.22	.13±0.01	.27	.20	.27	.21	.32	.18	.24	.28	.17	.22
MgO	15.7	14.6	15.9±0.3	15.5	15.1	14.8	15.3	15.3	14.5	14.9	15.1	15.1	15.0
CaO	22.7	22.2	22.7±0.1	22.7	23.8	22.7	22.5	21.0	23.7	22.3	22.3	23.0	22.8
Na_2O	.22	.30	.19±0.02	.17	.10	.24	.25	.40	.14	.23	.23	.22	.16
Total	100.45	98.71	99.19	99.08	99.93	100.28	100.09	99.75	99.93	99.82	100.96	100.48	100.10
Formula per four cations													
Si	1.919	1.877	1.897	1.871	1.915	1.871	1.893	1.895	1.859	1.822	1.915	1.892	1.904
Al^{VI}	.081	.123	.103	.129	.085	.129	.107	.105	.141	.177	.085	.108	.096
Al^{VI}	.032	.024	.019	.001	.018	.017	.003	.015	.014	.000	.018	.031	.023
Ti	.012	.020	.011	.020	.012	.020	.017	.020	.022	.023	.016	.014	.016
Cr	.009	---	.007	.001	.003	.001	.002	.002	.001	.001	.000	.004	.001
Fe^{3+}	.032	.079	.068	.105	.047	.089	.085	.076	.091	.146	.051	.061	.050
Fe^{2+}	.147	.139	.098	.128	.131	.135	.134	.167	.113	.092	.188	.137	.163
Mn	.004	.007	.004	.008	.006	.008	.007	.010	.006	.007	.009	.005	.007
Mg	.859	.814	.878	.858	.832	.815	.843	.846	.800	.826	.827	.827	.825
Ca	.890	.894	.901	.862	.943	.898	.890	.836	.942	.889	.876	.906	.903
Na	.015	.022	.014	.017	.007	.017	.018	.029	.010	.017	.016	.016	.011
Wo	46.92	48.41	48.01	46.63	49.47	48.58	47.65	45.22	50.79	48.20	46.32	48.44	47.77
En	45.30	44.08	46.77	46.44	43.67	44.11	45.16	45.77	43.12	45.70	43.74	44.24	43.60
Fs	7.78	7.51	5.22	6.94	6.86	7.31	7.19	9.01	6.09	5.09	9.93	7.32	8.63

Table 4. Chemical compositions and structural formulas of selected samples of olivine from rocks of the Lower Coon Mountain pluton

[Electron-microprobe analyses in weight percent; analyst, F. Gray. Total iron determined as FeO. —, not detected; n.d., not determined]

Sample	82CMG30	82CMG30	82CMG30	82CMG36	82CMG36	82CMG36	82CMG77	82CMG131	82CMG131	82CMG136	82CMG136
Unit (fig. 4)	Jl	Jl	Jl	Jo	Jo	Jo	Jc	Jp	Jp	Jp	Jp
Major-element oxides											
SiO_2	49.7	49.1	49.4	44.9	44.3	44.9	45.1	44.9	44.7	45.4	44.4
Al_2O_3	31.9	32.7	32.4	35.1	35.1	35.0	35.2	34.8	35.6	33.8	34.8
FeO	.38	.30	.32	.33	.37	.37	.42	.36	.40	.65	.46
MgO	.12	.06	.05	.04	.04	.07	—	.05	.05	.18	—
CaO	15.5	16.1	15.6	18.9	18.6	19.0	18.8	18.5	18.6	18.5	18.3
Na_2O	2.64	2.45	2.61	1.09	1.11	1.06	.92	.93	.84	.97	1.07
K_2O	.07	.05	.04	.004	.01	.01	.004	.01	.01	.01	.05
BaO	—	—	—	—	—	n.d.	n.d.	—	—	n.d.	n.d.
SrO	.02	.05	.03	.17	.17	.13	—	.19	.17	n.d.	—
Total	100.33	100.81	100.45	100.534	99.7	100.54	100.444	99.74	100.37	99.51	99.08
Formula per 32 oxygens											
Si	9.066	8.925	9.001	8.277	8.180	8.283	8.306	8.264	8.234	8.353	8.126
Al	6.848	7.011	6.948	7.627	7.650	7.601	7.633	7.548	7.742	7.323	7.511
Fe	.058	.046	.049	.051	.057	.056	.065	.055	.062	.100	.070
Mg	.033	.016	.017	.012	.010	.020	—	.013	.014	.048	—
Ca	3.027	3.128	3.045	3.730	3.680	3.753	3.709	3.651	3.676	3.652	3.598
Na	.935	.864	.923	.388	.396	.379	.329	.333	.299	.346	.379
K	.016	.011	.009	.001	.001	.002	.001	.002	.002	.001	.011
Ba	—	—	—	n.d.	—	—	n.d.	—	—	n.d.	n.d.
Sr	.002	.005	.003	.018	.018	.014	—	.020	.019	n.d.	—
Z	15.970	15.982	15.998	15.955	15.887	15.94	16.004	15.867	16.038	15.776	15.707
X	3.980	4.003	3.980	4.137	4.095	4.148	4.039	4.006	3.996	3.999	3.988
Calculated Ab, An, and Or contents of plagioclase											
An	76.09	78.14	76.57	90.56	90.26	90.78	91.83	91.60	92.43	91.32	90.22
Ab	23.50	21.58	23.21	9.42	9.71	9.17	8.15	8.35	7.52	8.87	9.25
Or	.40	.27	.23	.02	.02	.05	.02	.05	.05	.03	.28

Table 4. Chemical compositions and structural formulas of selected samples of olivine from rocks of the Lower Coon Mountain pluton—Continued

Sample	82CMG136	82CMG146	82CMG146	82CMG146	82CMG150	82CMG150	82CMG150	82CMG150	82CMG150	82CMG172	82CMP3
Unit (fig. 4)	Jp	Jp	Jp	Jp	Jp	Jp	Jp	Jp	Jp	Jp	Jp
Major-element oxides											
SiO_2	44.6	45.8	46.5	46.5	51.1	52.7	48.1	50.0	51.9	44.0	45.4
Al_2O_3	34.7	34.7	33.6	33.7	30.3	29.3	32.3	31.7	30.5	34.4	35.4
FeO	.47	.35	.40	.53	.29	.30	.29	.37	.31	.35	.42
MgO	—	n.d.	.06	.04	.05	.05	.06	.17	.03	.06	.05
CaO	18.3	17.5	17.3	17.5	14.2	12.8	15.6	14.0	13.5	18.4	19.3
Na_2O	1.04	1.66	1.65	1.57	3.49	4.17	2.50	3.64	4.19	1.78	.78
K_2O	.02	.003	.03	.002	.04	.06	.03	.04	.04	.09	.01
BaO	—	—	—	—	—	—	—	—	—	—	—
SrO	—	.27	.18	.17	.05	.03	.03	.18	.19	.15	.14
Total	99.13	100.283	99.72	100.012	99.52	99.43	98.91	100.10	100.66	99.18	101.50
Formula per 32 oxygens											
Si	8.168	8.438	8.536	8.514	9.265	9.489	8.695	9.133	9.401	8.049	8.290
Al	7.475	7.531	7.260	7.329	6.474	6.225	6.879	6.820	6.505	7.419	7.605
Fe	.072	.055	.061	.082	.044	.045	.043	.056	.047	.054	.063
Mg	—	n.d.	.016	.012	.013	.014	.015	.047	.009	.015	.014
Ca	3.592	3.447	3.395	3.465	2.755	2.476	3.018	2.732	2.624	3.624	3.781
Na	.369	.593	.585	.562	1.228	1.457	.877	1.289	1.470	.417	.276
K	.003	.001	.006	—	.010	.014	.007	.009	.009	.021	.003
Ba	—	—	—	—	—	—	—	—	—	—	—
Sr	—	.029	.20	.018	.006	.003	.004	.019	.020	.015	.014
Z	15.715	16.024	15.856	15.985	15.783	15.759	15.617	16.009	15.953	15.522	15.958
X	3.964	4.041	4.006	4.045	3.999	3.950	3.906	4.049	4.123	4.077	4.074
Calculated Ab, An, and Or contents of plagioclase											
An	90.62	85.92	85.17	86.04	69.00	62.73	77.34	67.78	63.95	89.22	93.13
Ab	9.31	14.78	14.68	13.95	30.75	36.91	22.48	31.88	35.83	10.27	6.80
Or	.08	.02	.15	—	.25	.35	.18	.22	.22	.52	.07

Table 4. Chemical compositions and structural formulas of selected samples of olivine from rocks of the Lower Coon Mountain pluton—Continued

Sample	82CMP3	82CMP3	82CMP4	82CMP4	82CMP5	82CMP10	82CMP10	82CMP10	20CM81	20CM81	82CMG150	82CMG150
Unit (fig. 4)	Jp	Jp	Jp	Jp	Jp	Jc	Jc	Jc	Jg	Jg	Jp	Jp
Major-element oxides												
SiO_2	45.1	45.5	43.9	44.6	44.2	45.6	46.9	46.9	47.7	49.3	50.0	51.9
Al_2O_3	34.5	34.5	34.1	33.4	34.6	33.4	33.9	34.2	32.0	32.0	31.7	30.5
FeO	.40	.36	.46	.42	.51	.41	.40	.39	.28	.29	.37	.31
MgO	.04	.05	.05	.06	.06	.07	.06	.06	.03	.06	.17	.03
CaO	19.4	19.0	19.7	19.5	18.7	17.8	19.0	18.9	14.9	15.4	14.0	13.5
Na_2O	.66	.89	.80	.81	.74	1.78	1.10	1.14	2.25	2.75	3.64	4.19
K_2O	.01	.17	.02	.05	.01	.05	.003	.004	.04	.03	.04	.04
BaO	---	---	---	---	---	---	---	---	---	---	---	---
SrO	.19	.20	.16	.21	.18	.17	.14	.14	.06	.08	.18	.19
Total	100.66	100.67	99.19	99.05	99.00	99.28	101.503	101.73	97.76	99.91	100.10	100.66
Formula per 32 oxygens												
Si	8.335	8.380	8.106	8.201	8.097	8.384	8.542	8.526	8.514	9.024	9.133	9.401
Al	7.515	7.478	7.404	7.669	7.463	7.235	7.280	7.314	6.724	6.903	6.820	6.505
Fe	.062	.053	.071	.065	.078	.063	.061	.059	.041	.044	.056	.047
Mg	.011	.015	.014	.015	.017	.019	.015	.016	.009	.016	.047	.009
Ca	3.846	3.754	3.903	3.840	3.664	3.513	3.712	3.687	2.851	3.021	2.732	2.624
Na	.237	.316	.285	.291	.263	.634	.388	.402	.952	.975	1.289	1.470
K	.003	.040	.004	.012	.003	.012	.001	.001	.009	.007	.009	.009
Ba	---	---	---	---	---	---	---	---	---	---	---	---
Sr	.020	.021	.017	.023	.019	.018	.015	.014	.008	.008	.019	.020
Z	5.912	15.913	15.617	15.935	15.623	15.682	15.888	15.899	15.279	15.971	16.009	15.953
X	4.106	4.131	4.209	4.166	3.949	4.177	4.116	4.104	3.821	4.011	4.049	4.123
Calculated Ab, An, and Or contents of plagioclase												
An	94.13	91.34	93.11	92.69	93.20	84.47	90.51	90.15	74.79	75.47	67.78	63.95
Ab	5.80	7.69	6.80	7.02	6.69	15.24	9.46	9.83	24.97	24.36	31.88	35.83
Or	.07	.97	.10	.29	.08	.29	.02	.02	.24	.17	.22	.22

Table 5. Chemical compositions and structural formulas of selected samples of plagioclase from rocks of the Lower Coon Mountain pluton

[Electron-microprobe analyses in weight percent; analyst, F. Gray. Total iron determined as FeO. —, not detected; n.d., not determined]

Sample	82CMG30	82CMG30	82CMG30	82CMG36	82CMG36	82CMG36	82CMG77	82CMG131	82CMG131	82CMG136	82CMG136
Unit (fig. 4)	Jl	Jl	Jl	Jo	Jo	Jo	Jc	Jp	Jp	Jp	Jp
Major-element oxides											
SiO_2	49.7	49.1	49.4	44.9	44.3	44.9	45.1	44.9	44.7	45.4	44.4
Al_2O_3	31.9	32.7	32.4	35.1	35.1	35.0	35.2	34.8	35.6	33.8	34.8
FeO	.38	.30	.32	.33	.37	.37	.42	.36	.40	.65	.46
MgO	.12	.06	.05	.04	.04	.07	—	.05	.05	.18	—
CaO	15.5	16.1	15.6	18.9	18.6	19.0	18.8	18.5	18.6	18.5	18.3
Na_2O	2.64	2.45	2.61	1.09	1.11	1.06	.92	.93	.84	.97	1.07
K_2O	.07	.05	.04	.004	.01	.01	.004	.01	.01	.01	.05
BaO	—	—	—	—	—	n.d.	n.d.	—	—	n.d.	n.d.
SrO	.02	.05	.03	.17	.17	.13	—	.19	.17	n.d.	—
Total	100.33	100.81	100.45	100.534	99.70	100.54	100.444	99.74	100.37	99.51	99.08
Formula per 32 oxygens											
Si	9.066	8.925	9.001	8.277	8.180	8.283	8.306	8.264	8.234	8.353	8.126
Al	6.848	7.011	6.948	7.627	7.650	7.601	7.633	7.548	7.742	7.323	7.511
Fe	.058	.046	.049	.051	.057	.056	.065	.055	.062	.100	.070
Mg	.033	.016	.017	.012	.010	.020	—	.013	.014	.048	—
Ca	3.027	3.128	3.045	3.730	3.680	3.753	3.709	3.651	3.676	3.652	3.598
Na	.935	.864	.923	.388	.396	.379	.329	.333	.299	.346	.379
K	.016	.011	.009	.001	.001	.002	.001	.002	.002	.001	.011
Ba	—	—	—	n.d.	—	—	n.d.	—	—	n.d.	n.d.
Sr	.002	.005	.003	.018	.018	.014	—	.020	.019	n.d.	—
Z	15.970	15.982	15.998	15.955	15.887	15.94	16.004	15.867	16.038	15.776	15.707
X	3.980	4.003	3.980	4.137	4.095	4.148	4.039	4.006	3.996	3.999	3.988
Calculated Ab, An, and Or contents of plagioclase											
An	76.09	78.14	76.57	90.56	90.26	90.78	91.83	91.60	92.43	91.32	90.22
Ab	23.50	21.58	23.21	9.42	9.71	9.17	8.15	8.35	7.52	8.87	9.25
Or	.40	.27	.23	.02	.02	.05	.02	.05	.05	.03	.28

Table 5. Chemical compositions and structural formulas of selected samples of plagioclase from rocks of the Lower Coon Mountain pluton—Continued

Sample	82CMG136	82CMG146	82CMG146	82CMG146	82CMG150	82CMG150	82CMG150	82CMG150	82CMG150	82CMG172	82CMP3
Unit (fig. 4)	Jp	Jp	Jp	Jp	Jp	Jp	Jp	Jp	Jp	Jp	Jp
Major-element oxides											
SiO_2	44.6	45.8	46.5	46.5	51.1	52.7	48.1	50.0	51.9	44.0	45.4
Al_2O_3	34.7	34.7	33.6	33.7	30.3	29.3	32.3	31.7	30.5	34.4	35.4
FeO	.47	.35	.40	.53	.29	.30	.29	.37	.31	.35	.42
MgO	—	n.d.	.06	.04	.05	.05	.06	.17	.03	.06	.05
CaO	18.3	17.5	17.3	17.5	14.2	12.8	15.6	14.0	13.5	18.4	19.3
Na_2O	1.04	1.66	1.65	1.57	3.49	4.17	2.50	3.64	4.19	1.78	.78
K_2O	.02	.003	.03	.002	.04	.06	.03	.04	.04	.09	.01
BaO	—	—	—	—	—	—	—	—	—	—	—
SrO	—	.27	.18	.17	.05	.03	.03	.18	.19	.15	.14
Total	99.13	100.283	99.72	100.012	99.52	99.43	98.91	00.10	100.66	99.18	101.50
Formula per 32 oxygens											
Si	8.168	8.438	8.536	8.514	9.265	9.489	8.695	9.133	9.401	8.049	8.290
Al	7.475	7.531	7.260	7.329	6.474	6.225	6.879	6.820	6.505	7.419	7.605
Fe	.072	.055	.061	.082	.044	.045	.043	.056	.047	.054	.063
Mg	—	n.d.	.016	.012	.013	.014	.015	.047	.009	.015	.014
Ca	3.592	3.447	3.395	3.465	2.755	2.476	3.018	2.732	2.624	3.624	3.781
Na	.369	.593	.585	.562	1.228	1.457	.877	1.289	1.470	.417	.276
K	.003	.001	.006	—	.010	.014	.007	.009	.009	.021	.003
Ba	—	—	—	—	—	—	—	—	—	—	—
Sr	—	.029	.20	.018	.006	.003	.004	.019	.020	.015	.014
Z	15.715	16.024	15.856	15.985	15.783	15.759	15.617	16.009	15.953	15.522	15.958
X	3.964	4.041	4.006	4.045	3.999	3.950	3.906	4.049	4.123	4.077	4.074
Calculated Ab, An, and Or contents of plagioclase											
An	90.62	85.92	85.17	86.04	69.00	62.73	77.34	67.78	63.95	89.22	93.13
Ab	9.31	14.78	14.68	13.95	30.75	36.91	22.48	31.88	35.83	10.27	6.80
Or	.08	.02	.15	—	.25	.35	.18	.22	.22	.52	.07

Table 5. Chemical compositions and structural formulas of selected samples of plagioclase from rocks of the Lower Coon Mountain pluton—Continued

Sample	82CMP3	82CMP3	82CMP4	82CMP4	82CMP5	82CMP10	82CMP10	82CMP10	20CM81	20CM81	82CMG150	82CMG150
Unit (fig. 4)	Jp	Jp	Jp	Jp	Jp	Jc	Jc	Jc	Jg	Jg	Jp	Jp
Major-element oxides												
SiO_2	45.1	45.5	43.9	44.6	44.2	45.6	46.9	46.9	47.7	49.3	50.0	51.9
Al_2O_3	34.5	34.5	34.1	33.4	34.6	33.4	33.9	34.2	32.0	32.0	31.7	30.5
FeO	.40	.36	.46	.42	.51	.41	.40	.39	.28	.29	.37	.31
MgO	.04	.05	.05	.06	.06	.07	.06	.06	.03	.06	.17	.03
CaO	19.4	19.0	19.7	19.5	18.7	17.8	19.0	18.9	14.9	15.4	14.0	13.5
Na_2O	.66	.89	.80	.81	.74	1.78	1.10	1.14	2.25	2.75	3.64	4.19
K_2O	.01	.17	.02	.05	.01	.05	.003	.004	.04	.03	.04	.04
BaO	—	—	—	—	—	—	—	—	—	—	—	—
SrO	.19	.20	.16	.21	.18	.17	.14	.14	.06	.08	.18	.19
Total	100.66	100.67	199.19	99.05	99.00	99.28	101.503	101.73	97.76	99.91	100.10	100.66
Formula per 32 oxygens												
Si	8.335	8.380	8.106	8.201	8.097	8.384	8.542	8.526	8.514	9.024	9.133	9.401
Al	7.515	7.478	7.404	7.669	7.463	7.235	7.280	7.314	6.724	6.903	6.820	6.505
Fe	.062	.053	.071	.065	.078	.063	.061	.059	.041	.044	.056	.047
Mg	.011	.015	.014	.015	.017	.019	.015	.016	.009	.016	.047	.009
Ca	3.846	3.754	3.903	3.840	3.664	3.513	3.712	3.687	2.851	3.021	2.732	2.624
Na	.237	.316	.285	.291	.263	.634	.388	.402	.952	.975	1.289	1.470
K	.003	.040	.004	.012	.003	.012	.001	.001	.009	.007	.009	.009
Ba	—	—	—	—	—	—	—	—	—	—	—	—
Sr	.020	.021	.017	.023	.019	.018	.015	.014	.008	.008	.019	.020
Z	5.912	15.913	15.617	15.935	15.623	15.682	15.888	15.899	15.279	15.971	16.009	15.953
X	4.106	4.131	4.209	4.166	3.949	4.177	4.116	4.104	3.821	4.011	4.049	4.123
Calculated Ab, An, and Or contents of plagioclase												
An	94.13	91.34	93.11	92.69	93.20	84.47	90.51	90.15	74.79	75.47	67.78	63.95
Ab	5.80	7.69	6.80	7.02	6.69	15.24	9.46	9.83	24.97	24.36	31.88	35.83
Or	.07	.97	.10	.29	.08	.29	.02	.02	.24	.17	.22	.22

Table 6. Chemical compositions of rock samples from the contact area of the Lower Coon Mountain pluton

[X-ray-fluorescence analyses of major-element oxides in weight percent; analysts: J.S. Baker, A.J. Bartel, L. Espos, J. Taggart, and J.S. Wahlberg. Emission-spectrographic analyses of trace elements in parts per million; analyst, M. Malcolm. Fire-assay/atomic-absorption analyses of platinum-group elements in parts per billion; analysts: L. Bradley, C. Gent, J.M. McDade, R. Moore, and S. Wilson. n.d. not determined; H, interference; LOI, loss on ignition. All samples contained less than 20 ppm Ag and less than 0.05 ppm Au]

Rock type	Shale			Volcaniclastic rocks	Hornfels		Amphibolite
Sample	32CM81	74CM81	75CM81	73CM81	82CMG100	82CMG120	82CMG65
Major-element oxides							
SiO_2	63.1	63.9	63.7	43.6	57.6	41.7	44.0
Al_2O_3	17.0	16.9	15.1	3.14	18.6	14.5	14.4
Fe_2TO_3	5.75	5.95	9.27	19.3	6.36	13.2	13.3
Fe_2O_3	n.d.	n.d.	n.d.	n.d.	1.79	5.62	4.82
FeO	n.d.	n.d.	n.d.	n.d.	4.11	6.82	7.63
MgO	2.60	2.95	2.85	17.7	2.23	10.8	10.1
CaO	.83	.50	<.02	14.5	5.61	16.7	12.6
Na_2O	1.74	.71	.89	.35	7.04	.20	1.85
K_2O	2.72	3.55	2.35	<.02	.05	.05	.42
H_2O^+	n.d.	n.d.	n.d.	n.d.	1.57	3.51	2.49
H_2O^-	n.d.	n.d.	n.d.	n.d.	.19	.18	.26
TiO_2	.83	.80	.66	.96	.62	.83	1.47
P_2O_5	.18	.17	.07	<.05	.24	<.05	.19
MnO	.04	.08	.68	.19	.16	.15	.20
CO_2	n.d.	n.d.	n.d.	n.d.	.03	.04	.06
LOI	4.85	4.68	4.54	.98	1.58	2.71	1.69
Total	99.64	100.19	100.11	100.72	[1]99.84	[1]101.10	[1]100.49
Trace elements							
B	50	70	[2]30	<20	[3]<10	<10	17
Ba	1,000	1,000	1,500	10	60	<20	86
Co	<5	<5	20	70	13	58	53
Cr	150	150	30	300	11	270	250
Cu	50	50	300	3	12	15	100
Ga	20	20	30	H	18	18	21
Ni	20	15	50	150	19	150	110
Pb	10	20	20	<10	<10	<10	<10
Sc	20	15	15	70	11	60	52
Sr	200	100	30	20	360	700	390
V	200	300	150	300	67	450	390
Y	20	15	15	<10	26	11	28
Zn	<300	<300	<300	<300	66	H	H
Zr	100	100	100	10	140	48	83
Platinum-group elements							
Pd	3	4	9	1	n.d.	n.d.	n.d.
Pt	20	33	9	46	n.d.	n.d.	n.d.
Rh	<1	<1	<1	<1	n.d.	n.d.	n.d.
Ir	n.d.	n.d.	<20	<20	n.d.	n.d.	n.d.
Ru	n.d.	n.d.	<100	<100	n.d.	n.d.	n.d.

[1]Fe_2O_3 content and LOI not included in total.
[2]Sample contains 1.5 ppm Be and 10 ppm Nb.
[3]Sample contains 21 ppm La.

Table 7. Chemical and mineralogic data on rock samples from the layered sequence of the Lower Coon Mountain pluton

[X-ray-fluorescence analyses of major-element oxides in weight percent; analysts: J.S. Baker, A.J. Bartel, L. Espos, J. Taggart, and J.S. Wahlberg. Emission-spectrographic analyses of trace elements in parts per million; analyst, M. Malcolm. Fire-assay/atomic-absorption analyses of platinum-group elements in parts per billion; analysts: L. Bradley, C. Gent, J.M. McDade, R. Moore, and S. Wilson. Cross, Iddings, Pirsson, and Washington (CIPW) norms in weight percent; see text for FeO/Fe_2O_3 adjustments. Modes in volume percent; at least 800 points counted. —, not detected; n.d. not determined; H. interference; LOI, loss on ignition. All samples contained less than 20 ppm Ag, and less than 0.05 ppm Au, and less than 0.05 weight percent P_2O_5]

Unit	Clinopyroxene-olivine cumulate					Plagioclase-rich clinopyroxene-olivine cumulate						
Sample	82CMP6	82CMP7	4CM81	30CM81	79CM81	82CMG116	82CMP5	82CMP9	28CM81	83CM81	84CM81	85CM81
Major-element oxides												
SiO_2	39.9	42.0	40.7	40.2	42.4	43.1	41.5	41.8	40.7	40.3	40.2	46.2
Al_2O_3	4.16	3.55	3.47	3.80	3.88	4.67	7.88	10.3	9.24	6.31	8.18	1.63
Fe_2TO_3	21.5	19.4	20.9	21.0	19.4	17.8	17.8	18.6	17.8	20.6	18.9	11.1
Fe_2O_3	11.64	9.62	n.d.	n.d.	n.d.	7.64	7.71	7.35	n.d.	n.d.	n.d.	n.d.
FeO	8.87	8.80	n.d.	n.d.	n.d.	9.14	9.08	10.12	n.d.	n.d.	n.d.	n.d.
MgO	17.4	19.0	16.2	17.1	14.5	18.1	15.9	13.7	14.6	14.7	16.4	24.1
CaO	14.7	15.5	15.0	15.2	17.5	14.4	15.2	14.9	14.9	15.5	12.8	14.2
Na_2O	<.15	<.15	<.20	<.15	.20	.28	.25	.38	.37	.25	.34	<.15
K_2O	<.02	<.02	<.02	<.02	<.02	.03	.03	.09	<.02	.03	<.02	<.02
H_2O^+	2.67	1.37	n.d.	n.d.	n.d.	1.88	1.99	.85	n.d.	n.d.	n.d.	n.d.
H_2O^-	.35	.10	n.d.	n.d.	n.d.	.23	.15	.06	n.d.	n.d.	n.d.	n.d.
TiO_2	1.41	.37	1.55	1.30	1.80	1.21	1.22	1.66	1.27	1.66	1.12	.19
P_2O_5	<.05	<.05	<.05	<.05	<.05	<.05	<.05	<.05	<.05	<.05	<.05	<.05
MnO	.24	.21	.33	.23	.23	.32	.26	.28	.23	.28	.26	.17
CO_2	.05	.04	n.d.	n.d.	n.d.	.15	.08	<.01	n.d.	n.d.	n.d.	n.d.
LOI	2.31	.76	1.79	1.46	.71	1.89	1.57	.30	1.13	.88	1.64	2.63
Total	[1]101.39	[1]101.16	98.67	98.55	99.08	[1]100.85	[1]101.25	[1]101.49	98.90	98.78	98.28	99.50
Trace elements												
B	H	H	[2]<20	[2]<20	[2]<20	H	H	H	<20	<20	<20	<20
Ba	<20	<20	30	7	10	34	<20	<20	10	7	15	7
Co	93	94	70	70	70	87	79	80	70	70	100	30
Cr	410	640	300	300	300	820	420	280	300	300	500	1,500
Cu	22	17	15	10	10	33	100	110	20	30	5,000	3
Ga	H	H	H	H	H	H	H	H	H	H	H	H
Ni	160	200	150	100	100	240	150	120	100	70	200	300
Sc	H	H	70	70	70	H	H	H	70	70	100	70
Sr	21	23	7	15	20	82	140	260	150	70	150	7
V	790	570	300	300	500	410	680	730	300	300	700	100
Y	H	H	10	<10	15	H	H	H	<10	10	<10	<10
Zn	H	H	<300	<300	<300	H	H	H	<300	<300	<300	<300
Zr	49	42	10	10	20	55	45	50	<10	<10	<10	10
Platinum-group elements												
Pd	n.d.	n.d	1	1	<1	n.d.	n.d.	n.d.	8	4	191	5
Pt	n.d.	n.d	22	27	11	n.d.	n.d.	n.d.	25	19	230	64
Rh	n.d.	n.d.	<1	<1	<1	n.d.	n.d.	n.d.	<1	<1	<1	<1
Ir	n.d.	n.d.	<20	<20	<20	n.d.	n.d.	n.d.	n.d.	<20	<20	<20
Ru	n.d.	n.d.	<100	<100	<100	n.d.	n.d.	n.d.	n.d.	<100	<100	<100

Table 7. Chemical and mineralogic data on rock samples from the layered sequence of the Lower Coon Mountain pluton—Continued

Unit	Clinopyroxene-olivine cumulate					Plagioclase-rich clinopyroxene-olivine cumulate						
Sample	82CMP6	82CMP7	4CM81	30CM81	79CM81	82CMG116	82CMP5	82CMP9	28CM81	83CM81	84CM81	85CM81
CIPW norms												
or	0.1	0.1	—	—	—	0.2	0.2	0.5	—	—	—	[3]0.1
ab	1.3	.2	—	—	—	2.4	1.2	3.2	—	—	—	1.3
an	10.8	9.0	[3]9.5	[3]10.5	[3]9.8	11.5	20.5	26.0	[3]24.0	[3]16.3	[3]21.5	3.8
lc	—	—	.1	.1	.1	—	—	—	—	.1	.1	—
ne	—	.6	.9	.1	.9	—	.5	—	1.7	1.2	1.6	—
di	49.5	53.5	44.8	38.9	53.0	47.9	43.9	37.7	33.9	38.1	32.8	54.5
hy	.8	—	—	—	—	5.4	—	.1	—	—	—	3.4
ol	17.5	20.7	33.2	37.6	23.7	19.0	20.0	18.7	30.6	31.5	36.7	33.7
Ca-ortho	—	—	3.7	5.9	4.0	—	—	—	2.7	4.7	1.1	—
mt	17.1	14.0	4.6	4.2	4.9	11.2	11.3	10.6	4.1	4.7	3.9	2.5
il	2.7	1.8	3.0	2.5	3.5	2.3	2.3	3.1	2.5	3.2	2.2	.4
ap	.1	.1	.1	.1	.1	.1	.1	.1	.4	.1	.1	.1
di	41.9	43.9	27.0	23.5	32.4	37.8	34.2	27.7	21.0	22.5	20.3	41.9
he	4.6	6.5	16.7	14.4	19.2	7.6	7.6	8.3	12.0	14.7	11.6	10.0
wo	3.0	3.1	1.1	1.0	1.4	2.5	2.2	1.7	.9	.9	.9	2.7
fo	15.6	17.8	19.7	22.5	14.4	15.5	16.0	14.0	18.7	18.3	22.5	26.8
fa	1.8	2.9	13.5	15.2	9.3	3.4	3.9	4.7	11.8	13.2	14.2	7.0
en	.7	—	—	—	—	4.5	—	.1	—	—	—	2.8
fs	.1	—	—	—	—	.9	—	.03	—	—	—	.7
fo (pct)	89.1	86.0	59.4	59.7	60.6	81.9	80.4	75.1	61.3	58.1	61.3	79.4
en (pct)	90.0	—	—	—	—	83.3	—	77.4	—	—	—	80.9
Normative an (pct).	89.3	88.5	85.7	98.9	86.3	82.8	90.9	89.0	89.3	89.3	88.9	74.5
Modes												
di	67.2	67.1	n.d.	n.d.	n.d.	n.d.	53.8	43.1	n.d.	n.d.	n.d.	n.d.
ol	27.1	20.9	n.d.	n.d.	n.d.	n.d.	18.3	16.8	n.d.	n.d.	n.d.	n.d.
pl	—	—	n.d.	n.d.	n.d.	n.d.	19.0	29.1	n.d.	n.d.	n.d.	n.d.
mt	10.2	8.8	n.d.	n.d.	n.d.	n.d.	7.4	8.9	n.d.	n.d.	n.d.	n.d.
hb	1.3	2.8	n.d.	n.d.	n.d.	n.d.	1.2	1.8	n.d.	n.d.	n.d.	n.d.

[1]Fe_2TO_3 content and LOI not included in sum.
[2]Six-step semiquantitative spectrographic analysis.
[3]Calculated using correction $Fe_2O_3 = TiO_2 + 1.5$ of Irvine and Baragar (1971).

Table 8. Average major- and trace-element compositions of the layered sequence of the Lower Coon Mountain pluton

[Data from table 7. Major-element-oxides in weight percent; trace-element analyses in parts per million. —, no data]

Unit	Clinopyroxene-olivine cumulate	Plagioclase-rich clinopyroxene-olivine cumulate
Major-element oxides		
SiO_2	41.1±1.1	42.0±20
Al_2O_3	3.77±0.28	6.89±2.96
Fe_2TO_3	16.8±1.7	16.2±3.6
CaO	15.6±1.1	14.6±0.9
Na_2O	.20	.31±0.06
K_2O	<.02	.05±0.03
TiO_2	1.41±0.31	1.19±0.49
MnO	.25±0.05	.26±0.05
Trace elements		
B	<20	<20
Ba	15±13	15±11
Co	79±13	77±16
Cr	390±148	593±447
Cu	13±8	49±50
Ga	—	15
Ni	142±43	169±82
Sc	70	78±15
Sr	17±6	123±80
V	492±205	460±245
Y	12	<10
Zn	<300	<300
Zr	26±18	50±5

Table 9. Chemical and mineralogic data on rock samples from the layered clinopyroxene-olivine cumulate and olivine-clinopyroxene cumulate of the intrusive sequence of the Lower Coon Mountain pluton

[X-ray-fluorescence analyses of major-element oxides in weight percent; analysts: J.S. Baker, A.J. Bartel, L. Espos, J. Taggart, and J.S. Wahlberg. Emission-spectrographic analyses of trace elements in parts per million; analyst, M. Malcolm. Fire-assay/atomic-absorption analyses of platinum-group elements in parts per billion; analysts: L. Bradley, C. Gent, J.M. McDade, R. Moore, and S. Wilson. Cross, Iddings, Pirsson, and Washington (CIPW) norms in weight percent; see text for FeO/Fe_2O_3 adjustments. Modes in volume percent; at least 800 points counted. —, not detected; n.d. not determined; H. interference; LOI, loss on ignition. All samples contained less than 20 ppm Ag, and less than 0.05 ppm Au, and less than 0.05 weight percent P_2O_5]

Unit	Layered clinopyroxene-olivine cumulate							Olivine-clinopyroxene cumulate		
Sample	82CMG54	10CM81	24CM81	49CM81	50CM81	56CM81	67CM81	82CMG70(2)	82CMP2	82CMP27
Major elements										
SiO_2	46.7	44.4	48.8	46.9	42.5	42.8	48.3	39.1	48.1	43.9
Al_2O_3	2.70	2.93	2.24	3.61	2.27	3.90	2.43	1.37	1.29	7.26
Fe_2TO_3	10.8	15.2	8.32	12.0	16.9	18.0	9.11	17.8	9.31	13.4
Fe_2O_3	4.16	n.d.	n.d.	n.d.	n.d.	n.d.	n.d.	12.48	4.00	4.95
FeO	5.97	n.d.	n.d.	n.d.	n.d.	n.d.	n.d.	4.79	4.78	7.60
MgO	21.6	18.8	20.0	18.1	22.5	18.0	19.9	28.1	23.4	18.7
CaO	16.9	15.7	19.0	17.0	12.0	14.6	18.6	6.14	14.9	14.2
Na_2O	<.15	.18	<.15	.29	<.15	.16	.16	<.15	<.15	.16
K_2O	<.02	<.02	<.02	<.02	<.02	<.02	<.02	<.02	<.02	.09
H_2O^+	2.11	n.d.	n.d.	n.d.	n.d.	n.d.	n.d.	7.59	3.63	3.14
H_2O^-	.10	n.d.	n.d.	n.d.	n.d.	n.d.	n.d.	.51	.31	.24
TiO_2	.37	.84	.28	.59	.63	1.08	.32	.30	.13	.52
MnO	.18	.25	.13	.21	.26	.26	.15	.41	.16	.24
CO_2	.23	n.d.	n.d.	n.d.	n.d.	n.d.	n.d.	.25	.15	.07
LOI	2.10	2.17	1.45	1.62	3.40	2.61	1.45	7.97	3.71	2.67
Total	[1]101.01	99.25	99.78	99.40	100.46	98.97	99.76	[1]99.94	[1]101.28	[1]101.07
Trace elements										
B	<10	[2]<20	[2]<20	[2]<20	[2]<20	[2]<20	[2]<20	H	54	22
Ba	<20	7	7	15	7	7	15	140	<20	<20
Co	70	50	50	50	70	70	70	130	78	80
Cr	800	500	1,500	700	300	300	1,000	1,600	1,000	870
Cu	9.8	7	3	30	7	15	2	14	7.3	18
Ga	<10	H	H	H	H	H	H	<10	<10	10
Ni	200	100	150	150	200	150	150	670	280	280
Sc	85	70	70	70	70	70	100	H	75	61
Sr	28	15	15	70	10	10	10	<15	30	140
V	150	200	150	200	200	300	150	110	60	230
Y	<10	<10	<10	15	<10	10	<10	H	<10	14
Zn	<50	<300	<300	<300	<300	<300	<300	H	<50	H
Zr	30	<10	<10	15	<10	<10	<10	3	28	41
Platinum-group elements										
Pd	n.d.	<1	n.d.	10	<1	1	n.d.	n.d.	n.d.	n.d.
Pt	n.d.	17	n.d.	38	10	32	n.d.	n.d.	n.d.	n.d.
Rh	n.d.	<1	n.d.	<1	<1	<1	n.d.	n.d.	n.d.	n.d.
Ir	n.d.	<20	n.d.	<20	n.d.	<20	n.d.	n.d.	n.d.	n.d.
Ru	n.d.	<100	n.d.	<100	n.d.	<100	n.d.	n.d.	n.d.	n.d.

Table 9. Chemical and mineralogic data on rock samples from the layered clinopyroxene-olivine cumulate and olivine-clinopyroxene cumulate of the intrusive sequence of the Lower Coon Mountain pluton—Continued

Unit	Layered clinopyroxene-olivine cumulate							Olivine-clinopyroxene cumulate		
Sample	82CMG54	10CM81	24CM81	49CM81	50CM81	56CM81	67CM81	82CMG70(2)	82CMP2	82CMP27
CIPW norms										
or	—	—	[3]0.1	[3]0.1	[3]0.1	—	—	[3]0.1	[3]0.1	[3]0.6
ab	—	—	1.0	2.5	1.3	—	—	1.4	1.3	1.4
an	[4]6.7	[3]7.3	5.5	8.7	5.7	[3]7.3	[4]5.9	3.3	2.9	11.3
le	.1	.1	—	—	—	.2	.1	—	—	—
ne	.7	.9	.2	—	.02	.8	.7	—	—	—
di	57.9	58.0	71.3	61.8	45.1	53.9	66.6	23.7	57.1	50.6
hy	—	—	—	1.1	—	—	—	5.4	10.0	3.9
ol	31.3	28.3	18.6	21.4	43.1	31.4	24.1	62.6	25.5	28.0
Ca-ortho	1.8	.1	—	—	—	.3	1.1	—	—	—
mt	.7	3.5	2.6	3.1	3.2	3.9	.7	2.8	2.4	3.1
il	.7	1.6	.5	1.1	1.2	2.1	.6	.6	.3	1.0
ap	.1	.1	.1	.1	.1	.1	.1	.1	.4	.1
di	42.4	40.1	59.0	45.0	31.1	35.0	48.7	16.7	45.4	35.7
he	12.9	15.7	10.4	14.0	12.3	17.2	15.0	6.0	8.7	12.8
wo	2.6	2.2	3.9	2.7	1.7	1.7	2.9	1.0	3.0	2.0
fo	23.4	19.8	15.5	15.9	30.1	20.3	17.0	44.8	21.1	20.1
fa	7.8	8.6	3.1	5.5	13.1	11.0	6.1	17.8	4.5	7.9
rn	—	—	—	.9	—	—	—	3.9	8.4	2.8
fs	—	—	—	.3	—	—	—	1.4	1.6	1.0
fo (pct)	75.0	69.8	83.2	74.4	69.7	64.9	74.7	71.6	82.5	71.7
fn (pct)	—	—	—	76.3	—	—	73.5	83.9	91.5	—
Normative an (pct).	85.3	83.8	81.3	77.6	81.2	85.2	82.7	70.3	68.7	88.7
Modes										
di	64.9	n.d.	n.d.	n.d.	n.d.	n.d.	n.d.	n.d.	69.7	51.3
ol	33.7	n.d.	n.d.	n.d.	n.d.	n.d.	n.d.	n.d.	25.1	28.5
pl	—	n.d.	n.d.	n.d.	n.d.	n.d.	n.d.	n.d.	—	14.8
mt	1.0	n.d.	n.d.	n.d.	n.d.	n.d.	n.d.	n.d.	.3	2.1
hb	.2	n.d.	n.d.	n.d.	n.d.	n.d.	n.d.	n.d.	5.0	3.1

Table 9. Chemical and mineralogic data on rock samples from the layered clinopyroxene-olivine cumulate and olivine-clinopyroxene cumulate of the intrusive sequence of the Lower Coon Mountain pluton—Continued

Unit	Olivine-clinopyroxene cumulate									
Sample	17CM81	21CM81	36CM81	40CM81	41aCM81	41bCM81	41CM81	42CM81	43CM81	88CM81
Major elements										
SiO_2	43.2	48.0	42.2	39.8	42.0	42.8	45.7	33.1	42.8	43.5
Al_2O_3	3.20	2.67	2.88	5.70	4.06	3.70	3.20	.41	3.21	2.61
Fe_2TO_3	18.7	9.53	19.1	21.5	18.6	16.2	12.3	26.3	16.5	15.6
Fe_2O_3	n.d.	n.d.	n.d.	n.d.	n.d.	n.d.	n.d.	n.d.	n.d.	n.d.
FeO	n.d.	n.d.	n.d.	n.d.	n.d.	n.d.	n.d.	n.d.	n.d.	n.d.
MgO	16.1	20.1	18.8	12.0	15.7	17.7	19.3	31.7	19.5	19.6
CaO	15.9	18.2	15.1	15.1	16.5	15.7	16.9	.38	14.6	14.8
Na_2O	.19	.16	.18	<.15	<.15	<.15	.18	<.15	.17	<.15
K_2O	<.02	<.02	<.02	<.02	<.02	<.02	<.02	<.02	<.02	<.02
H_2O^+	n.d.	n.d.	n.d.	n.d.	n.d.	n.d.	n.d.	n.d.	n.d.	n.d.
H_2O^-	n.d.	n.d.	n.d.	n.d.	n.d.	n.d.	n.d.	n.d.	n.d.	n.d.
TiO_2	1.24	.35	1.16	1.25	1.30	1.12	.66	.47	.92	.81
MnO	.24	.17	.23	.37	.22	.22	.22	.33	.24	.23
CO_2	n.d.	n.d.	n.d.	n.d.	n.d.	n.d.	n.d.	n.d.	n.d.	n.d.
LOI	2.04	1.24	1.06	4.37	1.96	2.76	2.02	7.14	2.39	2.91
Total	99.28	100.61	100.85	100.26	100.71	100.01	100.6	100.00	100.45	100.33
Trace elements										
B	[2]<20	[2]<20	[2]<20	[2]<20	[2]<20	[2]<20	[2]<20	[2]<20	[2]<20	[2]<20
Ba	7	15	5	30	7	2	7	10	5	7
Co	70	70	70	100	70	70	50	150	70	70
Cr	700	1,000	300	1,000	300	300	500	700	500	700
Cu	10	3	7	20	7	7	7	15	7	7
Ga	H	H	H	H	H	H	H	H	M	H
Ni	200	150	150	300	150	150	150	300	150	200
Sc	70	100	70	300	70	70	70	15	70	70
Sr	7	10	10	20	5	5	5	<5	10	10
V	700	150	300	500	300	300	200	150	300	300
Y	15	<10	<10	30	10	<10	10	<10	10	10
Zn	<300	<300	<300	<300	<300	<300	<300	<300	<300	<300
Zr	15	10	10	15	10	<10	15	10	15	<10
Platinum-group elements										
Pd	2	<1	<1	4	1	1	1	2	2	2
Pt	40	33	35	12	20	27	25	25	33	13
Rh	<1	<1	<1	<1	<1	<1	13	<1	<1	<1
Ir	<20	<20	<20	< 20	<20	<20	<20	<20	<20	<20
Ru	<100	<100	<100	<100	<100	<100	<100	<100	<100	<100

Table 9. Chemical and mineralogic data on rock samples from the layered clinopyroxene-olivine cumulate and olivine-clinopyroxene cumulate of the intrusive sequence of the Lower Coon Mountain pluton—Continued

Unit	Olivine-clinopyroxene cumulate									
Sample	17CM81	21CM81	36CM81	40CM81	41aCM81	41bCM81	41CM81	42CM81	43CM81	88CM81
CIPW norms										
or	—	[3]0.1	—	—	—	—	—	—	—	—
ab	—	.6	—	—	—	—	—	—	—	—
an	[3]8.0	6.6	[3]7.1	[3]16.3	[3]10.7	[3]9.8	[3]8.1	[3]0.9	[3]8.2	[3]6.7
le	.1	—	.1	.1	.1	.1	.1	.1	.1	.1
ne	.9	.4	.8	.2	.7	.7	.8	.3	.8	.7
di	56.6	67.3	46.4	46.7	49.6	51.3	61.1	.6	49.9	55.2
hy	—	—	—	—	—	—	—	—	—	—
ol	26.8	21.4	35.7	27.8	28.3	31.0	24.9	93.8	34.0	31.9
Ca-ortho	.9	—	3.6	2.0	3.8	2.4	.4	.02	1.4	.3
mt	4.1	2.7	3.9	4.2	4.2	3.3	3.2	3.2	3.6	3.5
il	2.4	.7	2.2	2.5	2.5	1.3	1.3	1.0	1.8	1.6
ap	.1	.1	.1	.1	.1	.1	.1	.1	.1	.1
di	35.3	53.3	29.9	24.1	30.8	33.8	45.0	.4	34.0	38.1
he	19.8	11.5	15.0	22.0	13.4	15.9	13.4	.2	14.1	15.0
wo	1.6	3.4	1.5	.6	1.4	.7	2.7	—	1.8	2.1
fo	16.5	17.3	23.0	13.8	17.4	20.4	18.8	61.1	23.3	22.3
fa	10.2	4.2	12.7	14.0	10.8	10.6	6.2	32.8	10.7	9.6
en	—	—	—	—	—	—	—	—	—	—
fs	—	—	—	—	—	—	—	—	—	—
fo (pct)	61.8	80.5	64.4	49.8	61.7	65.9	75.3	65.1	68.6	69.8
en (pct)	—	—	—	—	—	—	—	—	—	—
Normative an (pct).	84.3	83.5	83.6	97.6	90.0	89.1	85.1	68.6	85.9	84.8
Modes										
di	n.d.	n.d.	n.d.	n.d.	n.d.	n.d.	n.d.	n.d.	n.d.	n.d.
ol	n.d.	n.d.	n.d.	n.d.	n.d.	n.d.	n.d.	n.d.	n.d.	n.d.
pl	n.d.	n.d.	n.d.	n.d.	n.d.	n.d.	n.d.	n.d.	n.d.	n.d.
mt	n.d.	n.d.	n.d.	n.d.	n.d.	n.d.	n.d.	n.d.	n.d.	n.d.
hb	n.d.	n.d.	n.d.	n.d.	n.d.	n.d.	n.d.	n.d.	n.d.	n.d.

[1]Fe_2TO_3 content and LOI not included in total.
[2]Six-step semiquantitative spectrographic analysis.
[3]Calculated by setting Fe_2O_3 = 0.5 weight percent.
[4]Calculated using correction $Fe_2O_3 = TiO_2 + 1.5$ of Irvine and Baragar (1971).

Table 10. Chemical and mineralogic data on rock samples from the olivine cumulate and dunite and the gabbro of the intrusive sequence of the Lower Coon Mountain pluton

[X-ray-fluorescence analyses of major-element oxides in weight percent; analysts: J.S. Baker, A.J. Bartel, L. Espos, J. Taggart, and J.S. Wahlberg. Emission-spectrographic analyses of trace elements in parts per million; analyst, M. Malcolm. Fire-assay/atomic-absorption analyses of platinum-group elements in parts per billion; analysts: L. Bradley, C. Gent, J.M. McDade, R. Moore, and S. Wilson. Cross, Iddings, Pirsson, and Washington (CIPW) norms in weight percent; see text for FeO/Fe_2O_3 adjustments. Modes in volume percent; at least 800 points counted. —, not detected; n.d. not determined; H. interference; LOI, loss on ignition. All samples contained less than 20 ppm Ag, and less than 0.05 ppm Au]

Unit	Olivine cumulate			Gabbro											
Sample	82CMG157	14CM81	63CM81	82CMG64	82CMG99	82CMG121	82CMP42	20CM81	28CM81	46CM81	47CM81	53CM81	54CM81	86CM81	101CM81
Major-element oxides															
SiO_2	45.3	35.6	36.3	44.2	43.5	39.1	43.7	44.3	41.0	43.3	43.6	42.1	48.4	39.8	40.5
Al_2O_3	4.48	1.07	.26	11.6	11.7	17.3	13.1	15.7	9.21	13.0	14.4	23.4	9.72	21.4	8.71
Fe_2TO_3	13.8	24.6	16.5	13.2	11.8	14.5	12.3	12.7	18.2	12.5	12.3	12.1	11.1	13.3	17.7
Fe_2O_3	4.61	n.d.	n.d.	5.55	3.48	5.83	4.22	n.d.	n.d.	n.d.	n.d.	n.d.	n.d.	n.d.	n.d.
FeO	8.27	n.d.	n.d.	6.88	7.49	7.80	7.27	n.d.	n.d.	n.d.	n.d.	n.d.	n.d.	n.d.	n.d.
MgO	21.7	28.1	34.7	13.2	16.9	9.10	11.8	10.3	14.1	12.0	11.6	4.20	11.9	4.93	14.6
CaO	12.1	3.88	.20	15.9	11.1	15.9	15.1	13.0	15.1	14.6	13.5	13.1	15.2	12.1	15.6
Na_2O	.44	<.15	<.15	.51	.53	.46	1.02	1.57	.39	.86	.74	2.24	1.58	1.59	.16
K_2O	.09	<.02	<.02	.30	.41	.21	.02	.16	<.02	.22	1.06	.17	.31	1.58	.08
H_2O^+	2.86	n.d.	n.d.	1.67	4.64	3.58	3.28	n.d.	n.d.	n.d.	n.d.	n.d.	n.d.	n.d.	n.d.
H_2O^-	.18	n.d.	n.d.	.24	.57	.15	.22	n.d.	n.d.	n.d.	n.d.	n.d.	n.d.	n.d.	n.d.
TiO_2	.46	.56	.06	.66	.39	1.23	.91	1.63	1.37	.65	.80	.83	.76	1.71	1.18
P_2O_5	<.05	<.05	<.05	<.05	<.05	<.05	<.05	<.05	<0.05	<.05	<.05	.83	.1	.80	<.05
MnO	.25	.31	.26	.18	.19	.15	.17	.19	.27	.20	.17	.10	.22	.13	.23
CO_2	.17	n.d.	n.d.	.11	.08	.11	.07	n.d.	n.d.	n.d.	n.d.	n.d.	—	—	n.d.
LOI	2.68	5.78	11.6	1.43	4.57	2.59	2.74	.60	1.15	3.02	2.18	1.33	.76	2.68	2.97
Total	[1]101.83	99.90	99.88	[1]100.89	[1]100.57	[1]100.92	[1]100.88	100.38	100.79	100.35	100.35	100.50	100.05	100.02	101.73
Trace elements															
B	36	50	<20	15	27	H	17	<20	<20	<20	<20	<20	<20	<20	<20
Ba	32	5	5	77	73	60	<20	50	20	20	70	70	70	300	15
Co	88	150	100	59	70	56	55	50	70	50	50	30	30	30	70
Cr	1,400	700	700	480	932	100	480	200	500	300	300	15	300	10	300
Cu	18	15	7	210	15	290	100	70	70	150	70	150	30	150	30
Ga	11	H	H	13	11	H	18	20	20	H	15	30	15	30	H
Ni	380	300	300	140	370	91	170	70	70	70	70	15	70	15	100
Sc	55	30	15	64	40	H	51	30	70	30	70	20	70	30	70
Sr	93	7	<5	320	290	840	490	200	100	300	200	1,000	200	700	150
V	180	300	30	390	120	570	440	300	700	300	300	300	300	300	500
Y	17	<10	<10	12	10	H	14	20	15	<10	10	15	10	20	10
Zn	<50	<300	<300	<50	120	H	H	<300	<300	<300	<300	<300	<300	<300	<300
Zr	59	10	7	37	32	41	43	30	15	15	15	20	30	<10	10
Platinum-group elements															
Pd	n.d.	4	<1	n.d.	n.d.	n.d.	n.d.	12	10	13	16	2	1	6	33
Pt	n.d.	62	28	n.d.	n.d.	n.d.	n.d.	24	32	28	26	15	14	15	62
Rh	n.d.	<1	<1	n.d.	n.d.	n.d.	n.d.	<1	<1	<1	<1	<1	<1	<1	<1
Ir	n.d.	<20	<20	n.d.	n.d.	n.d.	n.d.	<20	<20	<20	<20	<20	<20	n.d.	<20
Ru	n.d.	<100	<100	n.d.	n.d.	n.d.	n.d.	<100	<100	<100	<100	<100	<100	n.d.	<100
CIPW norms															
or	1.1	[2,3]0.1	1.8	2.5	[4]1.2	.1	[2]1.0	—	[2]1.3	6.4	[5]1.3	[3]1.9	[3]9.7	—	—
ab	3.8	—	1.4	4.3	4.6	3.6	8.1	13.4	—	4.1	2.8	14.5	13.6	3.6	—
an	9.8	[3]2.4	—	28.5	29.3	41.6	30.0	35.7	[3]41.1	32.1	33.8	8.8	18.8	48.4	[3]23.4
lc	—	.1	—	—	—	—	—	—	.1	—	—	—	—	—	.4
ne	—	.7	—	—	—	—	.4	—	1.8	1.9	2.0	—	—	5.6	.8
di	40.1	14.5	.6	39.8	21.8	25.5	37.8	22.6	10.8	34.6	28.1	66.5	46.0	7.0	33.3
hy	10.9	—	15.7	.7	11.6	16.2	—	.7	—	—	—	—	.9	—	—
ol	25.1	77.7	79.3	14.3	22.8	—	15.3	18.4	26.9	21.3	21.8	—	13.9	15.5	31.2
Ca-ortho	—	.1	—	—	—	—	—	—	2.4	—	—	—	—	—	4.6
mt	8.1	3.2	2.6	9.2	6.5	7.9	6.3	4.6	4.2	3.2	3.4	—	3.3	4.8	4.0

Table 10. Chemical and mineralogic data on rock samples from the olivine cumulate and dunite and the gabbro of the intrusive sequence of the Lower Coon Mountain pluton—Continued

Unit	Olivine cumulate			Gabbro											
Sample	82CMG157	14CM81	63CM81	82CMG64	82CMG99	82CMG121	82CMP42	20CM81	28CM81	46CM81	47CM81	53CM81	54CM81	86CM81	101CM81
CIPW norms—Continued															
il	.9	1.2	.1	1.3	.8	2.2	1.8	3.1	2.6	1.3	1.6	2.1	1.5	3.4	2.3
ap	.1	.1	.1	.1	.1	.1	.1	.5	.1	.1	.1	.2	.2	1.9	.1
di	31.9	9.3	.5	31.4	16.7	18.2	27.9	8.8	14.8	24.5	18.5	27.4	31.6	3.6	20.5
he	6.1	4.7	.1	6.4	3.9	6.2	8.2	6.5	5.1	12.0	8.7	39.2	12.7	3.4	11.9
wo	2.1	.5	.03	2.1	1.1	1.1	1.7	2.9	.9	1.1	.9	2.9	1.7	.1	.9
fo	20.7	50.0	60.8	11.7	18.1	—	11.6	12.5	19.5	13.9	14.4	—	9.6	7.7	19.0
fa	4.4	27.7	18.5	2.6	4.7	—	3.8	5.9	7.4	7.5	7.5	—	4.2	7.9	12.1
en	9.2	—	12.3	.6	9.4	12.1	—	.5	—	—	—	—	.6	—	—
fs	1.8	—	3.4	.1	2.2	4.1	—	.2	—	—	—	—	.2	—	—
fo (pct)	2.6	64.3	76.7	81.8	79.4	—	75.5	68.1	72.5	65.0	65.8	—	69.3	49.4	60.8
en (pct)	84.0	—	78.4	83.2	81.8	74.5	—	67.2	—	—	—	—	71.3	—	—
Normative an (pct).	72.2	65.6	—	86.8	86.3	92.0	77.2	72.7	93.2	81.7	84.7	34.9	58.1	78.9	94.9
Modes															
di	n.d.	n.d.	n.d.	87.0	34.1	n.d.	n.d.	n.d.	n.d.	n.d.	n.d.	n.d.	n.d.	n.d.	n.d.
ol	n.d.	n.d.	n.d.	12.5	13.4	n.d.	n.d.	n.d.	n.d.	n.d.	n.d.	n.d.	n.d.	n.d.	n.d.
pl	n.d.	n.d.	n.d.	32.0	47.8	n.d.	n.d.	n.d.	n.d.	n.d.	n.d.	n.d.	n.d.	n.d.	n.d.
mt	n.d.	n.d.	n.d.	4.6	.9	n.d.	n.d.	n.d.	n.d.	n.d.	n.d.	n.d.	n.d.	n.d.	n.d.
hb	n.d.	n.d.	n.d.	13.7	3.5	n.d.	n.d.	n.d.	n.d.	n.d.	n.d.	n.d.	n.d.	n.d.	n.d.

[1] Fe_2TO_3 content and LOI not included in total.
[2] Calculated using correction $Fe_2O_3 = TiO_2 + 1.5$ of Irvine and Baragar (1971)
[3] Contains 0.04 weight percent acmite.
[4] Contains 1.8 weight percent quartz.
[5] Contains 4.3 weight percent quartz, 8.8 weight percent acmite, and 0.07 weight percent Na-metasilicate.

Table 11. Average major- and trace-element-oxide compositions of rocks of the intrusive sequence of the Lower Coon Mountain pluton

[Data from tables 9 and 10. Major-element-oxide analyses in weight percent; trace-element analyses in parts per million]

Unit	Layered clinopyroxene-olivine cumulate	Olivine-clinopyroxene cumulate	Olivine cumulate and dunite	Gabbro
Major-element oxides				
SiO_2	45.8±2.6	42.6±3.9	39.1±5.4	42.8±2.5
Al_2O_3	2.73±0.48	3.20±1.81	1.94±2.24	14.1±4.7
Fe_2TO_3	12.9±3.8	16.5±4.7	18.3±5.6	13.5±2.3
MgO	19.8±1.7	20.1±5.2	28.2±6.5	11.2±3.7
CaO	16.3±2.4	13.7±4.9	5.39±6.09	14.2±1.6
Na_2O	.2±0.06	.17±0.1	.44	.97±0.64
K_2O	<.02	.09	.09	.41±0.48
TiO_2	.59±0.29	.79±0.41	.36±0.26	1.02±0.41
MnO	.21±0.05	.25±0.07	.27±0.03	.18±0.05
Trace elements				
B	<20	22	43	20±6
Ba	10±4	23±42	14±16	75±78
Co	61±11	83±28	113±33	52±15
Cr	729±427	728±371	933±404	326±254
Cu	11±10	10±5	13±6	111±82
Ga	<10	10	11	19±7
Ni	157±35	241±144	327±46	104±94
Sc	76±12	87±70	33±20	50±20
Sr	23±22	23±39	50	324±154
V	193±53	277±170	170±135	377±154
Y	13	15±8	17	14±4
Zn	<300	<300	<300	120
Zr	23	18±10	25±29	23±14

Table 12. Chemical and mineralogic data on rock samples from dikes in the Lower Coon Mountain pluton

[X-ray-fluorescence analyses of major-element oxides in weight percent; analysts: J.S. Baker, A.J. Bartel, L. Espos, J. Taggart, and J.S. Wahlberg. Emission-spectrographic analyses of trace elements in parts per million; analyst, M. Malcolm. Fire-assay/atomic-absorption analyses of platinum-group elements in parts per billion; analysts: L. Bradley, C. Gent, J.M. McDade, R. Moore, and S. Wilson. Cross, Iddings, Pirsson, and Washington (CIPW) norms in weight percent; see text for FeO/Fe_2O_3 adjustments. Modes in volume percent; at least 800 points counted. —, not detected; n.d. not determined; H. interference; LOI, loss on ignition. All samples contained less than 20 ppm Ag, and less than 0.05 ppm Au]

Sample	82CMG137	82CMG138	33CM81	44CM81
Major-element oxides				
SiO_2	50.2	49.5	60.7	56.4
Al_2O_3	11.6	15.3	19.0	13.7
Fe_2TO_3	10.5	10.9	6.01	6.66
Fe_2O_3	1.54	2.73	n.d.	n.d.
FeO	8.06	7.35	n.d.	n.d.
MgO	12.3	7.54	1.70	8.40
CaO	10.9	9.67	3.52	7.47
Na_2O	1.28	3.32	4.41	5.05
K_2O	.48	.10	1.06	.15
H_2O^+	3.15	2.62	n.d.	n.d.
H_2O^-	.15	.10	n.d.	n.d.
TiO_2	.67	1.15	.55	.36
P_2O_5	.15	.19	.28	.07
MnO	.18	.19	.22	.14
CO_2	.15	.33	n.d.	n.d.
LOI	2.62	2.24	2.40	1.17
Total	[1]100.81	[1]100.09	99.85	99.57
Trace elements				
B	<10	23	<20	<20
Ba	260	100	300	70
Co	47	36	15	30
Cr	700	140	3	300
Cu	65	130	7	7
Ga	11	21	30	H
Ni	200	130	50	150
Sc	43	32	7	30
Sr	290	650	500	300
V	230	290	70	150
Y	18	25	30	<10
Zn	170	80	<300	<300
Zr	98	120	100	30

Sample	82CMG137	82CMG138	33CM81	44CM81
Platinum-group elements				
Pd	n.d.	n.d.	<1	4
Pt	n.d.	n.d.	13	26
Rh	n.d.	n.d.	<1	<1
Ir	n.d.	n.d.	<20	<20
Ru	n.d.	n.d.	<100	<100
CIPW norms				
qz	[2]0.02	—	[3,4]20.3	[3]0.3
or	2.9	.6	6.5	.9
ab	11.1	28.9	38.5	43.6
an	25.2	27.4	16.1	14.6
di	23.7	16.9	—	14.6
hy	33.2	14.9	8.8	18.8
ol	—	4.5	—	—
mt	2.3	4.5	3.1	2.8
il	1.3	2.3	1.1	.7
ap	.4	.4	.7	.2
di	16.1	10.8	—	13.5
he	6.7	5.6	—	3.9
wo	.9	.5	—	.8
fo	—	2.9	—	—
fa	—	1.6	—	—
en	23.4	9.8	4.4	6.7
fs	9.7	5.1	4.5	2.0
fo (pct)	—	63.7	—	—
en (pct)	70.6	66.0	49.3	77.5
Normative an (pct).	69.3	48.6	29.5	25.0

[1]Fe_2TO_3 and LOI not included in total.
[2]Contains 17 ppm Pb.
[3]Calculated using correction $Fe_2O_3 = TiO_2 + 1.5$ of Irvine and Baragar (1971).
[4]Contains 5.0 weight percent corundum.

Table 13. Analyses of titanium dioxide and selected trace and platinum-group elements in rock samples from the Lower Coon Mountain pluton

[Six-step semiquantitative spectrographic analyses of trace elements in parts per million; TiO_2 contents in weight percent. Fire-assay/atomic-absorption analyses of platinum-group elements in parts per billion; analysts: L. Bradley, C. Gent, J.M. McDade, R. Moore, and S. Wilson. n.d., not determined]

Sample		Platinum-group elements				Trace elements					
	TiO_2	Cu	Ni	Co	Cr	V	Pd	Pt	Rh	Ir	Ru
LAYERED SEQUENCE											
Clinopyroxene-olivine cumulate											
4CM81	0.5	15	150	70	300	300	1	22	<1	<20	<100
30CM81	.5	10	100	70	300	300	1	27	<1	<20	<100
71CM81	n.d.	n.d.	n.d.	n.d.	n.d.	n.d.	1	15	<1	<20	<100
79CM81	.7	10	100	70	300	500	1	11	<1	<20	<100
100CM81	.5	70	30	30	70	300	4	35	<1	<20	<100
101CM81	.5	30	100	70	300	500	33	62	<1	<20	<100
82CMG78	.2	5	70	30	500	300	1	<10	<1	n.d.	n.d.
82CMG88	.2	5	70	50	500	300	1	<10	<1	n.d.	n.d.
82CMG92	.2	15	150	30	500	300	1	<10	<1	n.d.	n.d.
82CMG103	.3	50	100	30	300	300	16	42	<1	<20	<100
82CMG107	.2	10	70	30	300	700	31	65	<1	n.d.	n.d.
82CMG108	.3	15	150	30	500	300	8	23	1	<20	<100
82CMG110	.3	15	150	50	300	300	2	<10	1	<20	<100
82CMG110DUP	.15	7	70	30	300	300	2	42	<1	n.d.	n.d.
82CMG127	.15	5	70	30	300	300	9	45	2	n.d.	n.d.
82CMG133	.15	3	100	30	500	200	1	10	1	n.d.	n.d.
82CMG172	n.d.	n.d.	n.d.	n.d.	n.d.	n.d.	5	13	<1	n.d.	n.d.
82CMP6	.82	22	160	93	410	790	2	<10	<1	n.d.	n.d.
82CMP7	.56	17	200	94	640	570	1	<10	<1	n.d.	n.d.
82CMP8	.15	7	50	30	700	150	2	<10	<1	n.d.	n.d.
82CMP10	.2	7	50	30	150	300	2	<10	<1	n.d.	n.d.
82CMP11	.3	7	50	50	200	500	1	<10	<1	n.d.	n.d.
82CMP34	.3	10	50	50	300	500	3	24	<1	<20	<100
82CMP36	n.d.	n.d.	n.d.	n.d.	n.d.	n.d.	1	<10	<1	n.d.	n.d.
Plagioclase-rich clinopyroxene-olivine cumulate											
84CM81	191	230	<1	<20	<100	n.d.	n.d.	n.d.	n.d.	n.d.	n.d.
82CMG19	4	<10	<1	n.d.	n.d.	n.d.	n.d.	n.d.	n.d.	n.d.	n.d.
82CMG75	9	22	<1	n.d.	n.d.	20	70	30	500	70	.2
82CMG77	14	20	<1	n.d.	n.d.	50	70	30	500	200	.15
82CMG116	4	12	<1	<20	<100	33	240	87	820	410	.67
82CMG131	3	14	<1	<20	<100	100	70	50	200	300	.3
82CMG134	9	15	<1	n.d.	n.d.	100	70	50	300	500	.3
82CMG136	2	<10	<1	n.d.	n.d.	20	50	30	200	300	.2
82CMG146	7	<10	<1	n.d.	n.d.	n.d.	n.d.	n.d.	n.d.	n.d.	n.d.
82CMG146DUP	6	10	<1	n.d.	n.d.	50	70	30	500	300	.3
82CMG150	6	<10	<1	n.d.	n.d.	50	50	30	300	300	.3
82CMG152	33	37	<1	n.d.	n.d.	10	70	50	500	500	.3

Table 13. Analyses of titanium dioxide and selected trace and platinum-group elements in rock samples from the Lower Coon Mountain pluton—Continued

Sample		Platinum-group elements				Trace elements					
	TiO_2	Cu	Ni	Co	Cr	V	Pd	Pt	Rh	Ir	Ru
Plagioclase-rich clinopyroxene-olivine cumulate—Continued											
82CMP4	5	10	<1	n.d.	n.d.	20	50	50	200	300	.3
82CMP9	8	32	<1	<20	<100	110	80	120	280	730	1.1
82CMP30	1	<10	<1	n.d.	n.d.	100	30	20	150	150	.2
82CMP32	3	<10	<1	n.d.	n.d.	20	50	30	300	200	.2
INTRUSIVE SERIES											
Layered olivine-clinopyroxene cumulate											
10CM81	<1	17	<1	<20	<100	7	100	50	500	200	0.2
49CM81	10	38	<1	<20	<100	30	150	50	700	200	.15
50CM81	<1	10	<1	n.d.	n.d.	7	200	70	300	200	.2
56CM81	1	32	<1	<20	<100	15	150	70	300	300	.3
82CMG28	1	<10	<1	n.d.	n.d.	n.d.	n.d.	n.d.	n.d.	n.d.	n.d.
82CMG34	1	13	1	n.d.	n.d.	7	100	30	200	300	.3
82CMG37	1	<10	<1	n.d.	n.d.	1	70	30	700	150	.1
82CMG58	47	81	1	n.d.	n.d.	30	150	30	700	300	.15
82CMG96	3	<10	<1	n.d.	n.d.	20	70	30	700	200	.15
82CMG97	8	20	<1	n.d.	n.d.	15	150	20	700	150	.15
82CMG176	3	<10	<1	n.d.	n.d.	n.d.	n.d.	n.d.	n.d.	n.d.	n.d.
82CMP5	5	10	<1	n.d.	n.d.	100	79	150	420	680	.82
82CMP16	3	62	1	n.d.	n.d.	1	70	30	1,000	150	.1
82CMP17	1	18	<1	n.d.	n.d.	2	70	30	500	100	.07
82CMP21	2	<10	<1	n.d.	n.d.	7	70	30	300	150	.15
82CMP24	4	210	<1	n.d.	n.d.	10	70	30	500	200	.2
82CMP24DUP	3	<10	<1	n.d.	n.d.	15	50	30	700	300	.3
82CMP35	<1	14	<1	n.d.	n.d.	n.d.	n.d.	n.d.	n.d.	n.d.	n.d.
82CMP39	2	<10	<1	n.d.	n.d.	n.d.	n.d.	n.d.	n.d.	n.d.	n.d.
82CMP40	2	<10	<1	n.d.	n.d.	n.d.	n.d.	n.d.	n.d.	n.d.	n.d.
17CM81	2	40	<1	<20	<200	10	200	70	700	700	.7
21CM81	<1	33	<1	<20	<100	3	150	70	1,000	150	.15
36CM81	<1	35	<1	<20	<100	7	150	70	300	300	.5
40CM81	4	12	<1	<20	<100	20	300	100	1,000	500	.7
41CM81	1	25	13	<20	<100	7	150	50	500	200	.2
41ACM81	1	20	<1	<20	<100	7	150	70	300	300	.3
42CM81	2	25	<1	<20	<100	15	300	150	700	150	.15
43CM81	2	33	<1	<20	<100	7	150	70	500	300	.3
82CMG3	<1	27	<1	n.d.	n.d.	1.5	70	30	700	150	.07
82CMG4	1	82	4	n.d.	n.d.	3	300	70	1,500	70	.03
82CMG8	6	40	1	n.d.	n.d.	7	150	50	500	200	.2
82CMG10	1	<10	<1	n.d.	n.d.	n.d.	n.d.	n.d.	n.d.	n.d.	n.d.
82CMG32	1	40	<1	n.d.	n.d.	n.d.	n.d.	n.d.	n.d.	n.d.	n.d.
82CMG56	8	23	1	n.d.	n.d.	n.d.	n.d.	n.d.	n.d.	n.d.	n.d.
82CMG56DUP	2	12	<1	n.d.	n.d.	7	150	30	700	300	.2
82CMG63	3	12	<1	n.d.	n.d.	7	100	30	700	150	.15
82CMG68	<1	<10	<1	n.d.	n.d.	5	100	50	700	100	.15

Table 13. Analyses of titanium dioxide and selected trace and platinum-group elements in rock samples from the Lower Coon Mountain pluton—Continued

Sample		Platinum-group elements				Trace elements					
	TiO_2	Cu	Ni	Co	Cr	V	Pd	Pt	Rh	Ir	Ru
INTRUSIVE SERIES—Continued											
Layered olivine-clinopyroxene cumulate—Continued											
82CMG140	5	35	<1	n.d.	n.d.	15	700	70	1,000	70	.07
82CMP1	1	23	1	n.d.	n.d.	7	100	70	300	700	.5
82CMP2	<1	13	<1	n.d.	n.d.	7.3	70	280	100	60	.09
82CMP23	1	<10	<1	n.d.	n.d.	7	70	30	700	150	.1
82CMP26	1	<10	<1	n.d.	n.d.	10	100	30	1,500	150	.1
82CMP38	2	<10	<1	n.d.	n.d.	n.d.	n.d.	n.d.	n.d.	n.d.	n.d.
Olivine cumulate and dunite											
14CM81	4	62	<1	<20	<100	15	300	150	700	300	0.2
63CM81	<1	28	<1	<20	<100	7	300	100	700	30	.03
82CMG33	1	50	<1	n.d.	n.d.	n.d.	n.d.	n.d.	n.d.	n.d.	n.d.
82CMG62	5	13	<1	n.d.	n.d.	10	150	70	100	150	.1
82CMG94	8	<19	2	n.d.	n.d.	10	300	30	1,000	70	.05
82CMG98	1	<10	1	n.d.	n.d.	7	300	70	500	200	.2
82CMG113	10	15	1	n.d.	n.d.	20	300	70	700	100	.07
82CMG117	3	<10	1	n.d.	n.d.	20	200	50	1,000	100	.05
82CMG122	1	<10	<1	n.d.	n.d.	7	200	70	15	10	.01
82CMG123	2	4	<1	n.d.	n.d.	10	200	70	10	7	.007
Gabbro											
20CM81	12	24	<1	<20	<100	70	70	50	200	300	0.7
28CM81	10	32	<1	<20	<100	70	70	70	500	700	.7
35CM81	3	33	<1	<20	<100	15	150	70	500	700	.7
46CM81	13	28	<1	<20	<100	150	70	50	300	300	.2
47CM81	16	26	<1	<20	<100	70	70	50	300	300	.3
86CM81	1	14	<1	<20	<100	150	15	30	10	300	.3
98CM81	18	60	<1	<20	<100	7	100	70	300	300	.5
82CMG64	16	<10	<1	n.d.	n.d.	210	59	140	480	390	.35
82CMG64DUP	16	24	<1	n.d.	n.d.	150	100	30	300	300	.15
82CMG87	24	36	<1	n.d.	n.d.	7	30	20	150	300	.2
82CMP22	8	<10	<1	n.d.	n.d.	100	50	20	150	300	.2
82CMP29	7	<10	<1	n.d.	n.d.	20	50	20	200	150	.3
Intrusive feldspathic pyroxenite											
82CMG112	1	<10	<1	n.d.	n.d.	1.5	70	20	300	100	0.05
82CMG36	13	12	<1	n.d.	n.d.	1	70	30	700	150	.1

Table 13. Analyses of titanium dioxide and selected trace and platinum-group elements in rock samples from the Lower Coon Mountain pluton—Continued

Sample		Platinum-group elements				Trace elements					
	TiO_2	Cu	Ni	Co	Cr	V	Pd	Pt	Rh	Ir	Ru
POSTPLUTONIC INTRUSIVE DIKES											
33CM81	<1	13	<1	<20	<100	7	50	15	3	70	0.3
44CM81	4	26	<1	<20	<100	7	150	30	300	50	.2
53CM81	2	15	<1	<20	<100	150	15	30	15	300	.5
82CMG12	1	<10	<1	n.d.	n.d.	n.d.	n.d.	n.d.	n.d.	n.d.	n.d.
COUNTRY ROCKS											
73ACM81	1	46	<1	20	<100	3	50	70	300	300	0.5
74CM81	4	33	<1	n.d.	n.d.	50	15	<5	150	300	.5
75CM81	9	9	<1	<20	<100	300	50	20	30	150	.3

Table 14. Analyses of selected trace and platinum-group elements in soils developed on the Lower Coon Mountain pluton

[Six-step semiquantitative visual-spectrographic analyses of trace elements (Co, Cr, Cu, Ni, V) in parts per million; analysts: L. Bradley and M. Malcolm. Fire-assay/atomic-absorption analyses of platinum-group elements (Pd, Pt, Rh) in parts per billion; analysts: L. Bradley, J.M. McDade, and R. Moore. —, not detected; n.d., not determined]

	Soils											
Sample	5aCM81	5bCM81	6aCM81[1]	6bCM81[2]	6cCM81	7aCM81	7bCM81	7cCM81	7dCM81	11aCM81[3]	11bCM81[3]	22aCM81
Depth interval (cm).	0–10	11–21	0–10	11–21	25–30	0–10	11–20	21–27	28–37	0–10	10–20	0–9
Pd	1	3	2	2	3	2	2	3	3	16	15	2
Pt	18	27	37	23	64	40	140	34	22	33	31	49
Rh	1	1	2	1	2	1	<1	2	2	<1	1	<1
Co	100	150	100	100	100	150	150	150	150	70	70	100
Cr	700	1,000	1,000	1,500	1,500	1,500	1,500	1,500	1,000	500	700	1,500
Cu	15	50	30	50	50	20	20	30	30	30	30	10
Ni	200	200	300	200	300	150	200	200	200	150	150	300
V	700	700	700	700	700	700	700	500	500	200	300	300

	Protolith											
Sample	4CM81		4CM81							10CM81		
Unit	Jc		Jc			Jc				Ji		
Pd	1		1							<1		
Pt	22		22							17		
Rh	<1		<1							<1		
Co	70		70							50		
Cr	300		300							500		
Cu	7		7							7		
Ni	150		150							100		
V	300		300							200		

	Soil/rock ratio											
Pd	.1	3	2	2	3					<16	<15	n.d.
Pt	.81	1.2	1.7	1.0	2.9					1.9	1.8	n.d.
Rh	<1	<1	<2	<1	<2					<1.0	<1.0	n.d.
Co	1.4	2.1	1.4	1.4	1.4					1.4	1.4	1.4
Cr	2.3	3.3	3.3	5.0	5.0					1.0	1.4	1.5
Cu	2.1	7.1	4.3	7.1	7.1					4.3	4.3	3.3
Ni	1.3	1.3	2.0	1.3	2.0					1.5	1.5	2.0
V	2.3	2.3	2.3	2.3	2.3					1.0	1.5	2.0

Table 14. Analyses of selected trace and platinum-group elements in soils developed on the Lower Coon Mountain pluton—Continued

Soils												
Sample	22bCM81	22cCM81	23aCM81	23bCM81	23cCM81	23dCM81	26aCM81	26bCM81	26cCM81	27aCM81	27bCM81	27cCM81
Depth interval (cm).	10–15	16–24	0–7	8–17	18–24	25–28	0–11	12–20	21–23	0–8	9–17	18–26
Pd	1	33	<1	1	1	1	2	2	2	2	2	1
P	45	115	53	63	47	51	175	181	144	120	160	84
Rh	2	<1	1	2	2	<1	3	3	2	<1	2	<1
Co	100	100	70	70	70	50	150	150	100	100	100	100
Cr	1,500	1,000	1,000	1,000	1,000	700	2,000	2,000	2,000	3,000	3,000	2,000
Cu	10	10	2	2	1.5	1.5	15	15	7	7	10	5
Ni	300	300	100	150	150	100	300	300	300	300	300	300
V	500	500	150	150	150	100	150	150	150	150	200	200

Protolith				
Sample	21CM81			
Unit	Joc	Jl	Jl	Joc
Pd	n.d.			
Pt	n.d.			
Rh	n.d.			
Co	70			
Cr	1,000			
Cu	3			
Ni	150			
V	150			

Soil/rock ratio				
Pd	n.d.	n.d.		
Pt	n.d.	n.d.		
Rh	n.d.	n.d.		
Co	1.4	1.4		
Cr	1.5	1.0		
Cu	3.3	3.3		
Ni	2.0	2.0		
V	3.3	3.3		

Table 14. Analyses of selected trace and platinum-group elements in soils developed on the Lower Coon Mountain pluton—Continued

Soils												
Sample—	37aCM81[4]	37bCM81	60aCM81	60bCM81	60cCM81	62aCM81	62bCM81	64aCM81	64bCM81	70aCM81	70bCM81	70cCM81
Depth interval (cm).	0–11	12–17	0–9	10–15	16–29	0–12	13–28	0–14	15–23	0–13	14–21	22–36
Pd	3	4	1	<1	1	1	1	2	3	2	3	2
Pt	49	59	20	44	44	128	150	119	46	61	55	107
Rh	1	1	<1	<1	<1	1	4	33	<1	<1	<1	1
Co	150	150	100	100	70	50	70	150	150	70	70	70
Cr	1,000	700	300	300	200	1,500	1,500	3,000	2,000	1,000	1,000	1,000
Cu	20	20	7	10	7	3	3	15	15	7	7	7
Ni	200	150	150	150	150	150	150	700	700	150	150	150
V	700	700	700	700	700	150	70	150	150	500	300	500

Protolith												
Sample—	36CM81					67CM81		63CM81		71CM81		
Unit—	Jl		Jc			Jl		Jl		Jp		
Pd	<1					1		<1		1		
Pt	<35					64		28		15		
Rh	<1					<1		<1		<1		
Co	70					70		100		150		
Cr	300					1,000		700		300		
Cu	7					2		7		15		
Ni	150					150		300		150		
V	300					150		30		700		

Soil/rock ratios											
Pd	<3	<4		1.0	1.0	<1.0	<3.0	2	3	2
Pt	1.4	1.7		2.0	2.3	4.3	1.6	4.1	3.7	7.1
Rh	<1.0	<1.0		<1.0	<4.0	<3.0	<1.0	<1.0	<1.0	<1.0
Co	2.1	2.1		.7	1.0	1.5	1.5	.5	.5	.5
Cr	3.3	2.3		1.5	1.5	4.3	2.9	3.3	3.3	3.3
Cu	2.9	2.9		1.5	1.5	2.1	2.1	.5	.5	.5
Ni	1.3	1.3		1.0	1.0	2.3	2.3	1.0	1.0	1.0
V	2.3	2.3		1.0	.5	5.0	.7	.7	.4	.7

Table 14. Analyses of selected trace and platinum-group elements in soils developed on the Lower Coon Mountain pluton—Continued

	Soils		
Sample——	81aCM81	81bCM81	81cCM81
Depth interval (cm).	0–12	13–15	16–20
Pd——	1	2	2
Pt——	17	27	31
Rh——	1	1	1
Co——	70	100	70
Cr——	700	700	1,000
Cu——	7	7	30
Ni——	200	150	300
V——	1,000	700	500
	Protolith		
Unit——	Jc		
Pd——			
Pt——			
Rh——			
Co——			
Cr——			
Cu——			
Ni——			
V——			
	Soil/rock ratio		
Pd——			
Pt——			
Rh——			
Co——			
Cr——			
Cu——			
Ni——			
V——			

[1]Contains 220 ppb Au.
[2]Contains 70 ppb Au.
[3]Lateral auger hole in roadcut.
[4]Contains 130 ppm Ag.

Table 15. Estimated average major-element-oxide contents of rocks of the layered and intrusive sequences of the Lower Coon Mountain pluton and of ultramafic rocks on Duke Island, Alaska

[Major-element-oxide analyses in weight percent. —, insufficient data]

Sample	1	2	3	4	5	6	7	8	9
SiO_2	42.7	45.8	44.2	46.7	46.2	46.1	48.6	47.3	50.0
Al_2O_3	5.48	4.39	4.96	4.9	—	—	—	—	—
FeTO	17.5	13.3	15.5	10.5	13.0	18.9	14.1	16.6	11.2
MgO	17.0	19.6	18.2	19.4	22.4	18.3	20.8	19.5	20.8
CaO	15.5	15.5	15.5	16.9	18.4	16.7	16.5	16.6	18.1
Na_2O	.26	.29	.27	.6	—	—	—	—	—
K_2O	—	.09	.05	.07	—	—	—	—	—
TiO_2	1.34	.74	1.05	.6	—	—	—	—	—
MnO	.26	.23	.25	.12	—	—	—	—	—
Total	100.04	99.94	99.98	99.79	100.0	100.0	100.0	100.0	100.1

SAMPLE 1. Layered sequence; average composition calculated from data in tables 1 and 8, normalized to 100 weight percent.
2. Intrusive sequence; average composition calculated from data in tables 1 and 11, normalized to 100 weight percent.
3. Lower Coon Mountain pluton; average composition calculated from data in tables 1, 8, and 11, normalized to 100 weight percent.
4. Duke Island ultramafic rocks; average composition reported by Irvine (1974, table 19, col. 1), normalized to 100 weight percent.
5. Composition of point *m* in figure 6B of Presnall (1966, p. 768), showing the join $CaSiO_3$-MgO-iron oxide-SiO_2 at 10^{-6} atm oxygen fugacity.
6. Column 1 recalculated to four oxides.
7. Column 2 recalculated to four oxides.
8. Column 3 recalculated to four oxides.
9. Column 4 recalculated to four oxides.

☆U.S. GOVERNMENT PRINTING OFFICE: 1993-784-052/80002